



universität
wien

DIPLOMARBEIT

Titel der Diplomarbeit

Investigating substrate specificities of picornaviral proteinases by
mutational analysis.

angestrebter akademischer Grad

Magister der Naturwissenschaften (Mag. rer.nat.)

Verfasser:
Matrikel-Nummer:
Studienrichtung (lt. Studienblatt):
Betreuer:

David Neubauer
0000921
Chemie A419
Ao. Univ.-Prof. Dr. Timothy Skern

Wien, am 27. September 2008



Intake of Wine, Beer, and Spirits and the Risk of Clinical Common Cold

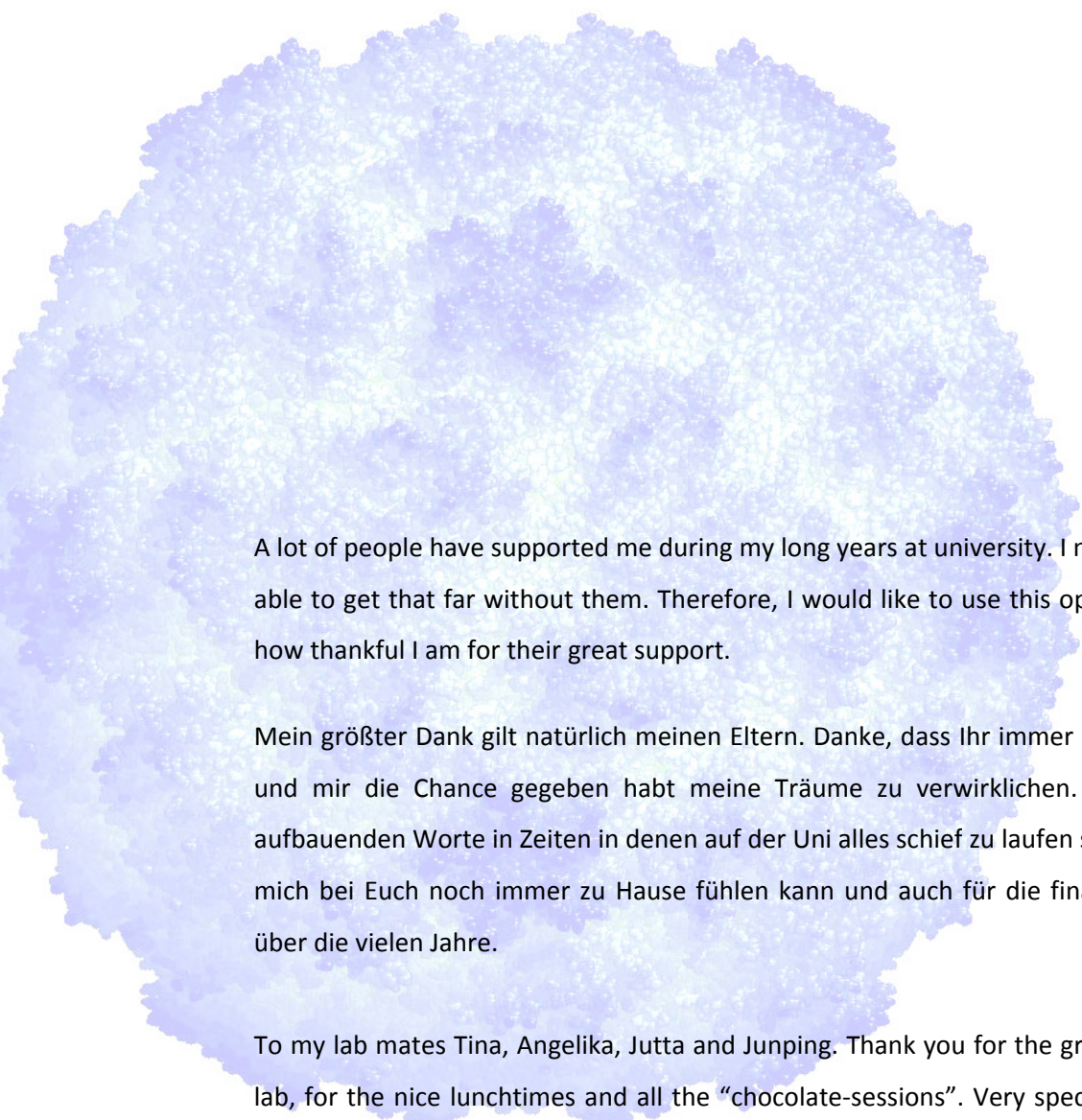
Bahí Takkouche,¹ Carlos Regueira-Méndez,¹ Reina García-Closas,² Adolfo Figueiras,¹ Juan J. Gestal-Otero,¹ and Miguel A. Hernán³

To examine whether intakes of wine, beer, spirits, and total alcohol are associated with the risk of common cold, in 1998–1999 the authors analyzed data from a cohort study carried out in a population of 4,272 faculty and staff of five Spanish universities. Usual alcohol intake was assessed at baseline by means of a standardized frequency questionnaire that was validated in a random sample of the population. The authors detected 1,353 cases of common cold. Total alcohol intake and beer and spirits consumption were not related to the occurrence of common cold, whereas consumption of wine was inversely associated with the risk of common cold. When drinkers of >14 glasses of wine per week were compared with teetotalers, the relative risk was 0.6 (95% confidence interval: 0.4, 0.8) after adjustment for age, sex, and faculty/staff status. The association was stronger for red wine. These results remained unaltered after adjustment for total alcohol intake and for other potential risk factors for common cold. Findings suggest that wine intake, especially red wine, may have a protective effect against common cold. Beer, spirits, and total alcohol intakes do not seem to affect the incidence of common cold. *Am J Epidemiol* 2002;155:853–8.

alcohol drinking; alcoholic beverages; cohort studies; common cold; wine

Common cold is one of the most frequent human diseases and, although its evolution is generally benign, causes the loss of at least 30 million days of work each year in the United States (1). Alcohol consumption has been shown to modulate the immune response and therefore could con-

epidemiologic study known (6). However, this study was conducted on volunteers artificially challenged with rhinovirus; therefore, no prospective data are available on the effect of alcohol consumption on the natural occurrence of common cold. Whether any specific type of alcoholic drink



A lot of people have supported me during my long years at university. I never would have been able to get that far without them. Therefore, I would like to use this opportunity to tell them how thankful I am for their great support.

Mein größter Dank gilt natürlich meinen Eltern. Danke, dass Ihr immer an mich geglaubt habt und mir die Chance gegeben habt meine Träume zu verwirklichen. Danke für die vielen aufbauenden Worte in Zeiten in denen auf der Uni alles schief zu laufen schien. Danke, dass ich mich bei Euch noch immer zu Hause fühlen kann und auch für die finanzielle Unterstützung über die vielen Jahre.

To my lab mates Tina, Angelika, Jutta and Junping. Thank you for the great atmosphere in the lab, for the nice lunchtimes and all the “chocolate-sessions”. Very special thanks go to Carla. Thank you so much for introducing me into the world of the laboratory and for answering my hundreds of questions so patiently.

I also want to mention all my friends. Life would be so boring without you. Thank you for listening to all my lab and scientific stories even when they bored you to death :-)

Last but not least I am deeply indebted to my supervisor Tim Skern. Thank you for giving me the chance to work on such an exciting topic, for the great support and all the important ideas and suggestions.

INDEX

1	ABSTRACT-ZUSAMMENFASSUNG	9
2	INTRODUCTION.....	15
2.1	PICORNAVIRUSES	17
2.2	HUMAN RHINOVIRUSES.....	17
2.2.1	<i>Taxonomy</i>	<i>17</i>
2.3	FOOT-AND-MOUTH DISEASE VIRUS	18
2.3.1	<i>Taxonomy</i>	<i>18</i>
2.4	THE VIRION.....	19
2.4.1	<i>Capsid</i>	<i>19</i>
2.4.2	<i>Genome.....</i>	<i>20</i>
2.5	LIFE CYCLE	22
2.5.1	<i>Attachment and entry.....</i>	<i>22</i>
2.5.2	<i>Decoding of the genetic information and polyprotein processing.....</i>	<i>26</i>
2.5.3	<i>Replication of the genome.....</i>	<i>27</i>
2.5.4	<i>Assembly and virus release.....</i>	<i>28</i>
2.5.5	<i>Host cell shutoff.....</i>	<i>29</i>
2.6	2A ^{PRO}	31
2.6.1	<i>Function</i>	<i>31</i>
2.6.2	<i>Structure</i>	<i>32</i>
2.6.3	<i>Substrate specificity.....</i>	<i>33</i>
2.7	L ^{PRO}	35
2.7.1	<i>Function</i>	<i>35</i>
2.7.2	<i>Structure</i>	<i>36</i>
2.7.3	<i>Substrate specificity.....</i>	<i>37</i>
2.8	AIMS.....	39
3	MATERIAL & METHODS.....	41
3.1	PLASMIDS	43
3.2	OLIGONUCLEOTIDES	45
3.3	DNA METHODS.....	48
3.3.1	<i>Agarose gel electrophoresis.....</i>	<i>48</i>
3.3.2	<i>DNA restriction reactions.....</i>	<i>48</i>
3.3.3	<i>Dephosphorylation of DNA 5' ends.....</i>	<i>49</i>
3.3.4	<i>Kinasing and annealing of oligonucleotides</i>	<i>49</i>
3.3.5	<i>Ligation of DNA molecules.....</i>	<i>50</i>
3.3.6	<i>Phenol-chloroform extraction</i>	<i>50</i>
3.3.7	<i>Precipitation of DNA</i>	<i>50</i>
3.3.8	<i>Purification by column</i>	<i>51</i>
3.3.9	<i>Extraction of DNA from agarose gels.....</i>	<i>51</i>
3.3.10	<i>Introduction of mutations by standard PCR techniques</i>	<i>51</i>
3.3.11	<i>Manipulation of cleavage sites by cassette cloning.....</i>	<i>52</i>

3.4	BACTERIAL CULTURES.....	52
3.4.1	Preparation of competent cells.....	52
3.4.2	Transformation.....	53
3.4.3	DNA MINI preps.....	53
3.4.4	DNA MIDI preps.....	54
3.5	RNA METHODS.....	54
3.5.1	In vitro transcription.....	54
3.5.2	Precipitation of RNA.....	55
3.5.3	RNA agarose gel electrophoresis.....	55
3.6	PROTEIN METHODS.....	56
3.6.1	In vitro translation.....	56
3.6.2	SDS polyacrylamide gel electrophoresis.....	57
3.6.3	Fluorography.....	58
4	RESULTS.....	59
4.1	CLEAVAGE OF WILD-TYPE SUBSTRATES BY HRV2 AND HRV14 2A ^{PRO}	61
4.2	HRV2 2A ^{PRO} CANNOT ACCEPT THE VP1-2A ^{PRO} CLEAVAGE SITE OF HRV14.....	62
4.3	NUP62 CONTAINS SEQUENCES THAT WERE FOUND TO BE CLEAVED IN TRANS BUT CANNOT BE ACCEPTED IN CIS BY HRV2 2A ^{PRO}	67
4.4	MET5: A HINGE AT WHICH THE N-TERMINUS IS ROTATED INTO THE ACTIVE SITE DURING SELF-PROCESSING?.....	69
4.5	CONSTRUCTION OF HRV14/2 2A ^{PRO} HYBRIDS.....	72
4.6	DOES THE VIRAL PROTEIN 2B INFLUENCE 2A ^{PRO} SELF-PROCESSING?.....	74
4.7	METHIONINE AT POSITION 143 IN Lb ^{PRO} EXHIBITS COMPARABLE PERFORMANCE IN DISCRIMINATING PHENYLALANINE FROM P2 THAN LEUCINE AT POSITION 143.....	77
5	DISCUSSION.....	79
5.1	HRV2 2A ^{PRO} CANNOT ACCEPT THE VP1-2A ^{PRO} CLEAVAGE SITE OF HRV14.....	82
5.2	NUP62 CONTAINS SEQUENCES THAT WERE FOUND TO BE CLEAVED IN TRANS BUT CANNOT BE ACCEPTED IN CIS BY HRV2 2A ^{PRO}	84
5.3	MET5: A HINGE AT WHICH THE N-TERMINUS IS ROTATED INTO THE ACTIVE SITE DURING SELF-PROCESSING?.....	85
5.4	CONSTRUCTION OF HRV14/2 2A ^{PRO} HYBRIDS.....	90
5.5	DOES THE VIRAL PROTEIN 2B INFLUENCE 2A ^{PRO} SELF-PROCESSING?.....	91
5.6	METHIONINE AT POSITION 143 IN Lb ^{PRO} EXHIBITS COMPARABLE PERFORMANCE IN DISCRIMINATING PHENYLALANINE FROM P2 THAN LEUCINE AT POSITION 143.....	92
6	APPENDIX.....	95
6.1	ABBREVIATIONS.....	97
6.2	LIST OF AMINO ACIDS.....	98
6.3	REFERENCES.....	99

1 ABSTRACT- ZUSAMMENFASSUNG

Picornaviruses are small, non-enveloped, icosahedral viruses with an RNA genome of positive sense. The family is subdivided into nine genera that contain important human and animal pathogens. The genome contains only one large open reading frame from which a polyprotein is translated. This polyprotein is then processed by viral proteinases in order to obtain the mature viral proteins. The chymotrypsin-like proteinase 2A^{pro} performs the initial cleavage of this processing in human rhinoviruses (HRV). It cleaves between the C-terminus of the preceding structural protein VP1 and its own N-terminus in an intramolecular (*cis*) reaction. In foot and mouth disease virus (FMDV), the first cleavage in polyprotein processing is performed by the leader protease (L^{pro}). This papain-like proteinase cleaves between its own C-terminus and the N-terminus of the structural protein VP4. L^{pro} was shown to be able to do so in both *cis* (intramolecular) or in *trans* (intermolecular) reactions. However, it has been found that the reaction is most likely intramolecular *in vivo*.

Cells infected with HRVs or FMDV were found to be severely impaired in translation of their own capped mRNAs. This phenomenon, called the host cell shut-off, has been shown to be caused by either 2A^{pro} (HRV) or L^{pro} (FMDV). Both of these proteinases were found to specifically cleave the host cell factor eukaryotic initiation factor 4G (eIF4G). eIF4G acts as a scaffolding protein in the translation initiation complex. Thus, the cell can no longer recruit its capped mRNAs to the 40S ribosomal subunit when eIF4G is cleaved. In contrast, viral RNA is uncapped and translation is initiated via an internal ribosomal entry segment (IRES). Therefore, translation of viral RNAs is still possible and the virus can take over the host cell translation machinery.

The cleavage sites used in the self-processing reaction by HRV2 and HRV14 2A^{pro} are not conserved. We show here that HRV2 2A^{pro} is not able to accept the cleavage site of HRV14. The search for the minimal number of HRV14 residues that are able to cause this inability revealed that HRV14 residues at both sides of the cleavable bond are necessary to prevent HRV2 2A^{pro} from processing and that proline at P2' is important for HRV2 2A^{pro} to recognize its substrate. Furthermore, we were able to show that substrate requirements in *cis* do not necessarily need to fit the requirements in *trans*. Cleavage sites that were found to be utilized by HRV2 2A^{pro} in the cleavage of nuclear pore complex proteins could not be accepted in *cis*.

In the crystal structure of HRV2 2A^{pro}, the N-terminus is turned away from the active site and gives a picture of the protease after self-processing. Therefore, a rearrangement of the N-terminus will be needed to allow self-processing. It has been suggested that Met5 could act as a hinge at which the N-terminus is rotated into the active site. We speculated that this

rotation would bring the side chain of Met5 close to the positively charged side chain of Lys109 and that for this reason an arginine could not be accepted at P5. However, we could show that this idea was false. Another approach aimed to help to understand the differences in substrate requirements of HRV2 and HRV14 2A^{pro} and to reveal possible mechanistic differences in the self-processing of these two proteinases. For this purpose, we tried to construct active 2A^{pro} hybrids made up of the N-terminal domain of HRV14 2A^{pro} and the C-terminal domain of HRV2 2A^{pro}. Unfortunately, the 2A^{pro} hybrids were totally inactive and therefore only little information could be obtained by these experiments. Finally, the influence of the protein 2B on 2A^{pro} self-processing and on the different behavior of HRV2 and HRV14 2A^{pro} in respect to the inhibitor zVAM.fmk was to be explored. We show here that self-processing is slightly delayed in the presence of 2B. As our zVAM.fmk stocks were found to be out of date, these experiments had to be postponed.

In a last set of experiments, we investigated the S2 pocket of Lb^{pro}. It has been shown that Leu143 is an important determinant in discriminating phenylalanine from protruding into the S2 pocket. Leu143 is not conserved amongst FMDV strains. Also methionine can be found at this position. Thus, we tested whether methionine was able to maintain this specificity. We were able to show that methionine exhibits similar ability to discriminate phenylalanine, indicating that not cleaving substrates with phenylalanine has biological relevance for the virus.

Picornaviren sind kleine Viren ohne Lipidhülle, die die Symmetrie eines Ikosaeders aufweisen. Die Familie der Picornaviren wird in neun Genera geteilt und enthält wichtige Pathogene für Mensch und Tier. Als Genom besitzen Picornaviren RNA mit positiver Polarität. Dieses besitzt nur einen offenen Leserahmen von dem ein Polyprotein abgelesen wird. Um die einzelnen viralen Proteine zu erhalten wird dieses von viralen Proteasen prozessiert. In humanen Rhinoviren (HRV) führt dabei die Chymotrypsin-ähnliche Protease 2A^{pro} den ersten Schnitt durch. In einer intramolekularen (*cis*) Reaktion spaltet sie das Polyprotein zwischen dem C-Terminus des vorangehenden strukturellen Proteins VP1 und ihrem eigenen N-Terminus. Die Prozessierung des Polyproteins der Maul-und-Klauenseuche (FMDV) wird von der Leader Protease (L^{pro}) eingeleitet. Diese Papain-ähnliche Protease spaltet das Polyprotein zwischen ihrem eigenen C-Terminus und dem N-Terminus des strukturellen Proteins VP4. Es ist bekannt, dass diese Reaktion prinzipiell in *cis* (intramolekular) oder *trans* (intermolekular) möglich ist. Allerdings wurde gezeigt, dass *in vivo* wahrscheinlich die intramolekulare Reaktion bevorzugt wird.

Die Translation von zellulären gecappten mRNAs ist in HRV oder FMDV infizierten Zellen stark eingeschränkt. Dieses als Abschaltung der Wirtszelle bekannte Phänomen wird durch die Proteasen 2A^{pro} (HRV) beziehungsweise L^{pro} (FMDV) verursacht. Beide sind fähig den eukaryotischen Initiationsfaktor 4G der Wirtszelle spezifisch zu spalten. Dieser arbeitet als Verbindungsprotein im Translationsinitiationskomplex. Durch die Spaltung dieses Proteins ist es der Wirtszelle nicht mehr möglich die eigenen gecappten mRNAs zur 40S Untereinheit der Ribosomen zu rekrutieren. Die virale RNA ist aber nicht gecappt. Ihre Translation wird intern über ein sogenanntes internes ribosomales Eintrittssegment (IRES) initiiert. Die Translation dieser viralen RNAs ist deshalb trotzdem möglich und der Virus übernimmt die Kontrolle über die Translationsmaschinerie der Wirtszelle.

Die von HRV2 und HRV14 2A^{pro} bei der Selbstprozessierung benutzten Schnittstellen sind nicht konserviert. Wie wir hier zeigen, kann die Schnittstelle aus HRV14 von HRV2 2A^{pro} nicht akzeptiert werden. Die Suche nach der minimalen Anzahl an HRV14 Resten die dies verursachen ergab, dass HRV14 Reste auf beiden Seiten der Spaltstelle eingeführt werden müssen um HRV2 2A^{pro} daran zu hindern die Schnittstelle zu erkennen. Außerdem wurde entdeckt, dass die Aminosäure Proline an Position P2' für die Erkennung des Substrates der HRV2 2A^{pro} wichtig ist. Über dies hinaus konnten wir beweisen, dass die Anforderungen an das Substrat in der *cis* Reaktion nicht zwingendermaßen mit den Anforderungen der *trans* Reaktion übereinstimmen müssen. Schnittstellen die bei der Spaltung von Proteinen des nuklearen

Porenkomplexes in *trans* von HRV2 2A^{pro} benutzt werden, wurden in der *cis* Reaktion nicht akzeptiert.

In der Kristallstruktur von HRV2 2A^{pro} ist der N-Terminus vom aktiven Zentrum weggedreht. Dies entspricht der Situation nach der Prozessierung in *cis*. Um die Selbstprozessierung aber möglich zu machen, muss der N-Terminus neu angeordnet werden. Es wurde bereits vorgeschlagen, dass Met5 als Angelpunkt fungieren könnte an dem der N-Terminus in das aktive Zentrum gedreht wird. Dadurch würde die Seitenkette von Met5 nahe der positiv geladenen Seitenkette von Lys109 positioniert. Deshalb nahmen wir an, dass die Aminosäure Arginin an Position P5 von HRV2 2A^{pro} nicht akzeptiert werden würde. Wir zeigen hier allerdings, dass diese Theorie falsch war. Ein weiteres Experiment sollte helfen, die Unterschiede in der Substratspezifität von HRV2 und HRV14 2A^{pro} zu verstehen und zielte auch darauf ab, eventuell vorhandene mechanistische Unterschiede aufzuklären. Dabei versuchten wir aktive 2A^{pro} Hybride zu konstruieren, die aus der N-terminalen Domäne der HRV14 2A^{pro} und der C-terminalen Domäne der HRV2 2A^{pro} bestehen. Unglücklicherweise waren diese Hybride vollständig inaktiv weshalb nur sehr wenig schlüssige Information aus diesen Experimenten gewonnen werden konnte. Schließlich sollte auch noch der Einfluss des Proteins 2B auf die Selbstprozessierung der HRV2 und HRV14 2A^{pro} und deren unterschiedliche Reaktion auf den Inhibitor zVAM.fmk getestet werden. Wir konnten zeigen, dass in Anwesenheit des Proteins 2B die Selbstprozessierung leicht verzögert abläuft. Unsere zVAM.fmk Bestände stellten sich aber leider als zu alt heraus, weshalb diese Experimente verschoben werden mussten.

Abgesehen von diesen Experimenten wurde auch die S2 Tasche der Leader Protease (Lb^{pro}) untersucht. Es wurde gezeigt, dass Leu143 eine wichtige Determinante ist um Phenylalanin nicht in diese Tasche eindringen zu lassen. Leu143 an dieser Position ist aber nicht unter allen FMDV Stämmen konserviert. Manche Stämme besitzen auch Methionin an dieser Stelle. Deshalb testeten wir, ob auch Methionin diese Aufgabe erfüllen kann. Tatsächlich konnten wir zeigen, dass auch Methionin fähig ist, Phenylalanin aus der S2 Tasche zu verdrängen. Diese Fakten legen nahe, dass es von biologischer Relevanz für den Virus ist, Substrate mit Phenylalanin an P2 nicht zu spalten.

2 INTRODUCTION

2.1 PICORNAVIRUSES

Picornaviruses are small (30nm diameter), non-enveloped, icosahedral viruses with a RNA genome of positive sense. The name originates from its small size (pico) and the nature of its genome. The family contains several important human and animal pathogens such as poliovirus (PV), human rhinoviruses (HRV), hepatitis A virus (HAV) and foot and mouth disease virus (FMDV). The family is subdivided into nine genera named enterovirus, rhinovirus, cardiovirus, aphthovirus, hepatovirus, parechovirus, erbovirus, kobuvirus and teschovirus (Fauquet 2005). Recently, the international committee on taxonomy of viruses (ICTV) reported the reclassification of the genus rhinovirus into the genus of enterovirus (ICTV 2008), reducing the number of picornaviral genera to eight.

This thesis discusses experiments with the proteinases 2A^{pro} of human rhinoviruses and Lb^{pro} of FMDV. Therefore, the introduction is focused on the genera of rhinoviruses and aphthoviruses. Nevertheless, several unifying principles of picornaviruses were examined on PV that acts as a role model. Therefore, many references refer to experiments with this enterovirus.

2.2 HUMAN RHINOVIRUSES

Human rhinoviruses (HRV) are the main causative agent of the common cold (Makela *et al.* 1998). The sites of infection are the nose and the throat, explaining the name of the genus (Arruda *et al.* 1997). Common colds are one of the main reasons for short time absence from work and cause enormous economic loss (Savolainen *et al.* 2002). Moreover, HRVs were also reported to cause more severe diseases and were recently connected with severe respiratory-tract infection in children (Renwick *et al.* 2007). Neither vaccines nor anti-viral compounds are available for the control and treatment of HRVs.

2.2.1 TAXONOMY

In 2005, the international committee on taxonomy reported a total of 103 HRV serotypes (Fauquet 2005). There are two systems for classifying HRVs. The first one uses

sequence homologies in the capsid proteins VP1 and VP4 to cluster the serotypes into either genetic group A or B (Laine *et al.* 2006). Recently, Lau *et al.* reported the discovery of a new genetic cluster C that is associated with acute respiratory illness in children (Lau *et al.* 2007). The second classification system groups the serotypes based on the receptor used for attachment and entry. About 90% of all serotypes belong to the so called major group viruses that use the intercellular adhesion molecule 1 (ICAM-1) as a receptor (Greve *et al.* 1989, Staunton *et al.* 1989). The remaining serotypes use the low density lipoprotein receptor (LDLR) or another member of the LDLR family (Hofer *et al.* 1994) and belong to the so-called minor group of human rhinoviruses.

2.3 FOOT-AND-MOUTH DISEASE VIRUS

FMDV is an animal pathogen of global interest (Kitching 2005). It infects cloven-hoofed animals such as cattle, swine, sheep, goats or deer. The symptoms of the infection range from fever and lameness to vesicular lesions on the tongue, snout, feet and teats. FMDV is ranked amongst the most highly contagious pathogens of animals. Infection occurs via the respiratory route (Donaldson *et al.* 1987) or lesions of the skin or mucous membranes (Donaldson 1987). Virus is also shed via milk (Hyde *et al.* 1975) as well as semen, urine and feces (Donaldson 1987). Control strategies include mass slaughter and quarantine of areas in which an FMDV outbreak has been recognized. An effective vaccine is available (Bahnemann 1975) and was used for successful control in Western Europe. However, an effective anti-viral compound is desirable for regions that have been reported free of FMDV for a longer time and for the treatment of persistently infected animals.

2.3.1 TAXONOMY

The species FMDV belongs to the genus of aphthoviruses and is subdivided into seven serotypes: A, O, C, Asia 1 and South African Territories 1, 2 and 3. Each of these serotypes contains a number of subtypes (Fauquet 2005).

2.4 THE VIRION

2.4.1 CAPSID

The picornaviral capsid is made up of four structural proteins named VP1-VP4 (the term VP0 resembles a precursor that is cleaved into the two proteins VP4 and VP2). The building block of the capsid is the protomer that consists of one copy of each structural protein (Figure 2-1A). 60 of these protomers can be combined to build up a picornaviral capsid. Several cryo-EM and X-ray structures of picornaviral capsids are available. The first structure of a picornaviral capsid to be solved was the one of HRV14 (Rossmann *et al.* 1985). Structures of PV1 (Hogle *et al.* 1985), FMDV serotype O (Acharya *et al.* 1989), HRV16 (Oliveira *et al.* 1993) and coxsackievirus B3 (CVB3) (Muckelbauer *et al.* 1995) followed. All these structures revealed that picornaviral capsids are of icosahedral symmetry with a triangulation number of $T=3$ (Figure 2-1A). VP1-VP3 form the outer shell, while VP4 is hidden in the interior.

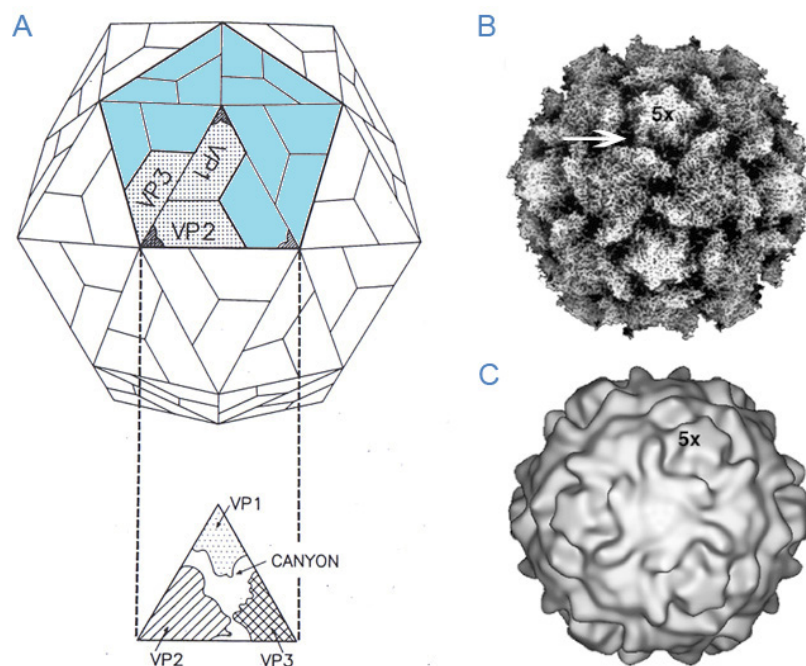


Figure 2-1 Structural features of picornaviral capsids. **(A)** Schematic representation of the capsid. The protomer with one copy of each structural protein is colored in grey (VP4 lies in the interior and cannot be seen). Five protomers build up a pentamer (light blue) (Fields *et al.* 2007). **(B)** X-ray structure of PV1. A 5-fold axis is labeled with “5x” and the canyon surrounding it is indicated by the arrow (Hogle *et al.* 1985). **(C)** Cryo-EM reconstruction of PV1. The star-shaped plateau at each 5-fold axis is surrounded by the 12Å deep canyon (Fields *et al.* 2007).

VP1, VP2 and VP3 share no sequence homology. Nevertheless, they all fold into a wedge shaped structure that is made up of an eight stranded antiparallel β -barrel. This barrel consists of two antiparallel β -sheets (Figure 2-2). Tight protein packing allows a number of protein-protein contacts enabling the assembly of a stable capsid. The C-termini of the structural proteins are exposed to the exterior of the shell while the N-termini are buried in the interior.

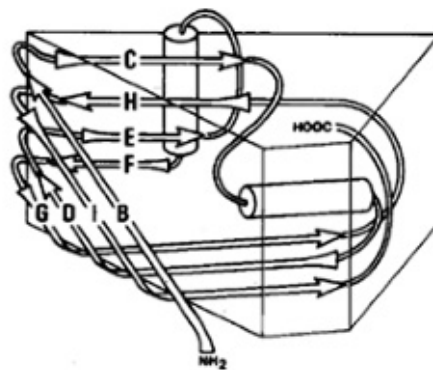


Figure 2-2 Secondary structure elements of the picornaviral structural proteins. The two antiparallel β -sheets form a wedge shaped β -barrel (Burke *et al.* 1991).

The capsid surface of rhinoviruses and enteroviruses exhibits plateaus at the 3-fold and 5-fold axes of symmetry. The 5-fold axis is surrounded by a deep cleft called the canyon (Figure 2-1B and C) which has been proven to be the receptor binding site for major group HRVs (see section 2.5.1.1). This canyon is not found on the surface of FMDV. It is filled by an insertion between the two β -strands β G and β H (Semler and Wimmer 2002). Another unique feature of FMDV capsids is the presence of a pore at the five-fold axis through which small molecules can pass (Acharya *et al.* 1989). The capsids of HRVs and FMDV are acid labile and therefore cannot pass the intestinal tract as PV (Fields *et al.* 2007).

2.4.2 GENOME

Picornaviruses have a single stranded RNA of positive polarity as their genome. The 5' uncapped and 3' polyadenylated RNA varies in length from about 7.1kb for HRVs to about 8.1kb for FMDV (Figure 2-3) (Stanway *et al.* 1984, Skern *et al.* 1985, Beard and Mason 2000). The viral protein VPg is covalently linked to the 5' end of picornaviral genomes (Lee *et al.*

1977). A long 5' untranslated region (UTR) is followed by a single, approximately 6.5-6.9kb long open reading frame (ORF). The 3' UTR is short (e.g. 47bp in HRV14) followed by the poly-A tail that is required for infectivity (Spector and Baltimore 1974). Both untranslated regions contain highly ordered structures that are involved in replication of the genome and initiation of cap independent translation (see sections 2.5.3 and 2.5.5).

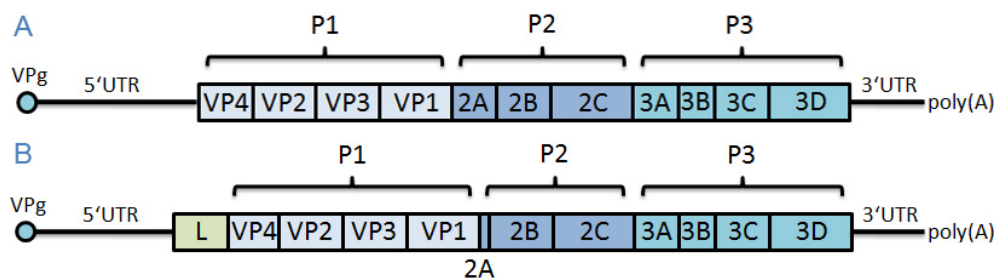


Figure 2-3 Picornaviral genome organization. **(A)** HRV. **(B)** FMDV. The single ORF is flanked by untranslated regions containing highly ordered structures. The RNA has the viral protein VPg covalently linked to its 5' end and is polyadenylated at its 3' end. The coding region is arranged in three regions called P1-P3. In FMDV the P1 region is preceded by the coding region for the L protein. (Fields *et al.* 2007)

The open reading frame is organized in three regions designated P1-P3. P1 contains the four structural proteins VP1-VP4. The protease 2A^{pro} and the accessory proteins 2B and 2C are encoded in region P2 while the P3 region codes for accessory proteins as well as the protease 3C^{pro} and the polymerase 3D^{pol}. In contrast to HRVs, FMDV codes for an additional protein, the so called leader protease (L). The coding region for this protein precedes the P1 region of structural proteins.

2.5 LIFE CYCLE

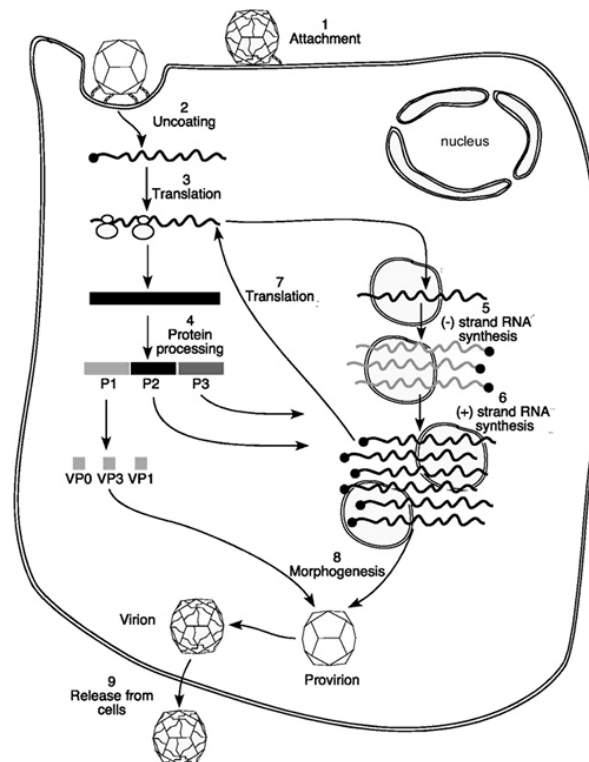


Figure 2-4 Schematic overview of the viral life cycle. After attachment and entry **(1)** the genome is released into the cytoplasm **(2)**. VPg is cleaved off and the ORF is translated into a long polyprotein **(3)**. This polyprotein is then proteolytically processed by viral proteinases **(4)**. Once the polymerase is synthesized, viral minus strand RNA intermediates are produced **(5)** which serve as template for the production of several new positive strands **(6)**. These new strands are either used for further translation **(7)** or packed into new particles **(8)**. The virus is then released from the cell upon cell lysis **(9)** (Fields *et al.* 2007).

2.5.1 ATTACHMENT AND ENTRY

2.5.1.1 ATTACHMENT AND ENTRY OF HUMAN RHINOVIRUSES

HRVs can be classified into the major and minor group based on the cellular receptor used for attachment and entry. Major group HRVs use the intercellular adhesion molecule 1 (ICAM-1) (Greve *et al.* 1989, Staunton *et al.* 1989) whereas minor group viruses use the low density lipoprotein receptor (LDLR) or other members of the LDLR family (low density lipoprotein receptor-related protein LRP or very low density lipoprotein receptor VLDLR)

(Hofer *et al.* 1994, Marlovits *et al.* 1998b). After attachment to the cell, the virus is taken up via endocytosis (Schober *et al.* 1998).

ICAM-1 is a member of the immunoglobulin superfamily. It is a transmembrane protein with a short intracellular, C-terminal domain (Staunton *et al.* 1988). The extracellular, N-terminal part of the protein consists of five immunoglobulin-like domains designated D1-D5 and is highly glycosylated. Its natural function is to bind the ligands leukocyte function-associated antigen-1 (LFA-1) and macrophage-1 antigen (Mac-1) at sites of infection.

The first atomic structure of an HRV particle (HRV14) revealed that a star shaped plateau at each five-fold axis of the icosahedral capsid is surrounded by a 12Å deep depression named the canyon (Figure 2-1B and C) (Rossmann *et al.* 1985). Soon, it was suggested that this 12-15Å wide canyon with its conserved residues at the floor could be the site of receptor binding. This theory was further strengthened by the finding that mutating residues at the canyon floor resulted in altered binding levels (Colonno *et al.* 1988). Finally, cryo-EM data of receptor-virus complexes showed that the canyon was indeed the site of receptor binding (Figure 2-5) (Olson *et al.* 1993). ICAM-1 was shown to bind the central region of the canyon of HRV16 with its N-terminal domain D1 penetrating about 10Å deep into the canyon.

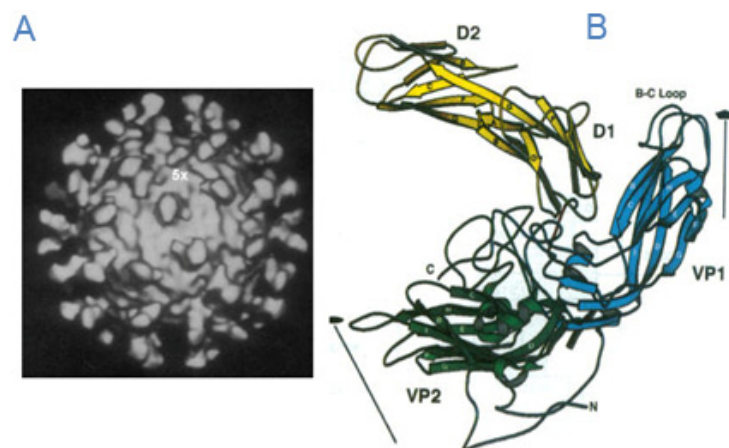


Figure 2-5 Cryo EM reconstruction of HRV16 bound to a recombinant fragment of ICAM-1. **(A)** Five molecules of the receptor bind to the canyon surrounding the plateau at each fivefold axis. **(B)** Schematic representation of the D1 domain of ICAM-1 binding to the floor of the canyon of the viral particle. (Olson *et al.* 1993).

The entry pathway of major group viruses is not yet completely understood. HRVs that use the canyon for receptor binding are destabilized upon binding. It has been shown that receptor binding alone is sufficient to induce conformational changes in the capsids of HRV14

and HRV16 (Hoover-Litty and Greve 1993). Binding of the D1 domain of ICAM-1 is thought to cause VP1 to slide slightly apart from the five-fold axis opening a channel through which the RNA could possibly be released (Kolatkar *et al.* 1999). This model is consistent with kinetic studies about the binding of the virus to the receptor. Nevertheless, also different entry modes are possible.

The LDLR family consists of proteins that contain variable numbers of repeats that are about 40 amino acids in length (so called “complement type A repeats”) (Yamamoto *et al.* 1984). The number of this repeats varies among different family members. LDLR is responsible for the binding and internalization of lipids that are transported in apolipoprotein complexes B or E into the cell. LDLR, which is strongly conserved through evolution, was found to serve as receptor for minor group HRVs.

The first hints in discovering the minor group receptor were obtained from binding experiments of HRV2 to detergent solubilized HeLa cell membranes. Mischak *et al.* showed that HRV2 could specifically bind a protein that was about 120 kDa in size (Mischak *et al.* 1988). This protein was further investigated by trypsin digestion, and N-terminal amino acid sequencing identified the protein as being human LDLR (Hofer *et al.* 1994). Marlovits *et al.* showed that recombinant LDLR was able to protect HeLa cells from infection with minor groups viruses, whereas HRV14 infection was unaffected (Marlovits *et al.* 1998c). Cryo-EM of recombinant VLDLR fragments complexed to HRV2 showed that the receptor binds at the star shaped plateau that is surrounded by the canyon (Figure 2-6) (Hewat *et al.* 2000). Furthermore, it was shown that already two of the complement type A repeats are sufficient to bind the virus (Marlovits *et al.* 1998a).

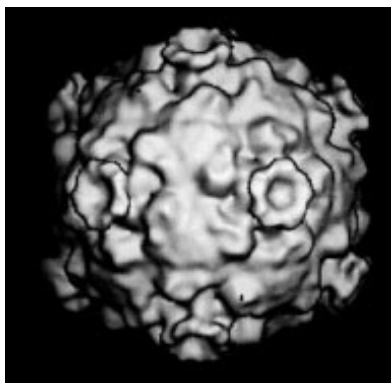


Figure 2-6 Cryo EM reconstruction of HRV2 bound to a VLDLR fragment. The receptor binds close to the five-fold axis of symmetry and builds up a ring-structure at the plateau (Hewat *et al.* 2000).

The uptake of the minor group HRV2 was shown to be much faster than the uptake of the major group HRV14 (Lonberg-Holm and Korant 1972). This is thought to be due to the lack of an internalization signal on ICAM-1. Still, HRV14 is dependent on an intact clathrin-dependent endocytosis pathway which suggests the involvement of a co-receptor (DeTulleo and Kirchhausen 1998). In contrast to major group HRVs, minor group HRVs are not destabilized upon receptor binding. They are therefore strongly dependent on the low pH that arises in the endosomes (Neubauer *et al.* 1987, Prchla *et al.* 1994) whereas HRV14 is able to uncoat in the presence of the drug bafilomycin A1 which blocks acidification of the endosomes (Schober *et al.* 1998, Bayer *et al.* 1999).

2.5.1.2 ATTACHMENT AND ENTRY OF FMDV

Early experiments showed that trypsin treatment of FMDV results in virus particles that are unable to bind cells (Moore and Cowan 1978). Subsequently, it was found that trypsin cleaves the capsid protein VP1 at position Arg144 (Robertson *et al.* 1983). This finding led to the speculation that this region may be involved in receptor binding. In 1984, Pierschbacher and Ruoslahti found that the tri-peptide ArgGlyAsp served as the recognition site for the fibronectin-receptor (Pierschbacher and Ruoslahti 1984b), a member of the integrin family. Interestingly, this RGD-sequence was also found in FMDV VP1 (Pierschbacher and Ruoslahti 1984a) and turned out to be a highly conserved motif (Pfaff *et al.* 1988).

Further experiments showed that peptides containing this motif were able to inhibit the binding of the virus to the cells (Fox *et al.* 1989, Baxt and Becker 1990), and site directed mutagenesis of the RGD-motif strengthened the idea of its involvement in the attachment of FMDV even further (Leippert *et al.* 1997). Finally, integrin $\alpha_v\beta_3$ was proven to be the receptor utilized by FMDV (Berinstein *et al.* 1995, Neff *et al.* 1998, Neff *et al.* 2000, Neff and Baxt 2001). However, it has also been shown that some FMDV strains can use heparan sulfate as a co-receptor (Jackson *et al.* 1996).

The exact route of entry and mode of uncoating of FMDV is still unclear. There is evidence that the virus is probably taken up into endosomes, followed by a breakdown of the capsid via acidification of the endosomes (Carrillo *et al.* 1984, Carrillo *et al.* 1985, Baxt 1987).

2.5.2 DECODING OF THE GENETIC INFORMATION AND POLYPROTEIN PROCESSING

Picornaviruses replicate in the cytoplasm of the host cell. Upon release of the viral RNA into the cytoplasm, the genome has to be translated before RNA replication can take place as the virus does not take its RNA dependent RNA polymerase with it. The viral RNA lacks a 5' cap structure but has the viral protein VPg covalently linked to its 5' end. However, it has been shown in PV that VPg is cleaved off by a cellular enzyme before translation can occur (Ambros and Baltimore 1980). Lacking the 5' cap structure, translation has to be initiated by a different mechanism. The 5' UTR of picornaviral genomes are 624 to 1119 nucleotides in length and contain highly structured regions (Fields *et al.* 2007). These structures are conserved among several members of picornaviruses, although they do not share sequence homology (Rivera *et al.* 1988). Deletions and mutations in this region of the genome were proven to effect translation (Bienkowska-Szewczyk and Ehrenfeld 1988, Trono *et al.* 1988), indicating that the secondary structures of the 5' UTR are involved in a cap independent internal translation initiation. The structures responsible for binding the 40S subunit of the ribosome were termed internal ribosomal entry segment (IRES). The mechanism of translation initiation will be discussed in section 2.5.5 in more detail in the context of the host cell shutoff.

Only one open reading frame is found on picornaviral genomes. Therefore, a large viral polyprotein is translated from this open reading frame. This polyprotein has to be processed by viral proteinases that specifically cleave the polypeptide chain to give the mature viral proteins. However, as the polyprotein is processed co-translationally (Toyoda *et al.* 1986), the whole polyprotein can never be detected.

In HRVs, the protease 2A^{pro} performs the initial cleavage on the polyprotein, cleaving between its own N-terminus and the C-terminus of the preceding structural protein VP1 (Figure 2-7A) (Toyoda *et al.* 1986). HRV2 2A^{pro} cleaves at the sequence IITTA*GPSD whereas HRV14 2A^{pro} uses the cleavage site DIKSY*GLGP.

The leader protease initiates polyprotein processing in FMDV by cleaving between its own C-terminus and the N-terminus of VP4 (Figure 2-7B) (Strebel and Beck 1986). The cleavage site used by the strain O_{1k} (the strain used in the experiments) is RKLK*GAGQ. Interestingly, initiation of protein synthesis can occur on two different AUG codons that are separated by 28 amino acids leading to the formation of two different forms of the L protease: Lab^{pro} and Lb^{pro} (Sangar *et al.* 1987). Although both forms have the same enzymatic activity (Medina *et al.* 1993), Lb^{pro} is the form predominantly produced in infected cells (Cao *et al.* 1995). The protein

2A of FMDV is only 18 amino acids in length and does not have proteolytic activity. Nevertheless, it has been shown that this sequence causes the interruption of the polyprotein chain between its own C-terminus and the N-terminus of 2B by a putative ribosomal skip (Ryan *et al.* 1991, Donnelly *et al.* 2001).

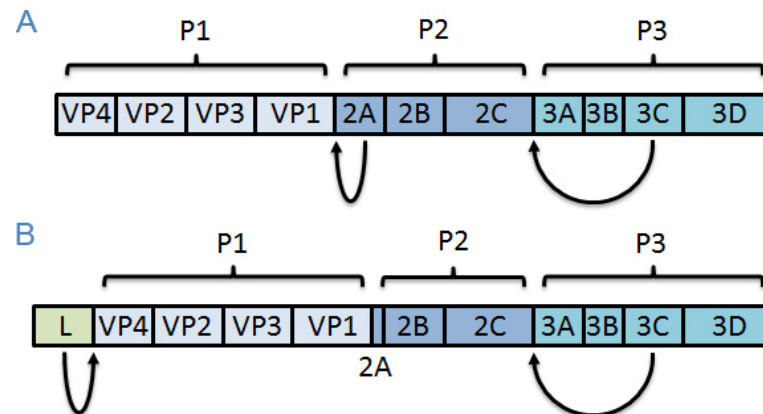


Figure 2-7 Schematic representation of the viral polyprotein of **(A)** HRV and **(B)** FMDV. The initial cleavages performed by $2A^{pro}$, L^{pro} and $3C^{pro}$ are indicated by arrows. $2A^{pro}$ cleaves between the C-terminus of VP1 and its own N-terminus, L^{pro} cleaves between its own C-terminus and the N-terminus of VP4 whereas $3C^{pro}$ performs its initial cleavage between 2C and 3A (Fields *et al.* 2007).

All other cleavages are carried out by the proteinase $3C^{pro}$ or its precursor $3CD^{pro}$. $3C^{pro}$ and $3CD^{pro}$ cleave between the amino acids glutamine and glycine. However, glutamine and glycine do not seem to be the only substrate requirements for $3C^{pro}$ as only nine of thirteen Gln*Gly junctions are cleaved in the PV polyprotein (Kitamura *et al.* 1981, Hanecak *et al.* 1982). The last event in polyprotein processing is the cleavage of VP0 into VP4 and VP2. VP0 is cleaved in the already assembled new viral particle in a maturation step. The mechanism of this cleavage remains unclear. The theory that the conserved Ser10 of VP2 could be responsible for the cleavage (Arnold *et al.* 1987) was discarded after it was found that mutating Ser10 to alanine did not affect cleavage. Subsequently, a conserved histidine was thought to act together with the RNA to cleave VP0 (Curry *et al.* 1997).

2.5.3 REPLICATION OF THE GENOME

A critical concentration of $3CD^{pro}$ is thought to initiate the switch from translation to negative strand RNA synthesis (Gamarnik and Andino 1998). Replication of the picornaviral

RNA genome is a highly complex process in which all but the structural proteins of the virus are involved. In infected cells, the bulk of the cytoplasm is occupied by virus induced membranous vesicles (Bienz *et al.* 1990) at which the RNA genome is replicated. Replication is performed by a viral encoded RNA dependent RNA polymerase which also covalently links the RNA to Tyr3 of VPg (Gerber *et al.* 2001a). As the polymerase cannot initiate RNA synthesis on a naked RNA strand, VPg serves as a primer (Gerber *et al.* 2001b). Recently, a model of the minus strand synthesis mechanism has been proposed in which the genome undergoes circularization by involvement of the cellular poly-A binding protein (PABP) (Herold and Andino 2001). Once a minus strand RNA has been produced by the polymerase, it serves as an intermediate for the production of several new positive strands (Novak and Kirkegaard 1991). No free minus strands are however observed in the cell. They are only found in an either fully double stranded replicative form or a replicative intermediate that consists of a full length minus strand coupled to a various number of complementary positive strands. While the viral polymerase can copy any primed RNA *in vitro*, it is known that *in vivo* it only replicates viral RNA. Structural patterns in the viral RNA such as the cloverleaf in the 5' UTR (Rivera *et al.* 1988), a single stem loop in the 3' UTR (Pilipenko *et al.* 1992) or internal *cis*-acting elements (Gerber *et al.* 2001a) ensure that the viral RNA is specifically recruited to the replicative complex.

2.5.4 ASSEMBLY AND VIRUS RELEASE

Assembly of the virus is a highly specific process in which only viral positive stranded RNA that is linked to VPg is encapsidated (Novak and Kirkegaard 1991). It is thought that this specificity is achieved by coupling the process of packing to the synthesis of positive stranded RNA (Halperen *et al.* 1964). Folding of the structural proteins starts co-translationally. Once HRV 2A^{pro} or FMDV 2A has separated them from the non-structural proteins, 3C^{pro} cleaves between VP0-VP3 and VP3-VP1 leading to the formation of the 5S protomer. The 5S protomer is the structural building block of the capsid containing one copy of each protein VP0, VP3 and VP1. Subsequently, 5 protomers assemble to build the 14S pentamer (Figure 2-8) (Palmenberg 1982). These important intermediates are capable of self-assembly to form an empty 80S capsid. There are two possible ways of packing the RNA into the capsid. Jacobson *et al.* stated a model in which RNA is inserted into fully built empty capsids (Jacobson and Baltimore 1968).

The second model claims that the RNA assembles with the 14S pentamers which then build up the provirion with the already encapsidated RNA (Nugent and Kirkegaard 1995). Finally, VP0 is cleaved by a yet unknown mechanism resulting in higher stability of the particle and acquisition of infectivity (Basavappa *et al.* 1994). Virus is then released from the cell upon cell lysis.

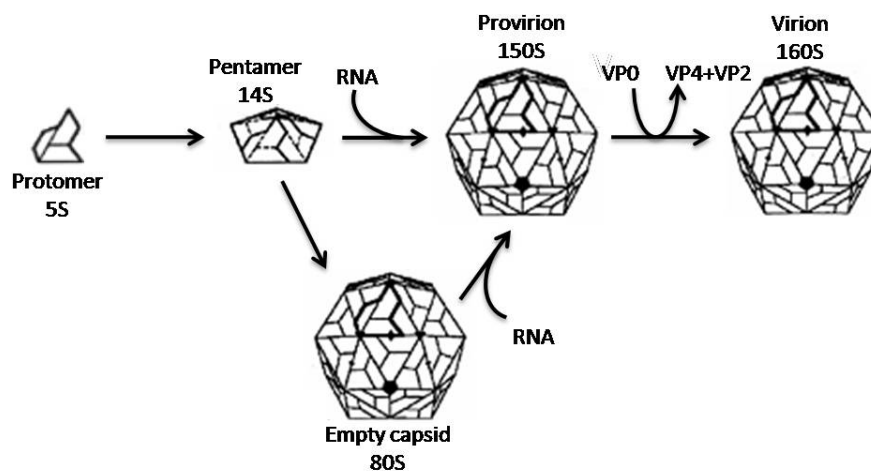


Figure 2-8 Assembly of the viral particle. Five protomers are combined to form a pentamer. This structure is capable of self-assembly to form an empty capsid. Whether the genome is inserted into a fully built capsid or is encapsidated while the particle is built up is still under debate. Finally VP0 is cleaved by an yet unknown mechanism in a maturation step (Rotbart 1995).

2.5.5 HOST CELL SHUTOFF

The so called host-cell shutoff is a phenomenon in which infected cells can no longer produce their own proteins (Etchison *et al.* 1982, Etchison and Fout 1985, Devaney *et al.* 1988). In contrast, viral proteins are still produced allowing the virus to take over its host-cell. However, the host-cell's mRNAs have been shown to be maintained intact. Therefore, the key event of this phenomenon has to be found in the process of translation.

Cellular mRNAs are 7-methyl-guanosine capped at their 5' end. This cap structure is important for the so-called 43S preinitiation complex (containing the 40S subunit of the ribosome) to recruit an mRNA. Subsequently, the 40S subunit scans for the AUG initiation codon, the 60S subunit of the ribosome binds and translation can occur. The recognition of the mRNA is mediated by several initiation factors (Figure 2-9A). Eukaryotic initiation factor 4E (eIF4E, also called cap binding protein) is capable of binding the cap structure of the mRNA

(Sonenberg *et al.* 1978). Additionally, it has a binding site for the N-terminal domain of eukaryotic initiation factor 4G (eIF4G) (Mader *et al.* 1995). eIF4G consists of two domains and acts as a central scaffolding protein for the initiation complex. With its C-terminal domain, it binds eukaryotic initiation factor 4A (eIF4A) and eukaryotic initiation factor 3 (eIF3) that in turn binds the 40S subunit of the ribosome (Lamphear *et al.* 1995). An additional site on the N-terminal domain of eIF4G binds poly-A binding protein (PABP), leading to a circularization of the complex (Imataka *et al.* 1998). The complex of eIF4A, eIF4G and eIF4E is called eIF4F. Figure 2-10 gives a schematic representation of the eIF4G binding domains.

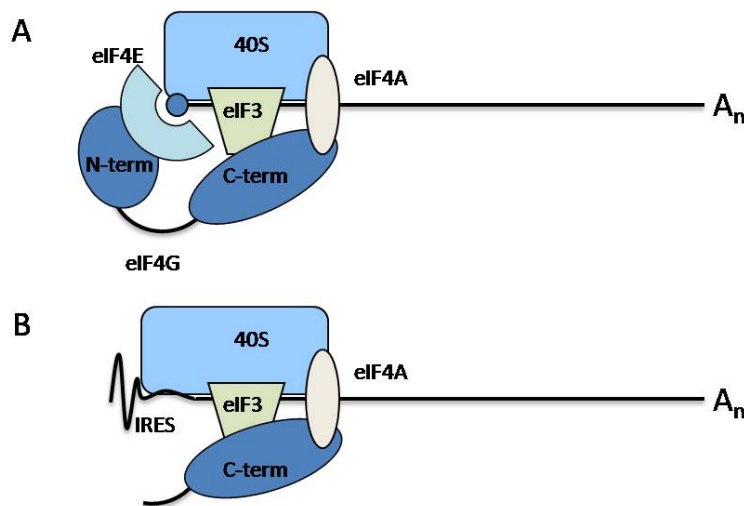


Figure 2-9 Schematic illustration of the initiation factors involved in cap-dependent and cap-independent translation initiation. **(A)** eIF4G acts as a scaffolding protein to bring together the capped mRNA and the 40S subunit of the ribosome. **(B)** eIF4G cleavage by 2A^{pro} or L^{pro} renders the complex unable to recruit capped RNA. However, viral RNAs can still be translated by cap-independent initiation via an internal ribosomal entry segment (IRES) (Fields *et al.* 2007).

It was first shown in PV infected HeLa cells that the initiation factor eIF4G is cleaved during the host-cell shut-off (Etchison *et al.* 1982). This leads to the loss of eIF4Gs scaffolding function and therefore to the loss of eIF4Fs ability to recruit capped mRNAs to the 40S subunit of the ribosome. However, viral RNAs initiating on an IRES are still able to be translated (Figure 2-9B). It has been shown that initiation of translation from an IRES works even more efficiently in the presence of the C-terminal cleavage product of eIF4G than in the presence of intact eIF4G (Borman *et al.* 1997). Thus, the virus is gaining advantage over the host cell.

The enzyme responsible for the cleavage of eIF4G in human rhinovirus infected cells was found to be the viral protease 2A^{pro}. Lamphear *et al.* showed that 2A^{pro} of HRV2 was

capable of directly cleaving eIF4G (Lamphear *et al.* 1993). In contrast, in FMDV infected cells eIF4G is cleaved by the leader protease (Devaney *et al.* 1988). In 1998, Gradi *et al.* reported the discovery of a homologue of eIF4G termed eIF4GII while the original protein was renamed eIF4GI (Gradi *et al.* 1998b). The two homologues share only 46% amino acid identity. Nevertheless, it has been shown that both homologues have to be cleaved to lead to the host cell shut-off (Gradi *et al.* 1998a). The cleavage sites of HRV2 2A^{pro} have been mapped as LSTR⁶⁸¹*GPPR at eIF4GI (Lamphear *et al.* 1993) and LLNV⁶⁹⁹*GSRR at eIF4GII (Gradi *et al.* 2003). The leader protease has been shown to cleave these two isoforms at FANLG⁶⁷⁴*RTTL (eIF4GI) and LLNVG⁷⁰⁰*SRRS (eIF4GII) (Kirchweiger *et al.* 1994, Gradi *et al.* 2004) (Figure 2-10).

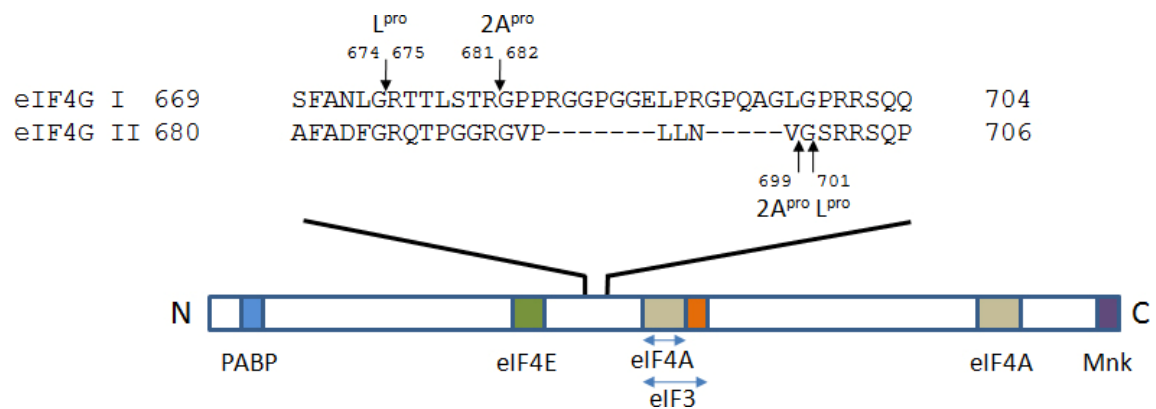


Figure 2-10 Organization of the scaffolding protein eIF4G. The binding domains for PABP, eIF4E, eIF4A, eIF3 and Mnk as well as the cleavages sites used by HRV2 2A^{pro} and FMDV Lb^{pro} are shown (Zhao *et al.* 2003).

2.6 2A^{PRO}

2.6.1 FUNCTION

The first cleavage performed by 2A^{pro} is the self-processing reaction in which it cleaves between the C-terminus of VP1 and its own N-terminus (Toyoda *et al.* 1986). The reaction is carried out co-translationally and in *cis*, freeing the structural proteins from the nonstructural ones. Subsequently, 2A^{pro} cleaves the two homologues of eIF4G leading to the host-cell shut-off. Besides this most important *trans*-cleavage, 2A proteinases of different picornaviruses were shown to cleave several other cellular proteins such as poly-A binding protein (Joachims *et al.* 1999, Kerekatte *et al.* 1999), dystrophin (Badorff *et al.* 1999), cytokeratin 8 (Seipelt *et al.*

2000) and members of the nuclear pore complex protein family (NUPs) (Gustin and Sarnow 2001, Park *et al.* 2008) (Table 2-1).

Protein	Cleaved by
PABP	PV 2A ^{pro} and 3C ^{pro} ; CVB3 2A ^{pro}
Dystrophin	CVB3 2A ^{pro}
Cytokeratin 8	HRV2 2A ^{pro} ; CVB4 2A ^{pro}
NUP98	HRV2 2A ^{pro}
NUP62	HRV2 2A ^{pro}

Table 2-1 Cellular proteins cleaved by picornaviral 2A proteinases.

2.6.2 STRUCTURE

Experiments with inhibitors revealed that 2A^{pro} is a member of the cysteine proteinases (Konig and Rosenwirth 1988) and modeling led to the prediction that it has a chymotrypsin-like fold (Bazan and Fletterick 1988). Only two atomic structures of picornaviral 2A proteinases are available at present. These are the crystal structure of HRV2 2A^{pro} (Petersen *et al.* 1999) (Figure 2-11) and the NMR structure of coxsackievirus B4 2A^{pro} (Baxter *et al.* 2006). Petersen *et al.* showed that HRV2 2A^{pro} indeed has a chymotrypsin-like fold but also shows some major differences to the structure of chymotrypsin (a prototypic serine proteinase). HRV2 2A^{pro} is made up of an N-terminal and a C-terminal domain connected by an interdomain-loop. The N-terminal domain is made up of four β -strands that form a β -sheet. This is one of the major differences to the structure of chymotrypsin with its eight β -strands in the N-terminal domain. The C-terminal domain is constructed of six β -strands that form a β -barrel. This domain contains a zinc ion which is co-ordinated by the 3 sulfurs of Cys52, Cys54 and Cys112 and the nitrogen of His114. However, this zinc ion is not involved in the catalytic activity. It is more likely thought to have an important role for the integrity of the structure (Sommergruber *et al.* 1994, Voss *et al.* 1995) by compensating the truncation of the N-terminal domain. The catalytic triad is made up of Cys106 (the nucleophile), His18 (the general base) and Asp35. Mutational analysis of these residues confirmed their role in catalysis (Sommergruber *et al.* 1997).

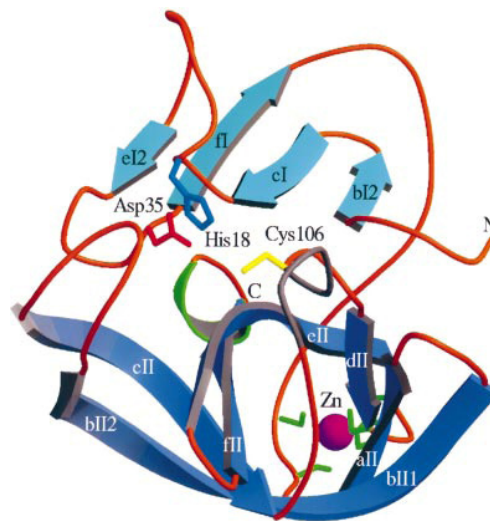


Figure 2-11 Overall structure of HRV2 2A^{pro}. The two domains are highlighted in light blue (N-terminal) and dark blue (C-terminal), respectively. The zinc ion is depicted in purple. The catalytic triad Cys106, His18 and Asp35 is rendered as stick-model (Petersen *et al.* 1999).

2.6.3 SUBSTRATE SPECIFICITY

To date, most of the work done on substrate specificity of 2A^{pro} has been performed with synthetic peptides. Only limited data is available from self-processing reactions. The only well conserved residue in HRV 2A^{pro} cleavage sites is Gly at position P1' (the nomenclature used here is the one of Berger and Schechter 1967). Consequently, peptides with Glu, Lys, Thr, Trp, Phe or Asp at P1' are not cleaved (Skern *et al.* 1991, Sommergruber *et al.* 1992) by HRV2 2A^{pro}, confirming the strong requirement for Gly at P1'. However, recently it has been shown that HRV2 2A^{pro} is able to cleave substrates with Ala at P1' in *trans* (Gustin K., pers. comm.). Another determinant of substrate specificity of HRV2 2A^{pro} is the residue at P2'. Peptides with Phe, Thr, Asp or Lys at P2' were cleaved about 2-5 fold less efficiently by HRV2 2A^{pro} than peptides with the wild-type proline (Sommergruber *et al.* 1992).

At the C-terminal end of VP1, the residues at P2 and P4 play an important role in substrate specificity. Experiments with peptides show that HRV2 2A^{pro} has a strong preference for Thr at P2. All peptides with differing residues at P2 were poorly recognized or not cleaved at all (Sommergruber *et al.* 1992). A substrate binding model by Petersen *et al.* (Figure 2-12A) may give an explanation for these results (Petersen *et al.* 1999). Threonine at P2 was found to form a hydrogen bond with Ser83. However, Tyr85 is found to stack on His18 and would have to rotate away from this stacked position in order to allow substrate binding (Figure 2-12B).

The formation of the hydrogen bond between threonine at P2 and Ser83 is thought to compensate for this rotation. The model also suggests that the narrowness and hydrophobicity of the S4 site is responsible for the preference for flexible hydrophobic residues at P4 (Figure 2-12A). At position P1, a number of residues can be accepted by HRV2 2A^{pro}. Met or Tyr at P1 even enhance the efficiency of cleavage. Peptides with Arg at P1 were processed with a relative efficiency of 0.56 with respect to a peptide corresponding to the wt cleavage site. This correlates well with the acceptance of the cleavage site TLSTR*GPPR found on eIF4GI. Recently, it was shown that this cleavage site can also be processed in the self-processing reaction by HRV2 2A^{pro} with only slight delays in kinetics (Sousa *et al.* 2006).

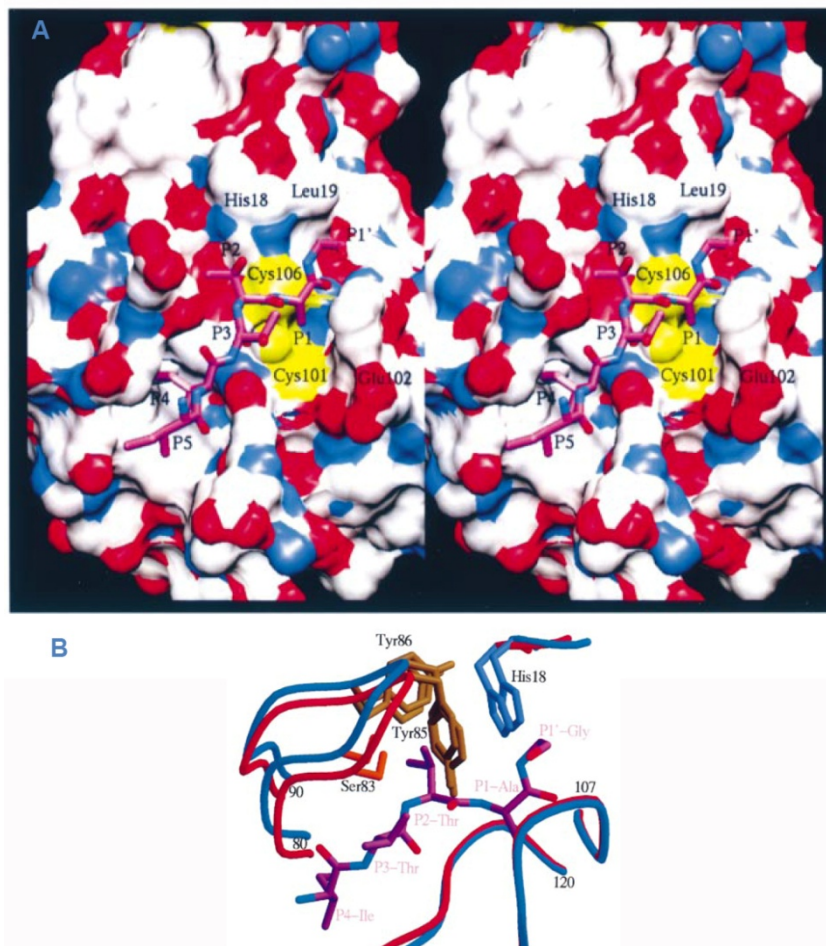


Figure 2-12 HRV2 2A^{pro} substrate binding model. A peptide representing the self-processing substrate from P5-P1' (IITTA*G) has been modeled into the substrate binding cleft of the HRV2 2A^{pro} structure. **(A)** Stereo drawing of the model. The enzyme is represented with its surface colored by atom type. Residues 82-89 have been removed to enable a better view on the substrate (pink stick model). **(B)** Recognition of the P2 residue. Both molecules in the structure are shown by a superimposition on each other. Threonine at P2 is able to form a hydrogen bond with Ser83. Tyr85 clashes with threonine at P2 and has to be rotated in order to allow substrate binding (Petersen *et al.* 1999).

Less is known about the specificity of HRV14 2A^{pro}. Experiments with recombinant HRV14 2A^{pro} and peptides revealed that HRV14 2A^{pro} accepts a peptide resembling its own polyprotein cleavage site very poorly. Interestingly, introduction of Pro at P2 improved the efficiency by more than tenfold. Furthermore, a peptide corresponding to the HRV2 2A^{pro} wild-type cleavage site was accepted even better (Wang *et al.* 1998). In contrast to HRV2 2A^{pro}, HRV14 2A^{pro} cannot process the eIF4GI site in *cis* (Sousa *et al.* 2006). Site directed mutagenesis showed that Arg at P1 is one of the residues preventing the HRV14 2A^{pro} from processing this site. Mutating Ala 104 to Cys or Ser was sufficient to restore some activity, but not to wild-type levels.

2.7 L^{PRO}

The translation of the FMDV polyprotein can be initiated on two start codons separated by 84 nucleotides. Thus, the leader proteinase exists in a full length (Lab^{pro}) and a shorter version (Lb^{pro}) (Sangar *et al.* 1987). Although the two forms have been shown to have the same enzymatic activity (Medina *et al.* 1993), Lb^{pro} was the form shown to be predominantly produced in the infected cell (Cao *et al.* 1995). Therefore, the experiments described in this thesis were performed with the shorter version, Lb^{pro}.

2.7.1 FUNCTION

In the initial cleavage event of the FMDV polyprotein processing, L^{pro} frees itself from the growing polypeptide chain by cleaving between its own C-terminus and the N-terminus of VP4 (Strebel and Beck 1986). It has been shown that this reaction can be catalyzed in *cis* as well as in *trans* (Belsham *et al.* 1990, Medina *et al.* 1993, Piccione *et al.* 1995). However, Glaser *et al.* have presented data which strongly suggests that self-processing occurs in *cis* (Glaser *et al.* 2001). Subsequently L^{pro}, like 2A^{pro}, cleaves the cellular translation initiation factor eIF4G (Devaney *et al.* 1988, Kirchweiger *et al.* 1994, Gradi *et al.* 2004), therefore being responsible for the host cell shut off in FMDV infected cells. No other substrates have been identified so far. However, a recent study revealed that L^{pro} is translocated to the nucleus of infected cells and is capable of regulating the activity of nuclear factor κ B (NF- κ B) (de Los Santos *et al.* 2007).

2.7.2 STRUCTURE

Both crystal and solution structures of Lb^{pro} are available (Guarne *et al.* 1998, Cencic *et al.* 2007). The proteinase has been found to have a papain-like fold and is made up of a globular domain (Met29-Tyr183) from which a C-terminal extension (CTE) protrudes (Figure 2-13). The globular domain is divided into two sub-domains. The N-terminal sub-domain is constructed of four α -helices and two very short antiparallel β -strands. The C-terminal sub-domain consists of a mixed β -sheet that is composed of seven strands, two of them running parallel (β 3- β 4) whereas the rest is arranged antiparallel. The active site is found at the interface of the two sub-domains. The nucleophile (Cys51) is positioned at the top of helix α 1. The general base His148 lies at the opposite site of the cleft together with Asp163 that positions His148 in the correct orientation.

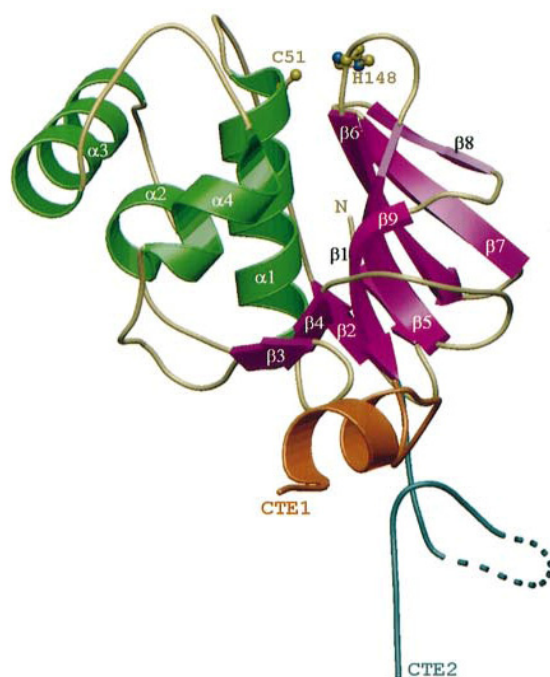


Figure 2-13 Crystal Structure of Lb^{pro} as determined by Guarné *et al.* The proteinase is made up of an N-terminal, α -helical (green) and a C-terminal, β -sheet (magenta) sub-domain. The active site (Cys51, His148) is located at the top of the inter-domain cleft. Both forms of the CTE (ordered and unordered) are depicted (CTE1 and 2).

Lb^{pro} molecules were found to form dimers in the crystal structure. The CTE of one molecule can be found in the active site of the other molecule and *vice versa*. In all four dimers

in the asymmetric unit always one CTE is fully ordered whereas the other one contains unordered residues that could not be traced in the electron density map (Glu186-Glu191). Dimerization was also found in the solution structure of Lb^{pro} (Cencic *et al.* 2007). Neither increasing the ionic strength (2M NaCl) nor decreasing protein concentration to 0.35mM was sufficient to tear the two molecules apart. These findings suggest that the quaternary structure of L^{pro} under physiological conditions may be a dimer, which would be in contrast to the idea of an intramolecular reaction during self-processing. However, Glaser *et al.* presented data which strongly argue for intramolecular self-processing. Further experiments will be needed to reveal the exact mechanism of L^{pro}.

2.7.3 SUBSTRATE SPECIFICITY

L^{pro} has developed a high degree of specificity, reflected by the fact that only three substrates of L^{pro} have been determined yet. These are the L^{pro}-VP4 junction of the polyprotein (Strebel and Beck 1986) and the two isoforms of eIF4G (Kirchweger *et al.* 1994, Gradi *et al.* 2004). However, the cleavage sites found at these substrates vary strongly (Table 2-2). L^{pro} prefers lysine at P1 in the self processing reaction. The P1 lysine is found to point away from the substrate binding cleft and is sandwiched by Glu96 and Glu147 (Figure 2-14, green surfaces), enabling the formation of electrostatic interactions. Interestingly, glycine is found at P1 in the *trans*-cleavage sites in eIF4GI and II (Kirchweger *et al.* 1994, Gradi *et al.* 2004) although also lysine could be accepted in a *trans*-reaction by the leader protease (Kirchweger *et al.* 1994, Gradi *et al.* 2004).

Substrate	P-region	↓	P'-region
Lb ^{pro} -VP4 junction	QRKLK		GAGQ
eIF4G I	FANLG		RTTL
eIF4G II	LLNVG		SRRS

Table 2-2 Overview of the substrates known to be cleaved by L^{pro}.

The requirements at position P2 were shown to be more stringent. The interactions between the P2 residue and the S2 binding pocket were found to be most important for substrate binding. Only leucine or valine are accepted at this position. This can be explained by

a deep and hydrophobic S2 pocket whose architecture is very similar to that found in other papain-like proteases (Guarne *et al.* 1998). Recently, Mayer *et al.* have shown that Leu143 (Figure 2-14, pink surface) of this hydrophobic pocket is a major determinant of the specificity at this site (Mayer *et al.* 2008). Widening of the pocket by mutating Leu143 to alanine rendered the protease able to accept phenylalanine at P2. The side-chain at P3 is pointing away from the substrate cleft and is not found to interact with the enzyme. Therefore, it is not surprising that asparagine can be accepted in the *trans*-reactions while during self-processing a lysine is found at this position. However, Kuehnel *et al.* have shown that aspartic acid at P3 is badly recognized by the leader proteinase in *cis* (Kuehnel *et al.* 2004). Also the residues found at P1' vary with *cis* or *trans*-cleavage. Glycine is found at the intramolecular cleavage site whereas arginine and serine are found on the eIF4G cleavage sites. Finally, it should be mentioned that it has been found that the CTE is involved in substrate specificity. Cencic *et al.* have shown that a leader protease with shortened CTE was not able to recognize a substrate in *trans* that was cleaved by the wild-type enzyme indicating that at least some of the residues of the CTE contribute to substrate recognition. The reason for the different substrate specificity of the shortened form may be due to its inability to form a dimer.

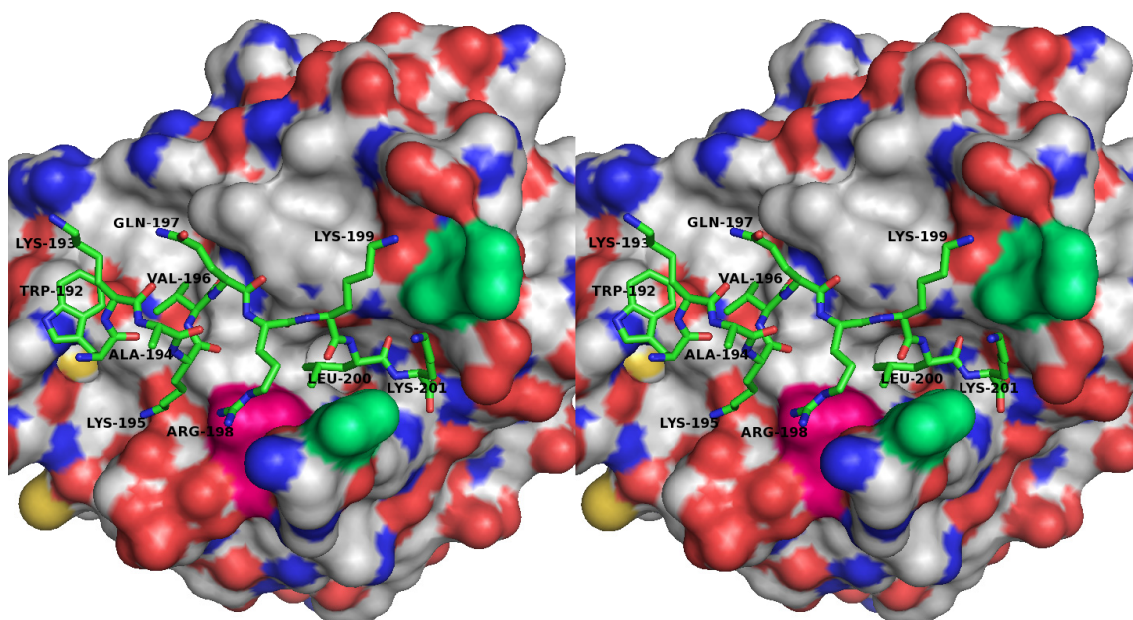


Figure 2-14 Stereo view of the Lb^{pro} substrate binding cleft with the CTE of the neighboring molecule bound. The surface of the enzyme is colored by element type with the exceptions of Glu96 and Glu147 (green) and Leu143 (pink) (generated with PyMOL (DeLano 2002)).

2.8 AIMS

Investigating protease substrate specificities plays an important role in the design of new protease inhibitors which have been shown to be promising agents for the development of anti-viral compounds. This thesis therefore analyzes substrate specificities of the two picornaviral proteinases 2A^{pro} of HRV2 and HRV14 as well as Lb^{pro} of FMDV.

2A^{pro} of HRV2 was shown to not accept the cleavage site found at the VP1-2A^{pro} junction of HRV14 (Schertler 2008). Therefore, we set out to investigate which of the HRV14 cleavage site residues are discriminated by HRV2 2A^{pro}. Subsequently, residues of the substrate binding cleft that are responsible for this discrimination should be identified. Furthermore, we tried to determine why only glycine can be accepted at P1' in the self-processing reaction while substrates with alanine at P1' can be cleaved in *trans* by HRV2 2A^{pro}. In another set of experiments, we intended to examine a hinge region at which the N-terminus is possibly rotated into the active site during self-processing. This mechanism has been proposed by Petersen *et al.* based on the structure of HRV2 2A^{pro} (Petersen *et al.* 1999) but has not been confirmed by biochemical methods at present.

Another aim was the construction of an active 2A^{pro} hybrid consisting of the N-terminal domain of HRV14 and the C-terminal domain of HRV2. This hybrid proteinase was thought to help to understand differences between the 2A proteinases of HRV2 and HRV14 and to examine possible mechanistic differences. Finally, the influence of the protein 2B on 2A^{pro} self-processing should be investigated.

Lb^{pro} is not able to accept phenylalanine in the S2 pocket. Leu143 was shown to be responsible for this discrimination (Mayer *et al.* 2008). Leu143 is not completely conserved amongst all FMDV serotypes, as also methionine is found at position 143. Therefore, we set out to investigate whether methionine at position 143 executes the same function in discriminating between phenylalanine and leucine.

3 MATERIAL & METHODS

3.1 PLASMIDS

The wild type plasmids pCITE HRV2 VP1-2A^{pro} and pCITE HRV14 VP1-2A^{pro} were kindly provided by Carla Sousa; pCITE Lb^{pro}-VP4-VP2 was obtained from Regina Cencic. The sequences coding for VP1-2A^{pro} and Lb^{pro}-VP4-VP2 are cloned into the plasmid pCITE (Novagen) downstream the internal ribosomal entry site (IRES) of the encephalomyocarditis virus (EMCV).

pCITE HRV2 VP1-2A^{pro} has been described (Glaser *et al.* 2003) and contains all but the first six basespairs of VP1 and the entire sequence coding for 2A^{pro} followed by two stop codons. The sequence contains an *MfeI* site 29bp upstream the VP1-2A^{pro} junction and a *BstEII* site 30bp downstream the junction which can be used for cassette cloning (Figure 3-1A).

pCITE HRV14 VP1-2A^{pro} contains the sequences for the entire VP1 and 2A^{pro} also followed by two stop codons (Sousa *et al.* 2006). An *AgeI* site in VP1 and a *SacII* site in 2A^{pro} have been introduced to enable proper cassette cloning (Figure 3-1B).

For the construction of pCITE HRV2 VP1-2A^{pro}-2B a 1610bp fragment was amplified from an HRV2 full length clone (fwd. Primer: TIM550; rev. Primer: TIM1637). The fragment contains VP1-2A^{pro}-2B followed by two stop codons and a *BamHI* restriction site. An *AgeI/BamHI* fragment of the amplified product was then cloned into pCITE HRV2 VP1-2A^{pro} (Figure 3-1C).

pCITE HRV14 VP1-2A^{pro}-2B was prepared in a similar way. A fragment containing 2A^{pro}-2B cDNA followed by two stop codons and a *BamHI* restriction site was amplified with the primers TIM1312 and TIM1650 from an HRV14 full length clone. The fragment and pCITE HRV14 VP1-2A^{pro} were prepared by digestion with *NsiI* and *BamHI* and ligated to give the plasmid pCITE VP1-2A^{pro}-2B (Figure 3-1D).

The construction of the plasmid for an HRV14/2 hybrid 2A^{pro} required introduction of an *MfeI* site into the plasmids pCITE HRV2 VP1-2A^{pro} and pCITE HRV14 VP1-2A^{pro} (TIM1618-TIM1621). A 290bp *MfeI/BamHI* fragment of pCITE HRV2 VP1-2A^{pro} was then used to exchange the corresponding fragment of pCITE HRV14 VP1-2A^{pro} (Figure 3-1E)

The plasmid pCITE Lb^{pro}-VP4-VP2 has been described (Glaser *et al.* 2001). It contains nucleotides 892-1896 from FMDV O1_k followed by two stop codons. The viral cDNA codes for the entire Lb^{pro} including three additional N-terminal amino acids, all 85 amino acids of VP4 and 78 amino acids of VP2. Cleavage sites can be modified by the exchange of a 38bp *Bpu10I/SacI* fragment in this plasmid (Figure 3-1F).

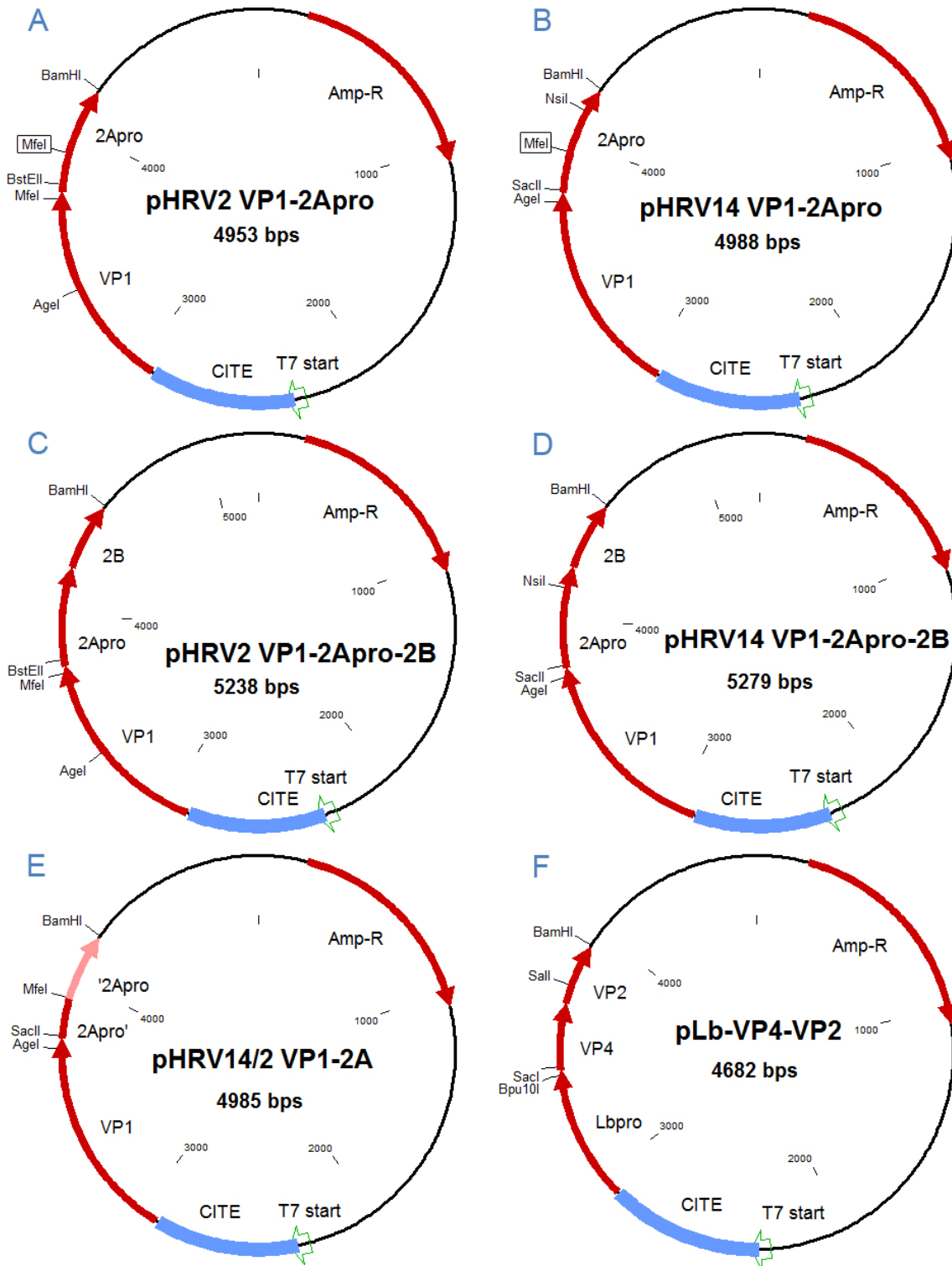


Figure 3-1 Schematic representations of the plasmids used in this thesis. Relevant restriction sites are listed. *MfeI* sites that are framed in **(A)** and **(B)** were introduced for the construction of the 2A^{pro} hybrid **(E)** but are not present in the wild-type plasmid.

A T7 promoter precedes the CITE and enables the *in vitro* transcription of mRNA by T7 RNA polymerase. The mRNAs contain the IRES in the 5' UTR enabling proper initiation of translation. An ampicillin resistance gene allows screening for bacterial clones that carry the plasmid.

3.2 OLIGONUCLEOTIDES

All oligonucleotides were purchased from VBC-Biotech Service GmbH, Vienna.

ID	Length	Sequence (5'→3')	Purpose
TIM1536	52	CCGGTAATTAAGAAGAGGAAAGGT ATTATCACTACAGCTGGCCGAGTC CGC	Introduction of the cleavage site IITTA*GPSP into pCITE HRV14/2 VP1-2A ^{pro} .
TIM1537	46	GGA CT CGGGCCAGCTGTAGTGATA ATACCTTTCCTCTCTTAATTA	
TIM1573	59	AATTGTGACCAGACCAATTATCACT ACAGCTGGCCTGGGCCCAATGTATG TTCATGTAG	Introduction of the cleavage site IITTA*GLGP into pCITE HRV2 VP1- 2A ^{pro} .
TIM1574	60	GTTACCTACATGAACATACATTGGG CCCAGGCCAGCTGTAGTGATAATTG GTCTGGTCAC	
TIM1590	59	AATTGTGACCAGACCAATTATCAAA TCATATGGCCCCAGTGACATGTATG TTCATGTAG	Introduction of the cleavage site IIKSY*GPSD into pCITE HRV2 VP1- 2A ^{pro} .
TIM1591	60	GTTACCTACATGAACATACATGTCA CTGGGGCCATATGATTTGATAATTG GTCTGGTCAC	
TIM1601	29	GGGCCCCGACCTAGGTATGGTGG GGTAG	Introduction of the cleavage site IITTA*GPGPRYGGVG into pCITE HRV2 VP1-2A ^{pro} .
TIM1602	36	GTTACCTACCCACCATACCTAGGT CCGGGGCCCGC	
TIM1603	29	GGGCCCAGTGACAGGTATGGTGG GATTG	Introduction of the cleavage site IITTA*GPSDRYGGI into pCITE HRV2 VP1-2A ^{pro} .
TIM1604	36	GTTACCAATCCCACCATACCTGTAC TCGGGGCCCGC	
TIM1605	29	GGGCCCAGTCCCATGTATGTTCA GTAG	Introduction of the cleavage site IITTA*GPSP into pCITE HRV2 VP1- 2A ^{pro} .
TIM1606	36	GTTACCTACATGAACATACATGGGA CTCGGGCCCGC	
TIM1642	29	GGGCCCAGTGACAGGTATGTTCA TG TAG	Introduction of the cleavage site IITTA*GPSDR into pCITE HRV2 VP1- 2A ^{pro} .
TIM1643	36	GTTACCTACATGAACATACCTGTCA CTCGGGCCCGC	

ID	Length	Sequence (5'→3')	Purpose
TIM1644	29	GGCCCCAGTGACATGTACGTACATGTAG	Introduction of the cleavage site IITTA*APSD into pCITE HRV2 VP1-2A ^{pro} .
TIM1645	36	GTTACCTACATGTACGTACATGTCACTGGGGGCCGC	
TIM1646	29	GGGCGCGAGTGACATGTACGTACATGTAG	Introduction of the cleavage site IITTA*GASD into pCITE HRV2 VP1-2A ^{pro} .
TIM1647	36	GTTACCTACATGTACGTACATGTCACTCGCGCCCGC	
TIM1648	59	AATTGTGACCAGACCAATTATCAAA TCATATGGCGCGAGTGACATGTACGTACATGTAG	Introduction of the cleavage site IIKSY*GASD into pCITE HRV2 VP1-2A ^{pro} .
TIM1649	60	GTTACCTACATGTACGTACATGTCACTCGGCCATATGATTTGATAATTG GTCTGGTCAC	
TIM1659	59	AATTGTGACCAGACCAATTATCACT TCATATGGCCTGAGTGACATGTATGTTTCATGTAG	Introduction of the cleavage site IITSY*GLSD into pCITE HRV2 VP1-2A ^{pro} .
TIM1660	60	GTTACCTACATGAACATACATGTCACTCAGGCCATATGAAGTGATAATTG GTCTGGTCAC	

Table 3-1 Oligonucleotides used for cassette-cloning.

ID	Length	Sequence (5'→3')	Purpose
TIM1599	21	ATCACTACCGCGGGCCCCAGT	Introduction of a <i>SacII</i> restriction site into pCITE HRV2 VP1-2A ^{pro} .
TIM1600	21	ACTGGGGCCCGCGGTAGTGAT	
TIM1607	27	AAATCATATGGCTTAAGTGACATGTAT	Introduction of the mutation P2L (2A ^{pro}) into pCITE HRV2 VP1-2A ^{pro} IIKSY*GPSD.
TIM1608	27	ATACATGTCACTTAAGCCATATGATTT	
TIM1609	27	TCATATGGCCCCGGGGACATGTATGTT	Introduction of the mutation S3G (2A ^{pro}) into pCITE HRV2 VP1-2A ^{pro} IIKSY*GPSD.
TIM1610	27	AACATACATGTCCCCGGGGCCATATGA	
TIM1611	27	TATGGCCCCAGTCCAATGTATGTTCAT	Introduction of the mutation D4P (2A ^{pro}) into pCITE HRV2 VP1-2A ^{pro} IIKSY*GPSD.
TIM1612	27	ATGAACATACATTGGACTGGGGCCATA	
TIM1618	27	ATACCACACTGCAATTGTACATCAGGT	Introduction of an <i>MfeI</i> restriction site into pCITE HRV14 VP1-2A ^{pro} .
TIM1619	27	ACCTGATGTACAATTGCAGTGTGGTAT	
TIM1620	27	CATTCCCTCTTGCAATTGTACCCAAGC	Introduction of an <i>MfeI</i> restriction site into pCITE HRV2 VP1-2A ^{pro} .
TIM1621	27	GCTTGGGTACAATTGCAAGAGGGATG	

ID	Length	Sequence (5'→3')	Purpose
TIM1623	27	GCTGGCATTTCATGAAGGGGCAA GAA	Introduction of the mutation L143M (Lb ^{pro}) into pCITE Lb ^{pro} -VP4-VP2.
TIM1624	27	TTCTTGCCCCTTCATGAAAATGCCA GC	
TIM1627	36	GGGGATCCAAGCCTATCATTGTCTT TCATTGTAAGG	Amplification of 2B including two stop codons and a <i>Bam</i> HI restriction site from an HRV14 full length clone. Erroneous primer that gives rise to the mutation I94N in 2B. Amplification of 2B including two stop codons and a <i>Bam</i> HI restriction site from an HRV14 full length clone.
TIM1650	39	CCGGGGGATCCAAGCCTATCATTGT CTTCAATGTAAGG	
TIM1637	42	AGCCCGGGGGATCCAAGCCTATCAT TCTTTGTGTATATAATT	Amplification of 2B including two stop codons and a <i>Bam</i> HI restriction site from an HRV2 full length clone.
TIM550	18	GGACGTGGTTTTTCCTTTG	
TIM1638	27	AATGTTAAAATAAGGAATTACCACT TG	Introduction of the mutation M17R (2A ^{pro}) into pCITE HRV14 VP1-2A ^{pro} .
TIM1639	27	CAAGTGGTAATTCCTTATTTTAACAT T	
TIM1640	27	AACCTTATTTATATGAATCTTCATCT T	Introduction of the mutation R15M (2A ^{pro}) into pCITE HRV2 VP1-2A ^{pro} IIKSY*GLSD.
TIM1641	27	AAGATGAAGATTCATATAAATAAG GTT	
TIM1651	27	GACTGTGGTGGGAATATTGCTATGCA AA	Introduction of the mutation K109I (2A ^{pro}) into pCITE HRV2 VP1-2A ^{pro} IITTA*GPSDR.
TIM1652	27	TTTGCATAGCAATATTCACCACAG TC	
TIM1653	27	GACTGCGGTGGGAAGTTGAGATGC ATA	Introduction of the mutation I112K (2A ^{pro}) into pCITE HRV14 VP1-2A ^{pro} .
TIM1654	27	TATGCATCTCAACTTCCCACCGCAGT C	
TIM1665	27	AGAAATCTTCATGCTTCAACTCTGA G	Introduction of the mutation L19A (2A ^{pro}) into pCITE HRV2 VP1-2A ^{pro} IITTA*APSD.
TIM1666	27	CTCAGAGTTGAAAGCATGAAGATTT CT	

Table 3-2 Primers used for site directed mutagenesis via PCR.

ID	Length	Sequence (5'→3')	Purpose
TIM20	16	GCTAAACATGTCAAGG	Forward sequencing primer for the HRV2 VP1-2A ^{pro} junction.
TIM1334	18	ATACATCAAGGTTTAGTG	Forward sequencing primer for the HRV14 VP1-2A ^{pro} junction.

ID	Length	Sequence (5'→3')	Purpose
TIM550	18	GGACGTGGTTTTTCCTTG	Forward sequencing primer for HRV2 and HRV14 VP1 and FMDV Lb ^{pro} .
TIM554	18	ATTTAGGTGACACTATAG	Reverse sequencing primer for HRV2 and HRV14 2A ^{pro} and FMDV VP2/VP4.

Table 3-3 Primers used for sequencing.

3.3 DNA METHODS

3.3.1 AGAROSE GEL ELECTROPHORESIS

Agarose gel electrophoresis was used throughout the cloning experiments to monitor the process. 1% agarose (Invitrogen) in 0.5x TAE-Buffer was used as a standard concentration. For the separation of smaller fragments, agarose concentration was raised up to 1.2%. An appropriate amount of 10x loading buffer was added to the samples before loading on the gel. 1µg of *HindIII* digested λ-DNA was used as a size marker. Electrophoresis was carried out in 0.5x TAE-Buffer at 80-110 Volts. Subsequently gels were soaked in ethidiumbromide solution for 15-30 minutes before being photographed on a UV trans-illuminator.

0.5x TAE-Buffer: 20mM Tris base, 5mM Sodiumacetate, 1mM EDTA.
 10x Loading Buffer: 1mM EDTA, 0.1% Orange G, 10% Ficoll in 0.5x TAE-Buffer
 Ethidiumbromide: 10⁻⁴% Ethidiumbromide in 0.5x TAE-Buffer

3.3.2 DNA RESTRICTION REACTIONS

Analytical digestions were typically performed in a total volume of 20µl. Restriction enzymes and associated buffers were delivered by NewEngland BioLabs. Samples were mixed well and incubated at the appropriate temperature for 1-3 hours.

x	µl	DNA
2	µl	NE Buffer (1-4)
0.3	µl	Enzyme
y	µl	H ₂ O MILI Q
20	µl	

Vectors for ligations were prepared in a total volume of 100 μ l. The amount of enzyme varied from 0.5 to 1.0 μ l. Again, the incubation was carried out at the adequate temperature for 2-14 hours.

x	μ l	DNA
10	μ l	NE Buffer (1-4)
0.5-1.0	μ l	Enzyme
<u>y</u>	<u>μl</u>	H ₂ O MILI Q
100	μ l	

3.3.3 DEPHOSPHORYLATION OF DNA 5' ENDS

Dephosphorylation was preceded by phenol-chloroform extraction followed by precipitation with 3M sodium acetate and absolute ethanol. The dry pellet was resuspended in 48.5 μ l H₂O MILI Q and 1 μ l of calf intestine alkaline phosphatase (CIP) (NewEngland BioLabs, 10u/ μ l) and 0.5 μ l 2M Tris-HCl (pH 8.0) were added. Samples were incubated at 37°C for 45 minutes followed by another 45 minutes at 65°C.

CIP is able to dephosphorylate the 5' ends of DNA and prevents vectors from re-ligation. Therefore, dephosphorylation is used to minimize the background in the cloning experiments.

3.3.4 KINASING AND ANNEALING OF OLIGONUCLEOTIDES

5'-phosphorylation of oligonucleotides was carried out using the enzyme T4 polynucleotide kinase (PNK) (NewEngland BioLabs, 10u/ μ l). The enzyme catalyzes the transfer of the γ -phosphate of ATP to the 5'-OH of DNA, RNA or oligonucleotides to prepare an insert for ligation with a cloning vector. The reaction was carried out in a total volume of 20 μ l.

2	μ l	100mM ATP
2	μ l	10x PNK Buffer
1	μ l	TIM XXXX (1 μ g/ μ l)
1	μ l	TIM XXXX (1 μ g/ μ l)
1	μ l	T4 PNK (NewEngland BioLabs, 10u/ μ l)
<u>13</u>	<u>μl</u>	H ₂ O MILI Q
20	μ l	

A thermocycler with a temperature program of 37°C / 30min; 90°C / 30sec; 37°C / 5min was used to incubate the samples and anneal the two oligonucleotides. Alternatively a program of 37° / 30min; 65°C / 10min; RT / 3hrs; 4°C / 4hrs was used.

3.3.5 LIGATION OF DNA MOLECULES

1µl of vector was loaded on an agarose gel to estimate the concentration of the DNA solution prior ligation. About 50ng of vector and 1µl of phosphorylation mix were incubated with 2µl 10x ligase buffer and 0.5µl T4-DNA-ligase (Promega, 3u/µl) in a total volume of 20µl at room temperature over night. Additional mixes with either no ligase or no insert served as negative controls.

3.3.6 PHENOL-CHLOROFORM EXTRACTION

In order to purify DNA, phenol-chloroform extraction followed by precipitation with sodium acetate and ethanol was used as a standard method. 3µl 0.5M EDTA (pH 8) per 100µl DNA solution were added followed by a 1x volume of phenol (containing 0.1% 8-hydroxyquinolin and equilibrated with 50mM Tris/HCl pH8). Samples were vortexed briefly and centrifuged for 1 minute at 13.000 rpm. The aqueous phase was transferred into a new tube and mixed with a 1x volume of chloroform. Vortexing, centrifuging and transfer of the aqueous phase was repeated as above.

3.3.7 PRECIPITATION OF DNA

Samples were mixed with 1/10 volume of 3M sodium acetate followed by 2 volumes of absolute ethanol. DNA was precipitated at -80°C for 15 minutes and centrifuged for 15 minutes at 14.000 rpm and 4°C. The supernatant was carefully removed and the pellet was dried on air for 30-60 minutes to remove any traces of ethanol. DNA was then redissolved in an appropriate volume of H₂O MILI Q.

3.3.8 PURIFICATION BY COLUMN

Alternatively, DNA was purified via an anion exchange mini column of the “Wizard® SV Gel and PCR Clean up System” by Promega. DNA was eluted from the column with an adequate volume of H₂O MILI Q.

3.3.9 EXTRACTION OF DNA FROM AGAROSE GELS

Bands were cut out under UV light and DNA was isolated from the gel by the use of the “Wizard® SV Gel and PCR Clean up System” by Promega. DNA was eluted from the column with an appropriate amount of H₂O MILI Q.

3.3.10 INTRODUCTION OF MUTATIONS BY STANDARD PCR TECHNIQUES

PCR with mutated primers was used to introduce mutations of one to a few basepairs. Complementary primers that carry the mutated site were designed and used in a PCR reaction with a proofreading polymerase. The 9-12 basepairs long regions flanking the mutated site allow proper hybridization of the primer with the template and therefore introduction of the mutation. The PCR product is then transformed into TOP 10F' cells which fix the gaps and create regular plasmids. A standard mix for this method contained:

0.5	μl	Template DNA
1	μl	Primer fwd (1μg/μl)
1	μl	Primer rev (1μg/μl)
4	μl	dNTP's (2.5mM) (GE Healthcare)
5	μl	10x Pfu Buffer (Promega)
1	μl	Pfu Polymerase (Promega, 3u/μl)
<u>38.5</u>	<u>μl</u>	H ₂ O MILI Q
50	μl	

Mixes lacking primers were used as a negative control. PCR was performed on a Perkin Elmer DNA Thermal Cycler 480 with a temperature program of:

95°C	2min	
95°C	30sec	
annealing Temperature	1min	30x
68°C	10min	
4°C	∞	

Annealing temperature was originally chosen 5-10°C below the calculated melting temperature of the primers and was adjusted in case of an unsatisfactory product. 10µl of the PCR mix were loaded on an agarose gel to check the quality of the product. The remaining 40µl were mixed with 4.5µl NE-Buffer 4 and 1µl of *DpnI* and incubated at 37°C for 5 hours. *DpnI* requires methylation of the adenines in its recognition sequence allowing specific digestion of the template DNA. 10µl of this mix were then transformed into TOP 10F' cells (see 3.4.2).

3.3.11 MANIPULATION OF CLEAVAGE SITES BY CASSETTE CLONING

Cassette cloning was chosen as the standard mutagenesis method to introduce a number of mutations at once. Oligonucleotides were delivered by VBC biotech (see 3.2). Two complementary oligonucleotides were 5'-phosphorylated and annealed (see 3.3.4) to form an insert with the correct sticky ends. Vectors were created by digestion with the appropriate restriction enzymes (see 3.3.2), dephosphorylated (see 3.3.3) and purified by gel extraction (see 3.3.9). Vector and insert were then ligated (see 3.3.5) and transformed into *E. coli* (strain TOP 10F') (see 3.4.2).

3.4 BACTERIAL CULTURES

3.4.1 PREPARATION OF COMPETENT CELLS

Both the TOP 10F' strain as well as the DH5α strain of *E. coli* were used for cloning experiments. Cells were made competent by using the CaCl₂ method. A starter culture was set up by inoculation of 3ml LB-Medium and shaking at 37°C over night. On the following day, 200ml LB-Medium were inoculated with the starter culture and grown at 37°C for 2-4 hours until an optical density of 0.4-0.5 was reached. Harvesting of cells was carried out by centrifugation in sterile Falcon-tubes at 5.000 rpm for 5 min in a swinging bucket (4°C). After harvesting, cells were constantly kept at 4°C. The bacterial pellet was resuspended in 25ml ice-cold 0.1M CaCl₂ solution and incubated on ice for 25min. Centrifugation was repeated, the pellet again resuspended in 10ml 0.1M CaCl₂ solution and incubated at 4°C over night. The

next day, the suspension was mixed gently with 2ml sterile glycerol, portioned into 200µl aliquots and frozen in liquid nitrogen. Competent cells were stored at -80°C.

LB-Medium: 1% Bacto-Trypton, 0.5% Yeast-Extract, 10mM Tris/HCl pH 7.5, 170mM NaCl
LB-Amp-Medium: contains 100mg/L Ampicillin

3.4.2 TRANSFORMATION

E. coli of the strains TOP 10F' and DH5α were used for transformation in the cloning experiments. A 200µl aliquot of competent cells per transformation was thawed and kept on ice for 10 minutes. Addition of 10µl ligation or PCR mutagenesis mix was followed by incubation for 15 minutes on ice. Samples were then heat shocked at 42°C for 30-60 seconds, transferred on ice again and mixed with 400µl preheated (37°C) LB-medium. After incubation at 37°C for 20-30 minutes, 150µl were plated on LB-Amp Agar-Agar plates. The remaining bacteria was spun down at 8.000 rpm for 20 seconds followed by the removal of all but about 100µl medium. Bacteria were resuspended in the remaining medium and plated on a separate LB-Amp Agar-Agar plate. Plates were incubated at 37°C over night to allow bacteria to form colonies.

LB-Amp Agar-Agar plates: Add 1.5% Agar-Agar to LB-Medium. Autoclave at 120°C for 20 minutes. Let cool down, add ampicillin (100mg/L) and pour plates.

3.4.3 DNA MINI PREPS

Small scale DNA preparations (MINI preps) from transformed *E. coli* were used to screen for positive mutants by digesting DNA with restriction enzymes. MINI preps purified by phenol-chloroform extraction or anion exchanger mini columns were also used for DNA-sequencing.

Colonies were picked from LB-Amp plates to inoculate 4ml of LB-Amp medium. Samples were incubated at 37°C over night in a bacterial shaker. On the next day cells were harvested in 1.5ml tubes by spinning down the solution at 6.000 rpm for 2 minutes and discarding the supernatant twice. The pellet was resuspended in 100µl Solution I and mixed gently with 200µl Solution II. After addition of 150µl Solution III, samples were again mixed

gently and centrifuged for 5 minutes at 14.000 rpm and 4°C. The supernatant was transferred to a new tube and DNA was precipitated by the addition of 1ml ice-cold absolute ethanol. Centrifugation was repeated as above and the supernatant was discarded. The DNA pellet that contains salt and RNA was then taken up in 200µl TE-Buffer. 200µl 5M LiCl were added followed by a step of centrifugation as above. Again, the supernatant was transferred to a new tube. DNA was once more precipitated with 1ml ice-cold absolute ethanol and collected by a final centrifugation as above. The supernatant was discarded and the pellet was dried on air for about 1 hour. Subsequently DNA was taken up in 50µl H₂O MILI Q and stored at -20°C.

Sol I: 50mM Tris/HCl pH 8.0, 10mM EDTA, 100µg/ml RNaseA
Sol II: 20mM NaOH, 1% SDS
Sol III: 2.8M Potassiumacetate pH 5.1
TE-Buffer: 10mM Tris/HCl pH 8.0, 1mM EDTA

3.4.4 DNA MIDI PREPS

Middle scale DNA preparations (MIDI preps) were used for preparation of larger amounts of very clean DNA for *in vitro* transcription. Both, the “Plasmid DNA Purification Kit” (Macherey-Nagel) and the “E.Z.N.A.[®] Plasmid Midi Prep Kit” (OMEGA BIO TEK) were used following the instructions of the respective company. DNA was resuspended in 200µl H₂O MILI Q and stored at -20°C.

3.5 RNA METHODS

3.5.1 IN VITRO TRANSCRIPTION

In all HRV plasmids the two stop codons at the end of 2A^{pro} are followed by a *Bam*HI restriction site. 20µl of plasmid from a MIDI prep were linearized at this site to avoid unnecessary long transcripts. In case of pCITE Lb^{pro}-VP4-VP2 this digestion was performed with *Sal*I. After checking the linearization on an agarose gel, DNA was purified via phenol-chloroform extraction and precipitated with 3M sodium acetate and absolute ethanol. The air dried pellet was resuspended in

20	μl	5x Transcription buffer (Promega)
5	μl	100mM DTT (Promega)
10	μl	2.5mM NTP mix (GE Healthcare)
3	μl	RNasin (Promega, 40u/μl)
1	μl	T7 RNA polymerase (Promega, 20u/μl)
<u>61</u>	<u>μl</u>	H ₂ O MILI Q
100	μl	

and incubated at 37°C for 90 minutes. Subsequently 0.6μl DNase I (Invitrogen, 512u/μl) were added followed by another 20 minutes of incubation at 37°C to digest the template DNA. The resulting RNA was purified via phenol-chloroform extraction (see 3.3.6) followed by precipitation with ammoniumacetate and absolute ethanol (see 3.5.2).

3.5.2 PRECIPITATION OF RNA

For precipitation, a 1/3 volume of 8M ammonium acetate and 2.5 volumes of absolute ethanol were added to the purified RNA and incubated at -80°C for 15 minutes. The RNA was then centrifuged for 15 minutes at 14.000 rpm and 4°C. The supernatant was discarded and the RNA pellet was washed with 500μl 70% ethanol. Centrifugation and discarding was repeated as above and the pellet was dried on air for about 1 hour. Subsequently, RNA was resuspended in 25μl H₂O MILI Q.

3.5.3 RNA AGAROSE GEL ELECTROPHORESIS

After *in vitro* transcription, 2μl of RNA were checked on a 1% agarose 0.1% SDS gel. Gels were washed in deionized water for 30 minutes before staining in 0.5x TAE-Buffer containing ethidiumbromide for 15-30 minutes. Subsequently, bands were visualized on a UV trans-illuminator.

3.6 PROTEIN METHODS

3.6.1 IN VITRO TRANSLATION

The ability of the viral proteases to perform self-processing was assayed by a time course *in vitro* translation. Rabbit reticulocyte lysate (RRL) was programmed with an *in vitro* transcribed mRNA coding for VP1-2A^{pro}, VP1-2A^{pro}-2B or Lb^{pro}-VP4-VP2 respectively. Aliquots of the newly synthesized viral proteins were taken at determined times, separated via SDS-PAGE and made visible by fluorography. To estimate the best amount of RNA for *in vitro* translation, a pilot reaction was performed.

3.6.1.1 PILOT REACTION

In vitro transcribed RNA was diluted 2:10, 3:10 and 4:10 to assay the best concentration for the time course experiment. For each dilution as well as for a negative control the following mix was prepared:

7	μl	RRL (Promega)
0.2	μl	1mM amino acids mix without methionine (Promega)
0.2	μl	RNasin (Promega, 40u/μl)
0.4	μl	10μM ³⁵ S methionine (1000Ci/mmol) (Hartmann Analytics)
<u>1.2</u>	<u>μl</u>	<u>H₂O MILI Q</u>
9	μl	

The mix was preheated to 30°C for 2 min before 1μl of each RNA dilution and 1μl H₂O for the negative control was added. Samples were incubated at 30°C for 20 min. Subsequently, 1μl ice-cold unlabeled methionine/cysteine mix (20mM) was added and the samples were placed on ice immediately to stop the translation. Samples were mixed with 25μl 2x Laemmli sample buffer and 15μl H₂O before being loaded on a 17.5% SDS-polyacrylamide gel (see section 3.6.2). After SDS-PAGE, gels were dried and the newly synthesized protein bands were visualized by fluorography (see 3.6.3).

2x Laemmli sample buffer: 20% Glycerol, 10% β-Mercaptoethanol, 6% SDS, 125mM Tris, 0.01% Bromophenol Blue, pH 6.8

3.6.1.2 TIME COURSE TRANSLATION

The results of the pilot reaction helped to decide on the best RNA concentration. In order to examine the *cis* cleavage of 2A^{pro} and Lb^{pro} over time, a time course translation was set up. It contained the time points of 0min, 10min, 20min, 30min, 60min, 120min, 180min and 300min for 2A^{pro}. In case of the leader protease the time points of 0min, 4min, 8min, 12min, 20min, 30min and 60min were chosen. Therefore, a x-times mastermix of the above translation mix was produced. 9µl of the mastermix were transferred into a new tube and served as a negative control. Samples were preheated to 30°C for 2 min before (x-1) µl of RNA and 1µl of water respectively were added to the tubes. Samples were incubated at 30°C. Aliquots of 10µl were taken at the given time points and put on an ice-cold mix of 1µl unlabeled methionine/cysteine (20mM), 25µl 2x Laemmli sample buffer and 15µl H₂O to stop the reaction. SDS-PAGE and fluorography served again as methods to visualize the newly synthesized viral proteins.

3.6.2 SDS POLYACRYLAMIDE GEL ELECTROPHORESIS

The SDS-polyacrylamide gelelectrophoresis system of Dasso & Jackson (Dasso and Jackson 1989) was used to analyze the translation products. This discontinuous system is made up of two gel-parts which differ in pH and are buffered with Tris-glycine. The 0.75mm thick gels were made up of a separating gel (pH 8.8) that contained 17.5% acrylamide covered by a 5% stacking gel (pH 6.8). Samples were heated to 95°C for 5 min before 10µl were loaded to the gel. Gels were run in 1x running buffer (Biorad PAGE system) at 10mA for the stacking gel and 15mA for the separation gel. ¹⁴C labeled CFA.626 (Amersham) was used as size marker.

Stacking Gel		Seperation Gel	
3.5 ml	30% Acrylamide	0.333 ml	30% Acrylamide
0.158 ml	2.5% Bisacrylamide	0.104 ml	2.5% Bisacrylamide
1.5 ml	4x Lower Gel Buffer	0.5 ml	4x Lower Gel Buffer
0.809 ml	H ₂ O	1.06 ml	H ₂ O
0.03 ml	10% Ammoniumpersulphate	0.02 ml	10% Ammoniumpersulphate
0.003 ml	TEMED	0.002 ml	TEMED

Table 3-4 Composition of SDS-Polyacrylamide gels.

4x Lower Gel Buffer:	1.5M Tris/HCl pH 8.8, 0.4% SDS
4x Upper Gel Buffer:	0.5M Tris/HCl pH 6.8, 0.4% SDS
10x Running Buffer:	500mM Tris, 3.85M Glycine, 1% SDS

3.6.3 FLUOROGRAPHY

Fluorography was used to visualize the newly synthesized and ³⁵S labeled proteins. Therefore, the gels were soaked 2x 15min in 100ml enhancing buffer, dried on a gel drier and exposed to a KODAK BioMax MR film for 20-90 hours. Films were developed on an AGFA Curix60.

Enhancing Buffer:	1M Sodiamsalicylate, 45% Methanol
-------------------	-----------------------------------

4 RESULTS

An *in vitro* system was used to investigate the *cis*-cleavage of the viral proteases on different cleavage sites. The viral genes of interest were cloned downstream of the EMCV IRES of the plasmid pCITE. The restriction sites *MfeI* and *BstEII* as well as *AgeI* and *SacII* respectively were used to modify the cleavage sites at the HRV2 and HRV14 VP1-2A^{pro} junctions by cassette cloning. In the plasmid pCITE Lb^{pro}-VP4-VP2 the cleavage site was modified by exchanging a *Bpu10I/SacI* fragment (see section 1.1). Mutations at positions lying apart of these cassettes were introduced by the use of standard PCR-techniques (see section 3.3.10). Plasmids were linearized by *BamHI* or *Sall* digestion prior *in vitro* transcription from the T7-start (see section 3.5.1). The mRNA obtained was then used for *in vitro* translation in RRL's. Proteins were labeled by the use of ³⁵S-Met. Aliquots were taken at specific time points of the reaction (see section 3.6.1). Proteins were then separated by SDS-PAGE and visualized by fluorography (see sections 3.6.2 and 3.6.3)

4.1 CLEAVAGE OF WILD-TYPE SUBSTRATES BY HRV2 AND HRV14 2A^{PRO}

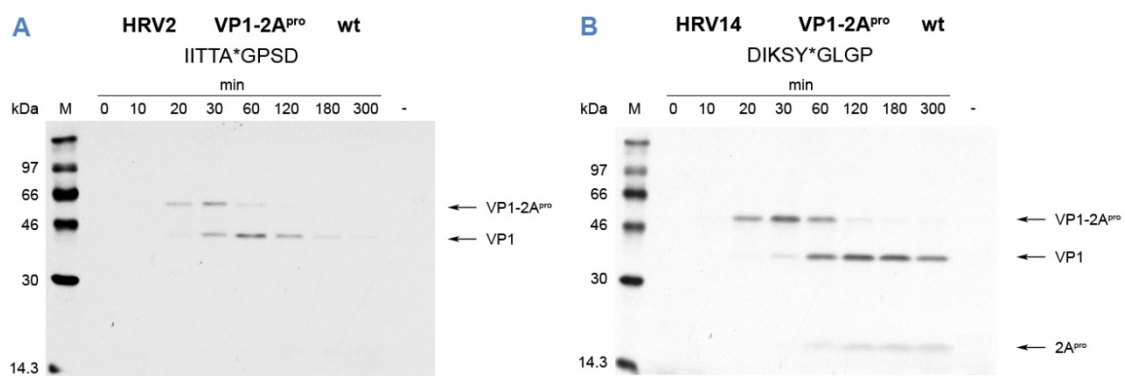


Figure 4-1 Self-processing of **(A)** HRV2 and **(B)** HRV14 2A^{pro} on the respective wild-type cleavage sites. Rabbit reticulocyte lysate was programmed with RNA coding for VP1-2A^{pro} (10ng/ μ l) and incubated at 30°C. Negative controls were prepared by adding water instead of RNA. 10 μ l aliquots were taken at the given time points and put on an icecold mix of 25 μ l 2x Laemmli sample buffer, 15 μ l H₂O and 1 μ l unlabeled methionine/cysteine (20mM). Viral proteins were then separated by SDS-PAGE on 17.5% gels and visualized by fluorography. Protein standards (M) in kDa are given on the left.

The kinetics of *cis*-cleavage by wild-type HRV2 and HRV14 2A^{pro} on their respective wild-type cleavage sites are very similar. For HRV2 2A^{pro}, the first cleavage products could be detected after 20 minutes and 50% of the precursor was cleaved after about 30 minutes

(Figure 4-1A). HRV14 2A^{PRO} performs this *cis* reaction slightly slower (Figure 4-1B). The first cleavage products were not detected before 30 minutes after start of translation and 50% of conversion was reached between 30 and 60 minutes. HRV2 2A^{PRO} could not be detected due to low sensitivity. In HRV2, VP1 contains seven methionine residues whereas 2A^{PRO} only contains two. 2A^{PRO} of HRV14 is generally easier to detect as it contains three methionine residues and only five methionines are found in VP1.

4.2 HRV2 2A^{PRO} CANNOT ACCEPT THE VP1-2A^{PRO} CLEAVAGE SITE OF HRV14

Recently, it has been shown that HRV2 2A^{PRO} is not able to accept the cleavage site of HRV14 (AspIleLysSerTyr*GlyLeuGlyPro) at the VP1-2A^{PRO} junction in *cis* (Schertler 2008). In our first experiment we were able to reproduce this finding (Figure 4-2A). No cleavage products could be detected, even at 300 minutes after start of translation. We set out to investigate which of these residues were responsible for this discrimination. Therefore, a number of HRV2 VP1-2A^{PRO} mutants with different combinations of cleavage sites was produced and tested for their ability to perform self-processing. Finally, residue 15 in HRV2 2A^{PRO} and residue 17 in HRV14 2A^{PRO} located in a putative S2' pocket were mutated to investigate their influence in recognizing the residue at P2'. Table 4-1 gives an outline of all mutants described in this section. Each of them will be discussed in detail below.

Serotype	VP1 ↓	2A ^{PRO}	Additional mutations	Figure
HRV2	<u>DI</u> KSY	<u>GL</u> GP		Figure 4-2A
HRV2	I I <u>TTA</u>	GP <u>SP</u>		Figure 4-2B
HRV2	I I <u>TTA</u>	<u>GL</u> GP		Figure 4-2C
HRV2	I I <u>KSY</u>	GP <u>SD</u>		Figure 4-2D
HRV2	I I <u>KSY</u>	GP <u>SP</u>		Figure 4-3A
HRV2	I I <u>KSY</u>	GP <u>GD</u>		Figure 4-3B
HRV2	I I <u>KSY</u>	<u>GL</u> SD		Figure 4-3C
HRV2	I I <u>TSY</u>	<u>GL</u> SD		Figure 4-3D
HRV2	I I <u>KSY</u>	<u>GL</u> SD	2A ^{PRO} : R15M	Figure 4-5A
HRV14	DIKSY	GLGP	2A ^{PRO} : M17R	Figure 4-5B

Table 4-1 Overview of the HRV2 and HRV14 VP1-2A^{PRO} mutants described in section 4.2. Residues at the VP1-2A^{PRO} junction are listed. Underlined residues in the HRV2 mutants differ from the wild-type sequence and are found at equivalent positions at the HRV14 VP1-2A^{PRO} junction. Time course translations of each mutant can be found in the figures listed on the right.

A major difference between the P' regions of HRV2 and HRV14 is the presence of the negatively charged residue aspartic acid at P4' in HRV2 and the hydrophobic amino acid proline at P4' in HRV14. Therefore, we wanted to investigate if the single mutation D4P in HRV2 2A^{pro} would stop the protease from processing this cleavage site. Figure 4-2B shows the result for this experiment. Very similar to the processing of the wild-type cleavage site, the first cleavage products were detected after 20 minutes (compare Figure 4-1A). 30 minutes after the start of translation, 50% of the VP1-2A^{pro} precursor was cleaved and the reaction was completed between 60 and 120 minutes.

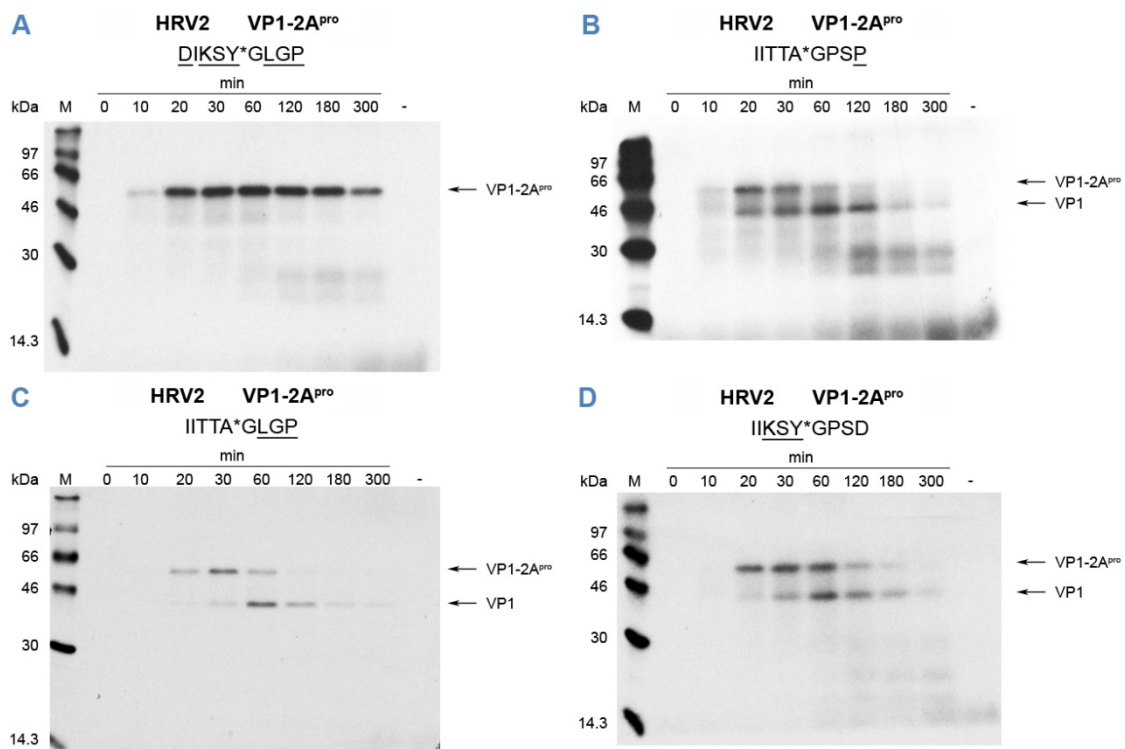


Figure 4-2 Self-processing of HRV2 2A^{pro} on cleavage sites containing residues found at the junction of HRV14 VP1-2A^{pro}: **(A)** entire cleavage site found in HRV14. **(B)-(D)** mixed cleavage sites. Underlined residues differ from the residues found in the wild-type cleavage site. Rabbit reticulocyte lysate was programmed with RNA coding for VP1-2A^{pro} (10ng/ μ l) and incubated at 30°C. Negative controls were prepared by adding water instead of RNA. 10 μ l aliquots were taken at the given time points and put on an icecold mix of 25 μ l 2x Laemmli sample buffer, 15 μ l H₂O and 1 μ l unlabeled methionine/cysteine (20mM). Viral proteins were then separated by SDS-PAGE on 17.5% gels and visualized by fluorography. Protein standards (M) in kDa are given on the left.

The single mutation D4P was not sufficient to prevent HRV2 2A^{pro} from cleaving at this site. Thus, further mutations in the P' region were thought to be necessary to affect self-processing. Introduction of three residues from HRV14 into the HRV2 VP1-2A^{pro} cleavage site

(LeuGlyPro instead of ProSerAsp at P2'-P4') resulted in a slight delay in self-processing (Figure 4-2C). Nevertheless, the time point of 50% conversion was only shifted to a minor degree and was found between 30 and 60 minutes, indicating that the changes in the P' region are not responsible for the discrimination of the HRV14 cleavage site by HRV2 2A^{pro}. For this reason, we wanted to investigate the influence of the region P3-P1 on self-processing by mutating the residues ThrThrAla to LysSerTyr that are found in the VP1-2A^{pro} cleavage site of HRV14. Surprisingly, the kinetics of cleavage were again only slightly slowed (Figure 4-2D). The first cleavage products could not be detected before 30 minutes and 50% of the precursor were cleaved at about 60 minutes. Nevertheless, all of the mutated cleavage sites so far investigated, were clearly processed by HRV2 2A^{pro} indicating that mutations upstream as well as downstream of the cleavable bond are necessary to stop HRV2 2A^{pro} from processing this cleavage site in *cis*.

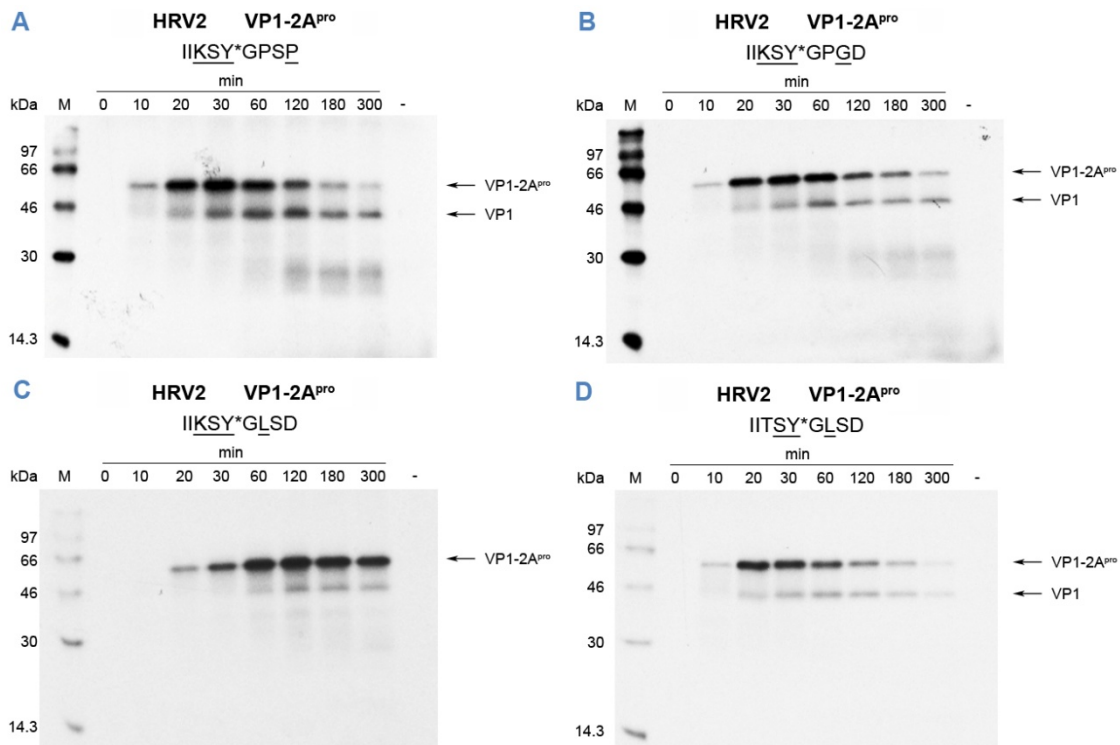


Figure 4-3 Self-processing of HRV2 2A^{pro} on cleavage sites containing residues found at the junction of HRV14 VP1-2A^{pro}. Underlined residues differ from the residues found in the wild-type cleavage site. Rabbit reticulocyte lysate was programmed with RNA coding for VP1-2A^{pro} (10ng/ μ l) and incubated at 30°C. Negative controls were prepared by adding water instead of RNA. 10 μ l aliquots were taken at the given time points and put on an icecold mix of 25 μ l 2x Laemmli sample buffer, 15 μ l H₂O and 1 μ l unlabeled methionine/cysteine (20mM). Viral proteins were then separated by SDS-PAGE on 17.5% gels and visualized by fluorography. Protein standards (M) in kDa are given on the left.

As the mutant with LysSerTyr at P3-P1 was the most severely affected, we decided to keep these mutations and introduce additional single mutations in the region P2'-P4'. Figure 4-3A shows the influence of the additional mutation aspartic acid to proline at P4'. HRV2 2A^{pro} was still able to process this cleavage site, albeit at a much lower rate than the wild-type cleavage site. Initial cleavage products could still be detected after 20 minutes. Nevertheless, 50% conversion of the precursor was not found until 120 minutes after start of translation, supporting the theory that mutations at both sides of the cleavable bond are necessary to stop HRV2 2A^{pro} from self-processing. Introduction of glycine instead of serine at P3' caused an even greater impairment of self-processing activity (Figure 4-3B). Although some cleavage product could still be detected after 20 to 30 minutes, a clear time point of 50% cleavage could not be detected any longer. Whether the detected cleavage product is still the result of specific cleavage by 2A^{pro} remains doubtful.

Finally, introduction of leucine at P2' in the background of LysSerTyr at P3-P1 results in a pattern comparable to the one found with the entire HRV14 cleavage site (Figure 4-3C). Only a very low amount of non-precursor protein could be detected indicating that HRV2 2A^{pro} was no longer able to process this cleavage site. Therefore, these four mutations prevent HRV2 2A^{pro} from self-processing. However, the minimal number of HRV14 residues that are sufficient to impair HRV2 2A^{pro} self-processing remains to be shown. Thus, we reintroduced the wild-type residue threonine at P3 and tested if the remaining HRV14 residues were still sufficient to prevent cleavage. Figure 4-3D shows that this mutant resulted in a pattern that was more comparable to the one found with the cleavage site IleLeuLysSerTyr*GlyProGlyAsp (compare Figure 4-3B).

These results strongly argue against our previous assumptions that the region P2'-P4' is not involved in the discrimination of the HRV14 cleavage site. Comparison of Figure 4-2D with Figure 4-3C shows that introduction of leucine at P2' in the background of LysSerTyr at P3-P1 severely impairs self-processing. Therefore, we wanted to investigate residues that are involved in the recognition of the P2' proline. Unfortunately, no structure of a 2A^{pro} with its substrate bound to the active site is available. The crystal structure of HRV2 2A^{pro} represents a picture of the protease after self-processing has taken place. The N-terminus is rotated out of the active site. Thus, the P2' proline is placed a long way off from its position during self-processing. Nevertheless, investigation of this crystal structure revealed a putative binding pocket for the proline at P2' (Figure 4-4A). It is made up of Arg15, Leu19, Phe20, Tyr39 and the main chain atoms of Asn16. Sequence alignments of several HRV serotypes showed that Arg15

is conserved among group A viruses whereas a conserved methionine is found at the equivalent position in group B viruses (Met17) (Figure 4-4B). This finding let us hypothesize that Arg15 may be involved in discriminating proline from this pocket although the relatively large distance from Arg15 from the active site (8.9 Å between the C α atoms of Cys106 and Arg15) argued against this.

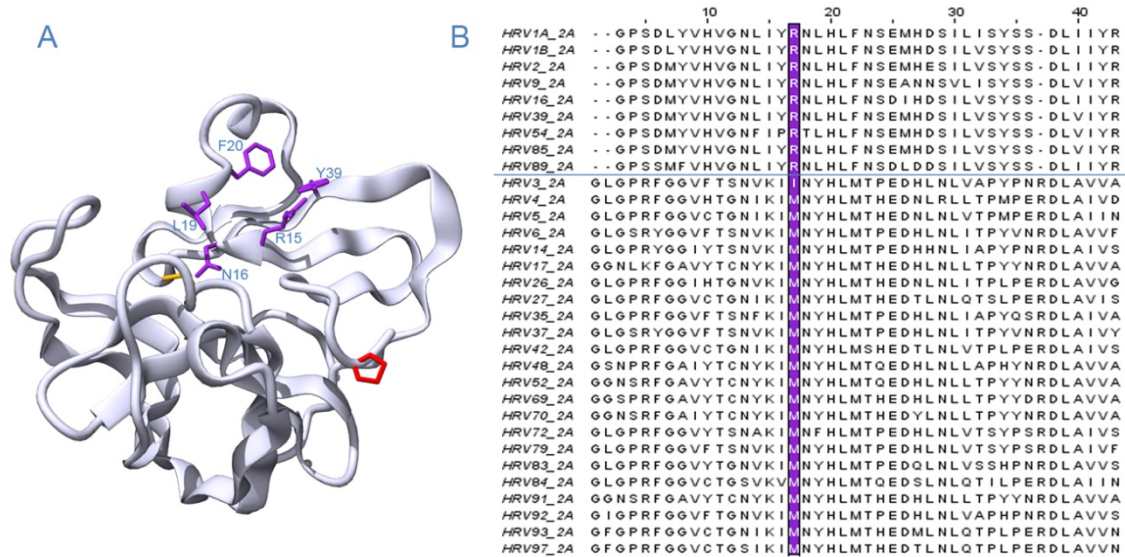


Figure 4-4 (A) Putative binding pocket for the P2' proline in HRV2 2A^{pro}. Residues forming the pocket are shown in purple. The P2' proline is depicted in red and the active site cysteine (Cys106) is colored yellow (generated with the “protein movie generator” (Autin and Tuffery 2007)). (B) Partial multiple sequence alignment of several HRV 2A^{pro} sequences. The position of R15 and M17 respectively is highlighted in purple. Blocks of Group A and Group B viruses are separated by a blue line (generated with JalView (Clamp *et al.* 2004)).

We therefore introduced the mutation R15M into the plasmid pHRV2 VP1-2A^{pro} llelleLysSerTyr*GlyLeuSerAsp and tested whether this was sufficient to compensate the effect of leucine at P2'. Figure 4-5A shows that self-processing could not be restored (compare Figure 4-3C), indicating that Arg15 is not involved in discriminating leucine from the P2' position. Nevertheless, in a reverse experiment, we tested for self-processing of a HRV14 2A^{pro} M17R mutant. Figure 4-5B shows that this mutant was unable to perform self-processing on the wild-type HRV14 cleavage site. This finding and the fact that position 15 (HRV2) and position 17 (HRV14) respectively are conserved within the two genetic groups suggests that this residue has some important function, albeit not in the recognition of the P2' residue.

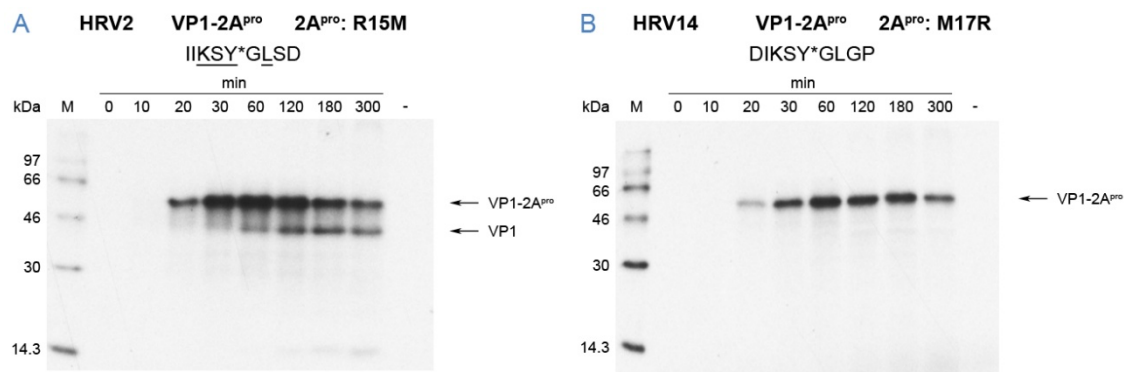


Figure 4-5 Self-processing of HRV2 and HRV14 2A^{PRO} mutants. **(A)** Effect of the mutation R15M in HRV2 2A^{PRO} on the self-processing of the sequence IlleLysSerTyr*GlyLeuSerAsp. Underlined residues differ from the residues found in the wild-type cleavage site. **(B)** Effect of the mutation M17R in HRV14 2A^{PRO} on the self-processing on its wild-type cleavage site. Rabbit reticulocyte lysate was programmed with RNA coding for VP1-2A^{PRO} (10ng/μl) and incubated at 30°C. Negative controls were prepared by adding water instead of RNA. 10μl aliquots were taken at the given time points and put on an icecold mix of 25μl 2x Laemmli sample buffer, 15μl H₂O and 1μl unlabeled methionine/cysteine (20mM). Viral proteins were then separated by SDS-PAGE on 17.5% gels and visualized by fluorography. Protein standards (M) in kDa are given on the left.

4.3 NUP62 CONTAINS SEQUENCES THAT WERE FOUND TO BE CLEAVED IN *TRANS* BUT CANNOT BE ACCEPTED IN *CIS* BY HRV2 2A^{PRO}

It has been shown that proteins of the nuclear pore complex (NUPs) are targets of 2A^{PRO} in *trans*-cleavages (Gustin and Sarnow 2001, Park *et al.* 2008). Moreover, recent studies revealed that HRV2 2A^{PRO} is able to directly cleave Nup62 at multiple sites (Park N. and Gustin K., pers. comm.). The cleavage sites used by HRV2 2A^{PRO} were identified by N-terminal sequencing and sequence analysis and are listed in Table 4-2. Alanine residues were found to be present at both the P1' and P2' position in these cleavage sites. Thus, we were interested whether HRV2 2A^{PRO} was also able to cleave substrates containing alanine either at P1' or P2' in *cis*. In agreement with our previous results that a mutation in the region P2'-P4' without additional mutations in the P3-P1 region did not significantly disturb self-processing, HRV2 2A^{PRO} was able to process a cleavage site with the single mutation proline to alanine at P2' at wild-type levels. First cleavage products could be detected at 20 minutes and 50% of the precursor were cleaved at about 30 minutes (Figure 4-6A, compare Figure 4-1A). As we knew that mutating proline at P2' in the background of LysSerTyr at P3-P1 had dramatic effects on self processing, we were interested how such a mutant with alanine at P2' would compare to

the mutant with leucine at P2'. Figure 4-6B shows that also alanine cannot be accepted in the background of the three mutated residues at P3-P1 (compare Figure 4-3C).

Cleavage site	P4	P3	P2	P1	↓	P1'	P2'	P3'	P4'
Self-processing	I	T	T	A		G	P	S	D
Nup62 ND/cp5	V	T	T	A		G	A	P	T
Nup62 ND/cp6	A	T	T	A		G	A	T	Q
Nup62 ND/cp3	L	K	P	L		A	P	A	G
Nup62 cp8/cp1	L	S	N	T		A	A	T	P

Table 4-2 Comparison of the HRV2 2A^{pro} self-processing cleavage site with cleavage sites found in the *trans*-cleavage of Nup62. ND=not detected, cp=cleavage product.

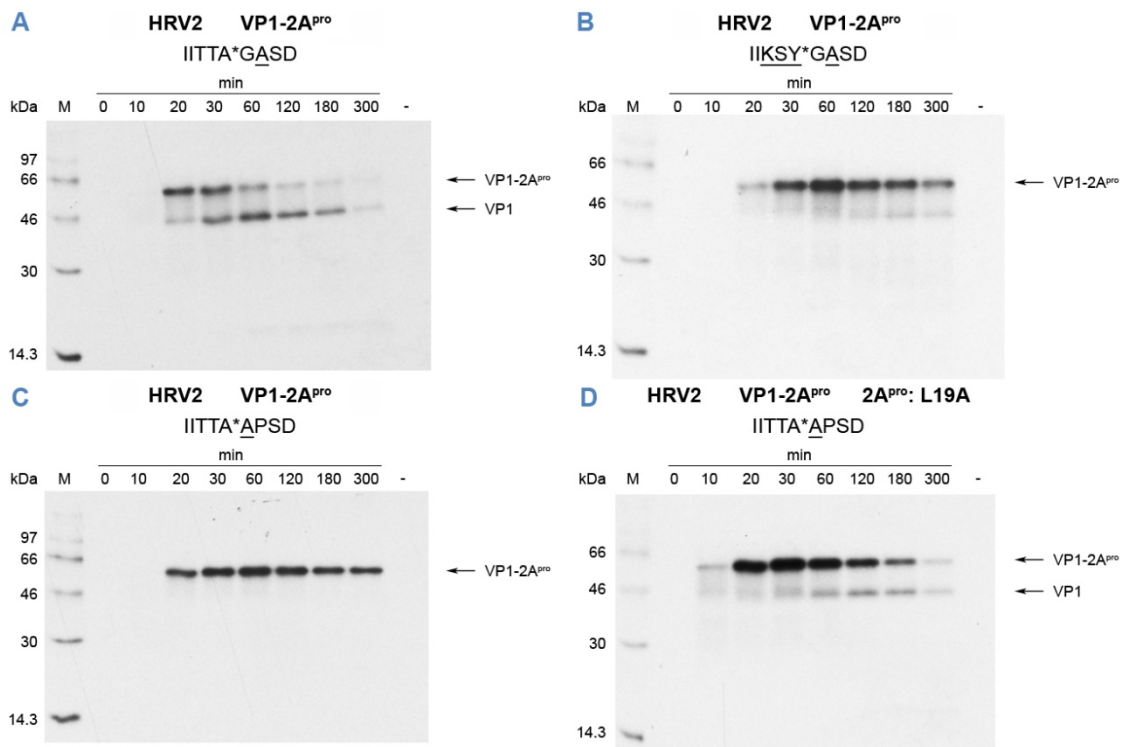


Figure 4-6 Self-processing of HRV2 2A^{pro} and a 2A^{pro} L19A variant on cleavage sites containing alanine at either P1' or P2'. Underlined residues differ from the residues found in the wild-type cleavage site. Rabbit reticulocyte lysate was programmed with RNA coding for VP1-2A^{pro} (10ng/μl) and incubated at 30°C. Negative controls were prepared by adding water instead of RNA. 10μl aliquots were taken at the given time points and put on an icecold mix of 25μl 2x Laemmli sample buffer, 15μl H₂O and 1μl unlabeled methionine/cysteine (20mM). Viral proteins were then separated by SDS-PAGE on 17.5% gels and visualized by fluorography. Protein standards (M) in kDa are given on the left.

Glycine at P1' is the only totally conserved residue found at the VP1-2A^{pro} junction of all HRV serotypes sequenced so far. Indeed, peptides with glutamic acid, lysine, threonine, phenylalanine or aspartic acid at P1' were shown to remain uncleaved by HRV2 2A^{pro} (Skern *et al.* 1991, Sommergruber *et al.* 1992), confirming this strong requirement for glycine at P1'. Nevertheless, we tested the ability of HRV2 2A^{pro} to accept a cleavage site containing alanine at P1'. Figure 4-6C shows that the single addition of a methyl group at this position results in total disruption of self-processing, indicating that glycine is really the only residue that can be accepted at P1' in the self-processing reaction. Petersen *et al.* suggested that Leu19 is responsible for discriminating any other residue from P1' by blocking any access to a possible S1' site (Petersen *et al.* 1999) (Figure 4-4A). Nevertheless, mutating Leu19 to alanine in order to provide more space for alanine at P1' did not significantly enhance self-processing (Figure 4-6D), suggesting that the occupancy of space by Leu19 is not the only reason for the strong requirement for glycine at P1'.

4.4 MET5: A HINGE AT WHICH THE N-TERMINUS IS ROTATED INTO THE ACTIVE SITE DURING SELF-PROCESSING?

Skern *et al.* have shown that a peptide with the sequence IVTRPIITTA*GPGPRYGGVG (underlined residues are the ones found in the equivalent positions of the HRV14 VP1-2A^{pro} junction) is not cleaved by HRV2 2A^{pro} (Skern *et al.* 1991). In order to test this cleavage site in the *cis* reaction we introduced it into the VP1-2A^{pro} junction of our *in vitro* system and tested for self-processing. Figure 4-7A shows that the cleavage site could not be processed by HRV2 2A^{pro} in *cis*, just as in *trans*. In order to exclude the possible influence of the altered P3' and P4' positions we introduced the cleavage site IITTA*GPSDRYGGI. Again we tested for self-processing and found that this cleavage site was not recognized by HRV2 2A^{pro} (Figure 4-7B).

Comparison of the HRV2 and HRV14 cleavage site revealed that the mutation of the hydrophobic residue methionine to the charged amino acid arginine at position P5' is one of the major differences and could cause the inability of HRV2 2A^{pro} to process these cleavage sites.

The crystal structure of HRV2 2A^{pro} gives a picture of the protease after the *cis* cleavage event, where the N-terminus is turned away from the active site. Petersen *et al.* proposed that any rearrangement beyond Met5 would probably alter the interactions within the N-terminal

β -sheet (Petersen *et al.* 1999). Thus, rearrangements of the first five residues must be sufficient to place the scissile bond in the active site (Figure 4-8).

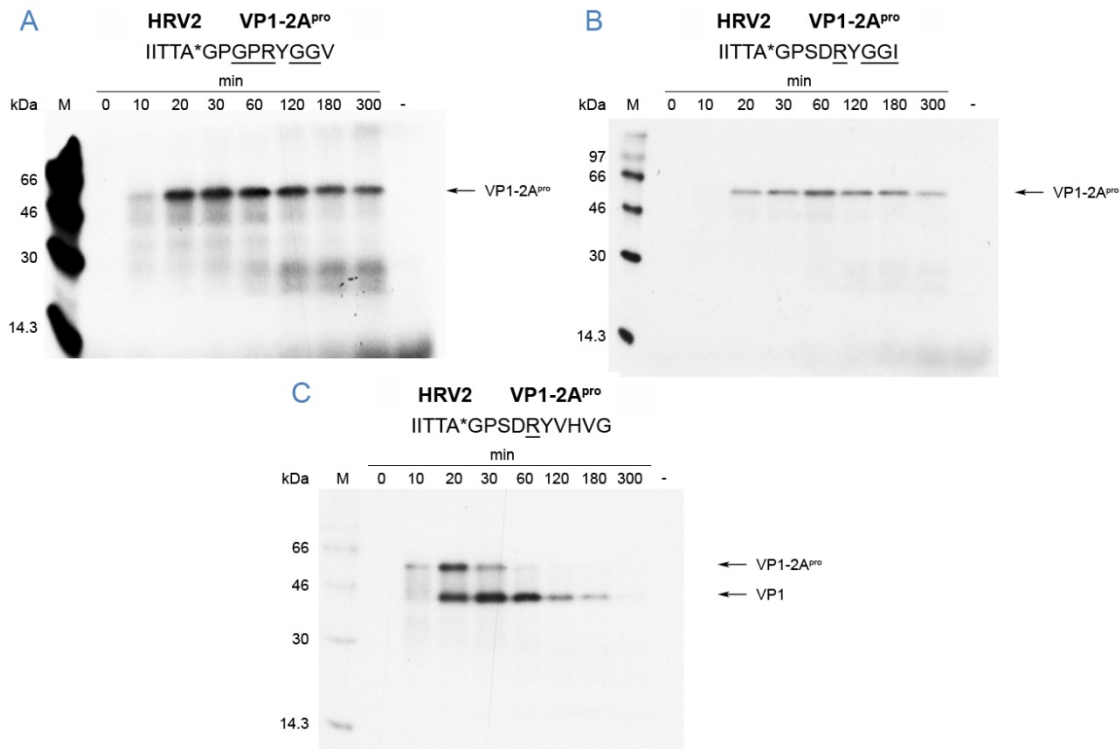


Figure 4-7 Self-processing of HRV2 2A^{pro} on substrates containing arginine at P5'. Underlined residues differ from the residues found in the wild-type cleavage site. Rabbit reticulocyte lysate was programmed with RNA coding for VP1-2A^{pro} (10ng/ μ l) and incubated at 30°C. Negative controls were prepared by adding water instead of RNA. 10 μ l aliquots were taken at the given time points and put on an icelcold mix of 25 μ l 2x Laemmli sample buffer, 15 μ l H₂O and 1 μ l unlabeled methionine/cysteine (20mM). Viral proteins were then separated by SDS-PAGE on 17.5% gels and visualized by fluorography. Protein standards (M) in kDa are given on the left.

Investigation of the structure showed that Met5 could act as a possible hinge region. Manipulation of the ϕ and ψ -angles of Met5 would bring the P1' glycine close to the active site. Furthermore, the Met5 side chain would end up in close proximity to Lys109 supporting the theory that HRV2 2A^{pro} cannot bear a positively charged amino acid at position P5' (Figure 4-8A). Sequence analysis revealed that Lys109 is conserved among group A viruses whereas an isoleucine is found in the equivalent position of HRV14 2A^{pro}. Therefore, we wanted to investigate the influence of the single mutation methionine to arginine at position P5'. Mutating Lys109 to isoleucine should then reveal if this residue is involved in this mechanism.

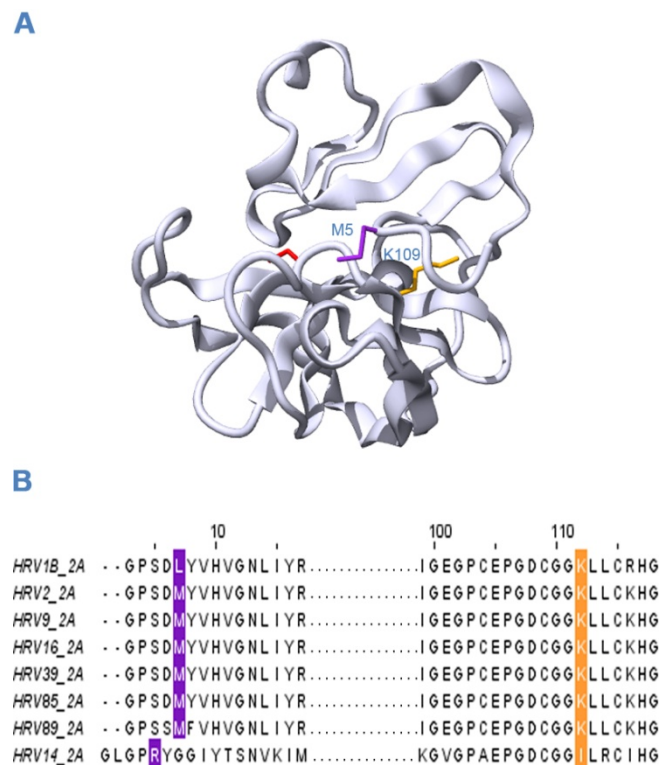


Figure 4-8 (A) Crystal structure of HRV2 2A^{pro}. The N-terminus is turned away from the active site (Cys 106, depicted in red). Rotation around Met5 (purple) could bring the N-terminus close to the active site. This rotation possibly would bring Met5 in proximity to Lys109 (yellow) (generated with the “protein movie generator” (Autin and Tuffery 2007)). (B) Multiple sequence alignment of 2A^{pro} sequences of several HRV serotypes. Methionine is the predominant residue at position P5’ in Group A viruses whereas an arginine is found at P5’ of HRV14 (a group B virus). Lysine at position 109 in HRV2 2A^{pro} is conserved among the listed Group A viruses. In HRV14 this position is taken by an isoleucine (generated with JalView (Clamp *et al.* 2004)).

Figure 4-7C shows that the sole introduction of arginine instead of methionine at P5’ does not influence self-processing, arguing against our theory that HRV2 2A^{pro} cannot accept arginine at P5’. Self-processing of this mutant is comparable to the wild-type kinetics. Self-processing at wild-type levels by the corresponding mutant K109I was therefore not surprising (Figure 4-9A). Figure 4-9B shows the result of the reverse experiment in which isoleucine at position 112 was substituted with lysine in HRV14 2A^{pro}. Self-processing of this mutant is strongly impaired. First cleavage products could only be detected after 30 minutes and 50% of processing was reached between 120 and 180 minutes. This fact indicates a difference in the 2A proteinases of HRV2 and HRV14. However, in the absence of a HRV14 2A^{pro} structure the reason for this difference remains doubtful.

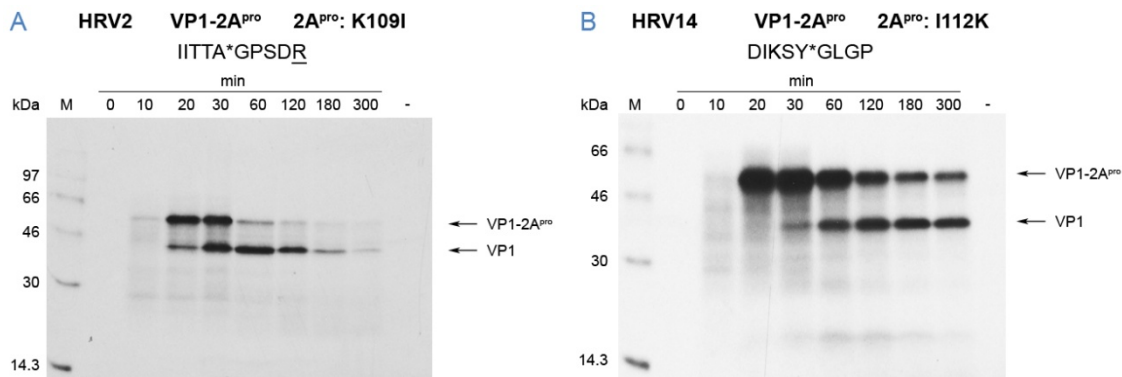


Figure 4-9 Role of Lys109 in HRV2 2A^{pro} and Ile112 in HRV14 2A^{pro} in contributing to a possible hinge region around P5'. Underlined residues differ from the residues found in the wild-type cleavage site. Rabbit reticulocyte lysate was programmed with RNA coding for VP1-2A^{pro} (10ng/μl) and incubated at 30°C. Negative controls were prepared by adding water instead of RNA. 10μl aliquots were taken at the given time points and put on an icecold mix of 25μl 2x Laemmli sample buffer, 15μl H₂O and 1μl unlabeled methionine/cysteine (20mM). Viral proteins were then separated by SDS-PAGE on 17.5% gels and visualized by fluorography. Protein standards (M) in kDa are given on the left.

4.5 CONSTRUCTION OF HRV14/2 2A^{PRO} HYBRIDS

The experiments in the previous chapters show that the 2A proteases of HRV2 and HRV14 show some noticeable differences. The cleavage sites in their self-processing reaction differ quite strongly. HRV2 2A^{pro} cleaves at IlleThrThrAlA*GlyProSerAsp, whereas HRV14 2A^{pro} cleaves at AspIlleLysSerTyr* GlyLeuGlyPro. Additionally, it has been shown that HRV2 2A^{pro} cannot accept the HRV14 cleavage site and *vice versa* (Schertler 2008). The need for proline at P2' in HRV2 2A^{pro} seems to be one reason for the discrimination of the HRV14 cleavage site by HRV2 2A^{pro} (see section 4.2). Furthermore, sequence alignments show that the N-terminal region of group B viruses exhibits two additional residues in respect to group A viruses (Figure 4-4B). In section 4.4 we found that the two proteinases showed different response to mutating the equivalent residues 109 (HRV2) or 112 (HRV14). Finally, Deszcz *et al.* have shown that the 2A proteinases of HRV2 and HRV14 show different responses to the specific 2A^{pro} inhibitor zVAM.fmk (Deszcz *et al.* 2006). zVAM.fmk inhibits both, the self-processing and *trans* cleavages of HRV14 2A^{pro}, whereas HRV2 2A^{pro} is only inhibited in its *trans* reaction.

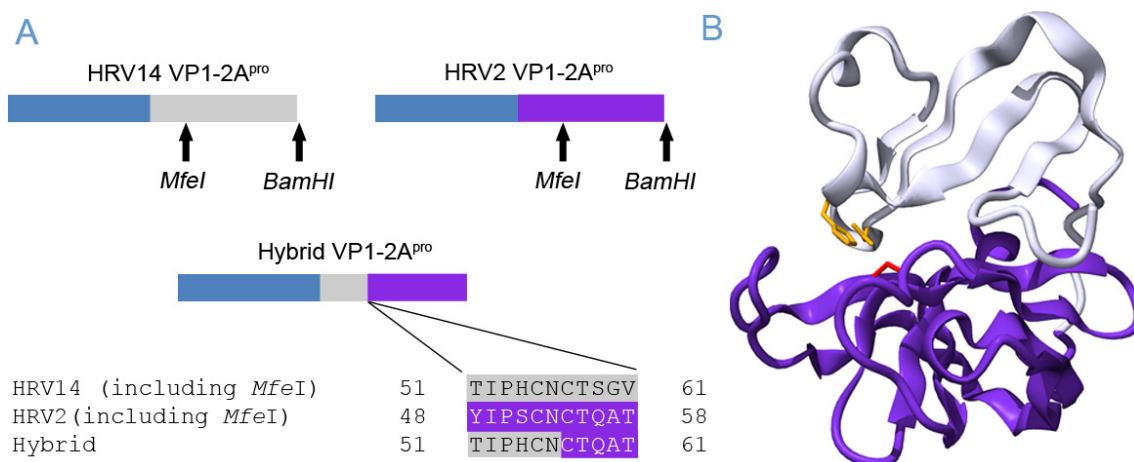


Figure 4-10 Construction of a hybrid $2A^{pro}$. **(A)** *MfeI* sites were introduced into the plasmids coding for either HRV2 or HRV14 VP1- $2A^{pro}$. *MfeI* and *BamHI* sites were then used to substitute the C-terminal domain and create a hybrid containing HRV14 VP1, the N-terminal $2A^{pro}$ domain of HRV14 and the C-terminal $2A^{pro}$ domain of HRV2. The sequence at the changeover is given separately. **(B)** Scheme of the two domains of HRV2 $2A^{pro}$. In a hybrid $2A^{pro}$ the grey N-terminal domain will be exchanged by the respective HRV14 $2A^{pro}$ domain. The catalytic triad (numbered according to HRV2 $2A^{pro}$) is colored in red (Cys106) and yellow (His18 and Asp35) (generated with the “protein movie generator” (Autin and Tuffery 2007)).

These findings suggest that the two proteinases do not only differ in substrate specificity, but could also differ in the general mechanism in which they perform self-processing. The construction of hybrid $2A$ proteinases could be a helpful tool to understand these differences.

Thus, we decided to construct a hybrid VP1- $2A^{pro}$ made up of HRV14 VP1, the N-terminal $2A^{pro}$ domain of HRV14 and the C-terminal $2A^{pro}$ domain of HRV2. Introduction of the restriction site *MfeI* was necessary to allow exchange of the cDNA coding for the C-terminal HRV2 $2A^{pro}$ domain (Figure 4-10A). The two domains of $2A^{pro}$ are combined at the end of the long interdomain loop at the amino acid Asn56 (Figure 4-10B). Therefore, the construction should not interfere with interactions of residues within one domain.

Figure 4-11A shows self-processing of the hybrid. No cleavage product could be detected, indicating that the hybrid was absolutely unable to perform self-processing. Most of the interactions involved in substrate recognition are found in the C-terminal domain of $2A^{pro}$. We therefore introduced the HRV2 cleavage site into the hybrid and tested for self-processing. Nevertheless, also this variant was absolutely inactive as no cleavage product could be detected even at 300 minutes (Figure 4-11B).

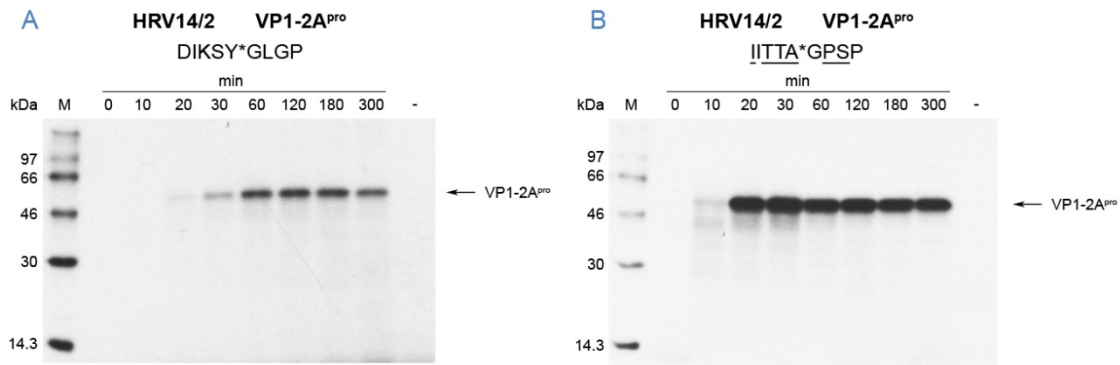


Figure 4-11 Self-processing of HRV14/2 hybrid 2A^{pro} on **(A)** the HRV14 cleavage site and **(B)** the HRV2 cleavage site. Underlined residues differ from the residues found in the wild-type HRV14 cleavage site. Rabbit reticulocyte lysate was programmed with RNA coding for VP1-2A^{pro} (10ng/μl) and incubated at 30°C. Negative controls were prepared by adding water instead of RNA. 10μl aliquots were taken at the given time points and put on an icecold mix of 25μl 2x Laemmli sample buffer, 15μl H₂O and 1μl unlabeled methionine/cysteine (20mM). Viral proteins were then separated by SDS-PAGE on 17.5% gels and visualized by fluorography. Protein standards (M) in kDa are given on the left.

4.6 DOES THE VIRAL PROTEIN 2B INFLUENCE 2A^{PRO} SELF-PROCESSING?

Recently, the group of Karla Kirkegaard showed that the viral protein 2B may influence the activity of 2A^{pro}. Poliovirus was grown in the presence of the specific 2A^{pro} inhibitor zVAM.fmk. The search for escape mutants revealed that resistance to zVAM.fmk did not predominantly map to 2A^{pro} but 2B, indicating that 2B is involved in 2A^{pro} activity (Kirkegaard K., pers. comm.). Therefore, we wanted to investigate the influence of 2B on self-processing. Furthermore, we were interested if the presence of 2B would influence the diverse ability of zVAM.fmk to inhibit HRV2 2A^{pro} and HRV14 2A^{pro} in the self-processing reaction. To this end, HRV2 2B and HRV14 2B were amplified from full length clones by standard PCR techniques and cloned into the respective plasmids downstream of 2A^{pro}. The resulting VP1-2A^{pro}-2B constructs were tested for their self-processing activity.

Self-processing of HRV2 VP1-2A^{pro}-2B is shown in Figure 4-12A. First cleavage products were detected at 20 minutes after start of translation. 50% cleavage of the precursor was achieved at about 60 minutes and cleavage was practically finished after 300 minutes. Thus, HRV2 VP1-2A^{pro}-2B performs self processing slower than the HRV2 VP1-2A^{pro} construct (compare Figure 4-1A). Proper folding of the precursor probably takes longer in the presence of 2B, giving an explanation for the delayed kinetics. HRV14 VP1-2A^{pro}-2B exhibits a similar

pattern (Figure 4-12B). First cleavage products were detected after 20 minutes and the time point of 50% cleavage was found at about 120 minutes. This finding is consistent with the fact that also HRV14 VP1-2A^{pro} is slightly slower than HRV2 VP1-2A^{pro}. Thus, the VP1-2A^{pro}-2B constructs exhibit normal self-processing albeit being slightly slower than the VP1-2A^{pro} constructs.

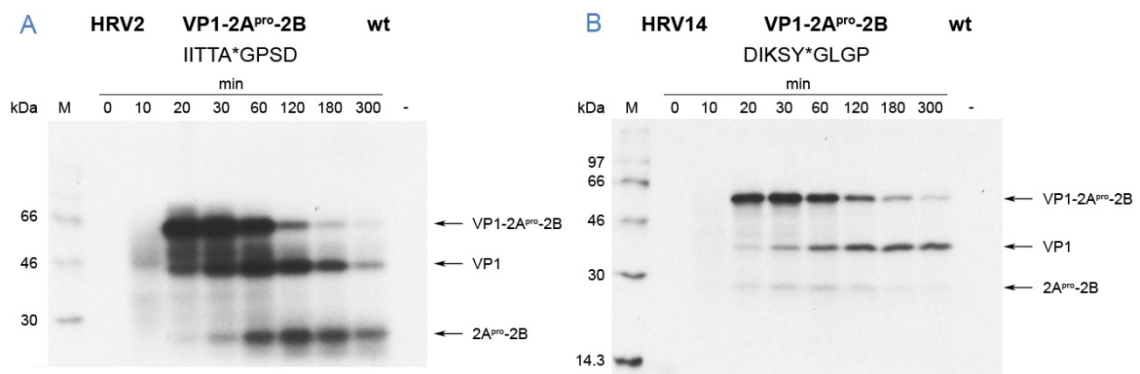


Figure 4-12 Self-processing of **(A)** HRV2 and **(B)** HRV14 VP1-2A^{pro}-2B constructs. Rabbit reticulocyte lysate was programmed with RNA coding for VP1-2A^{pro}-2B (10ng/ μ l) and incubated at 30°C. Negative controls were prepared by adding water instead of RNA. 10 μ l aliquots were taken at the given time points and put on an icecold mix of 25 μ l 2x Laemmli sample buffer, 15 μ l H₂O and 1 μ l unlabeled methionine/cysteine (20mM). Viral proteins were then separated by SDS-PAGE on 17.5% gels and visualized by fluorography. Protein standards (M) in kDa are given on the left.

An erroneous primer for PCR amplification of HRV14 2B gave rise to a HRV14 VP1-2A^{pro}-2B construct with a mutation in the C-terminal region of 2B (I94N). Surprisingly, this single mutation totally stopped 2A^{pro} from performing self-processing, strongly supporting the idea that 2B is involved in 2A^{pro} activity (Figure 4-13).

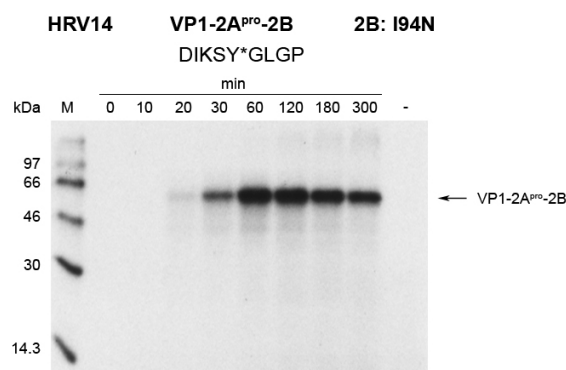


Figure 4-13 Self-processing of HRV14 VP1-2A^{pro}-2B with the mutation I94N in 2B. Rabbit reticulocyte lysate was programmed with RNA coding for VP1-2A^{pro}-2B (10ng/ μ l) and incubated at 30°C. Negative controls were prepared by adding water instead of RNA. 10 μ l aliquots were taken at the given time points and put on an icecold mix of 25 μ l 2x Laemmli sample buffer, 15 μ l H₂O and 1 μ l unlabeled methionine/cysteine (20mM). Viral proteins were then separated by SDS-PAGE on 17.5% gels and visualized by fluorography. Protein standards (M) in kDa are given on the left.

In next step, we wanted to test whether the presence of 2B influences the ability of zVAM.fmk to inhibit HRV14 2A^{pro} in *cis*. mRNA coding for HRV14 VP1-2A^{pro}-2B was used to program RRL's in the presence of different amounts of the specific 2A^{pro} inhibitor zVAM.fmk. Samples were incubated for 60 minutes followed by the addition of ice-cold Laemmli sample buffer and unlabeled methionine/cysteine in order to stop translation. zVAD.fmk (a caspase inhibitor found to be also active against 2A^{pro}) served as a positive control, 0.1% dimehtylsulfoxide (serves as the solvent for zVAM.fmk) as a negative control. Figure 4-14A shows that there is no significant difference between the increasing amounts of zVAM.fmk and when compared to the controls. Furthermore, the time point of 60 minutes seemed to be not optimal. In order to test if the inhibitors were active at all, we tested them under the conditions described by Deszcz *et al.* (Deszcz *et al.* 2006). We used mRNA coding for HRV14 VP1-2A^{pro} to program RRL's. Additionally we tested a fresh stock of zVAD.fmk as a positive control (indicated by zVAD^{new}). Figure 4-14B shows that only the highest concentration of zVAM.fmk was able to induce slight inhibition. However, according to Deszcz *et al.* sufficient inhibition should already be achieved at a concentration of 50 μ M indicating that the inhibitor was out of date and not active any more. This was supported by the finding that the fresh stock of zVAD.fmk did indeed inhibit self-processing of HRV14 VP1-2A^{pro} in the positive control.

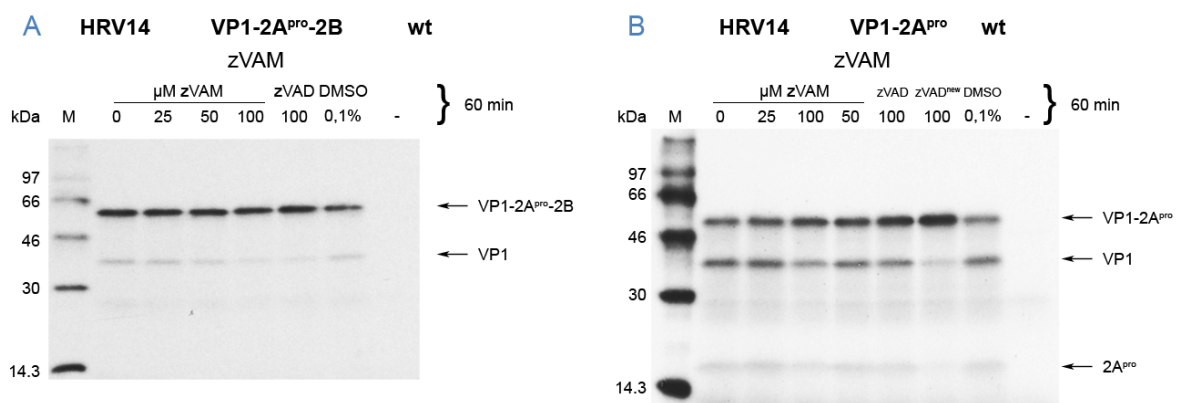


Figure 4-14 Inhibition of **(A)** HRV14 VP1-2A^{pro}-2B and **(B)** HRV14 VP1-2A^{pro} self-processing by zVAM.fmk and zVAD.fmk. Rabbit reticulocyte lysate was programmed with RNA coding for VP1-2A^{pro}-2B and VP1-2A^{pro} respectively (10ng/ μ l) and incubated at 30°C. Negative controls were prepared by adding water instead of RNA. The indicated amount of inhibitor was added 10 minutes after start of translation. Reaction was stopped after 60 minutes by adding an icecold mix of 25 μ l 2x Laemmli sample buffer, 15 μ l H₂O and 1 μ l unlabeled methionine/cysteine (20mM). Viral proteins were then separated by SDS-PAGE on 17.5% gels and visualized by fluorography. Protein standards (M) in kDa are given on the left.

4.7 METHIONINE AT POSITION 143 IN Lb^{PRO} EXHIBITS COMPARABLE PERFORMANCE IN DISCRIMINATING PHENYLALANINE FROM P2 THAN LEUCINE AT POSITION 143

FMDV codes for an additional protein preceding the genes for the structural proteins, the leader protease Lb^{PRO}. It is thought that in the initial self-processing reaction it cleaves itself off the polyprotein in an intramolecular reaction, although also intermolecular cleavage cannot be ruled out. Figure 4-15A shows the self-processing of the wild-type enzyme on its wild-type substrate. No precursor could be detected, demonstrating a very fast and efficient cleavage. Lb^{PRO} codes for four methionines whereas VP4-VP2 has only two. Therefore, the intensity of the Lb^{PRO} band is stronger than the VP4-VP2 band.

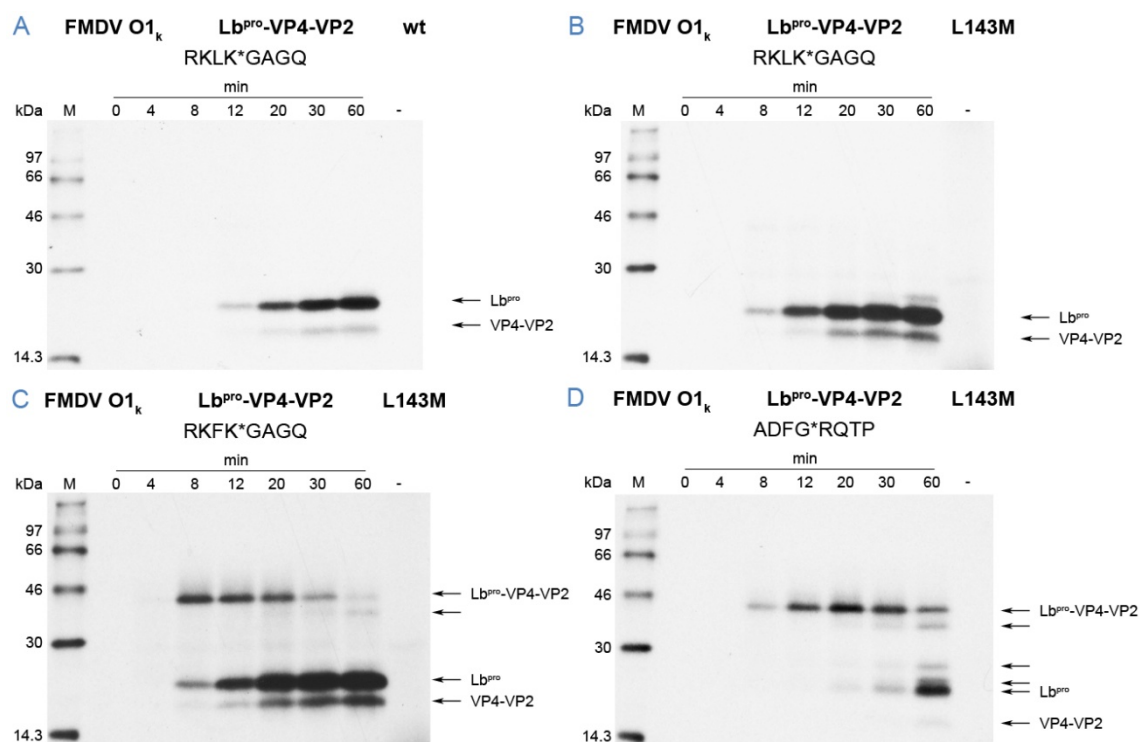


Figure 4-15 Self-processing of (A) FMDV Lb^{PRO}-VP4-VP2 wild-type and (B-D) variants carrying the mutation L143M. Rabbit reticulocyte lysate was programmed with RNA coding for Lb^{PRO}-VP4-VP2 (10ng/μl) and incubated at 30°C. Negative controls were prepared by adding water instead of RNA. 10μl aliquots were taken at the given time points and put on an icecold mix of 25μl 2x Laemmli sample buffer, 15μl H₂O and 1μl unlabeled methionine/cysteine (20mM). Viral proteins were then separated by SDS-PAGE on 17.5% gels and visualized by fluorography. Protein standards (M) in kDa are given on the left.

Recently, it has been shown that the leader protease is not able to process in *cis* the cleavage site AlaAspPheGly*ArgGlnThrPro present on eIF4GII (Kuehnel *et al.* 2004). Kuehnel *et al.* found that it was phenylalanine at P2 and aspartic acid at P3 that caused the discrimination. Leucine 143, found in the hydrophobic S2 pocket, was identified as preventing phenylalanine from protruding deeper into the pocket. Hence, substitution of leucine 143 by alanine rendered Lb^{pro} able to cleave a substrate with phenylalanine at P2 (Mayer *et al.* 2008). However, although Leucine 143 is not conserved among the seven serotypes of FMDV (Figure 4-16), the only other amino acids found at this position are isoleucine and methionine, which possess bulky and hydrophobic side-chains like leucine.

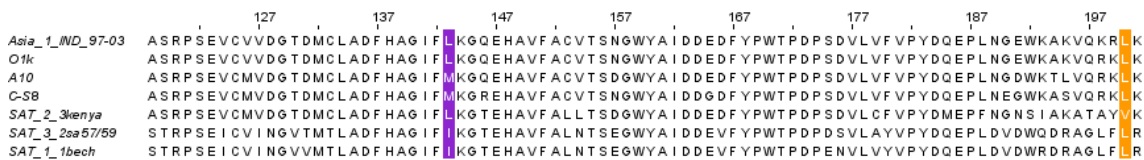


Figure 4-16 Multiple sequence alignment of Lb^{pro} sequences of one strain of each FMDV serotype. The bulky hydrophobic residues leucine, methionine and isoleucine can be found at position 143 (purple). Only leucine or valine is found in all sequenced FMDV strains at position 200 (P2) (orange) (generated with JalView (Clamp *et al.* 2004)).

Therefore, we wanted to investigate if methionine at position 143 would also be able to discriminate phenylalanine from the S2 pocket. Substitution of leucine 143 with methionine had no influence on the self-processing of the wild-type cleavage site (Figure 4-15B). No precursor could be detected, which is comparable with the wild-type enzyme. The L143M mutant was however impaired in its ability to cleave the substrate with phenylalanine at P2 (Figure 4-15C). The precursor could still be detected 30 minutes after start of translation. Additionally, an aberrant cleavage product could be detected at 60 minutes (labeled by arrow). However, comparison of the self-processing of the wild-type enzyme on the same cleavage sites shows that the L143M mutant is less impaired than the wild-type enzyme (Mayer *et al.* 2008). Finally, processing of the eIF4GII sequence AlaAspPheGly*ArgGlnThrPro by the L143M variant is severely impaired (Figure 4-15D) and is comparable to the self-processing activity of the wild-type enzyme on the same cleavage site. Cleavage products could not be detected before 30 minutes after start of translation. Moreover, additional aberrant cleavage products were detected.

5 DISCUSSION

The cleavage sites of HRV 2A proteinases vary amongst the different serotypes in the self-processing reaction. Furthermore, it was shown that 2A^{pro} cleavage sites for *trans*-cleavages vary even more than for *cis*-cleavages. For example, HRV2 2A^{pro} cleaves its own polyprotein at IleIleThrThrAla*GlyProSerAsp whereas HRV14 2A^{pro} cleaves at AspIleLysSerTyr*GlyLeuGlyPro. The two isoforms of eukaryotic initiation factor 4G (eIF4GI and eIF4GII) are cleaved at ThrLeuSerThrArg*GlyProProArg (Lamphear *et al.* 1993) and ProLeuLeuAsnVal*GlySerArgArg (Gradi *et al.* 2003) in *trans* by HRV2 2A^{pro}. The cleavage sites on eIF4GI and II used by HRV14 2A^{pro} have not been determined yet but are thought to be identical. Table 5-1 gives an overview of some serotypes and their respective cleavage sites on the polyprotein.

The strong variation of the cleavage sites makes it impossible to create a consensus sequence for HRV 2A^{pro} cleavage sites. HRV 2A proteinases vary in their substrates in *cis* and *trans* and are known to cleave several cellular proteins (Badorff *et al.* 1999, Joachims *et al.* 1999, Kerekatte *et al.* 1999, Seipelt *et al.* 2000, Park *et al.* 2008). Nevertheless, there are some requirements that render 2A^{pro} a specific proteinase such as the strong requirement for glycine at P1' or the preference of HRV2 2A^{pro} for threonine at P2. Lacking HRV 2A^{pro} structures bound to substrates or inhibitors and with only one human rhinoviral structure of 2A^{pro} available (Petersen *et al.* 1999), mutational analysis of the cleavage site plays an essential role in determining the exact substrate requirements of HRV 2A^{pro}.

Serotype	VP1	↓	2A ^{pro}
HRV 1B	SMKTV		GPSD
HRV 2	IITTA		GPSD
HRV 9	AVKNV		GPSD
HRV 85	SLTTA		GPSD
HRV 89	TVTNV		GPSS
HRV 14	DIKSY		GLGP

Table 5-1 Amino acid sequences at the VP1-2A^{pro} junctions of different HRV serotypes.

Recently, it has been shown that 2A^{pro} could be an important target for the development of antiviral drugs (Crowder and Kirkegaard 2005). Co-transfection of RNA coding for wild-type PV and a mutant that was unable to process the VP1-2A^{pro} junction (2A^{pro} C109R) resulted in a dominant-negative effect, inhibiting the replication of the wild-type virus. A similar effect is imaginable for the FMDV leader proteinase. Therefore, understanding of the substrate specificities of 2A^{pro} and Lb^{pro} is crucial for the development of new inhibitors.

5.1 HRV2 2A^{PRO} CANNOT ACCEPT THE VP1-2A^{PRO} CLEAVAGE SITE OF HRV14

HRV2 2A^{PRO} is not able to self-process at the VP1-2A^{PRO} junction when the wild-type cleavage site is replaced by the cleavage site of HRV14 (Asp11eLysSerTyr*GlyLeuGLyPro). We therefore wanted to investigate which of the residues in the HRV14 cleavage site were responsible for this discrimination. Comparison of the two cleavage sites shows that the major differences can be found at the positions P5, P3, P1, P2', P3' and P4' (Table 5-1). Sommergruber *et al.* showed that peptides with tyrosine at P1 were cleaved with even higher efficiency than peptides with the wild-type alanine by HRV2 2A^{PRO} (Sommergruber *et al.* 1992), indicating that tyrosine at P1 should not be the reason for the discrimination of the HRV14 cleavage site. When the crystal structure of HRV2 2A^{PRO} was solved, a peptide, spanning P5 to P1', was modeled into the substrate binding cleft (Petersen *et al.* 1999). In this model, the main chain of threonine at P3 is hydrogen bonded to the main chain of Gly124. Its side chain points away from the substrate binding cleft. Based on this model, it is quite possible that lysine is well accepted at the P3 position and is therefore also thought to be not responsible for the inability of HRV2 2A^{PRO} to accept the HRV14 cleavage site. Thus, investigation of the P' region seemed to be most interesting.

An interesting feature in the P' region of HRV2 2A^{PRO} is a stable type I reverse turn that is stabilized by a hydrogen bond between the carboxylate of Asp4 and the protonated α -amino group of Gly1 (Petersen *et al.* 1999). Additionally, the N-terminus is rotated out of the active site in the crystal structure. It has been speculated that this stable turn serves as a protection against product inhibition. However, this motif is not conserved. Furthermore, HRV2 2A^{PRO} could easily process the cleavage site with proline instead of aspartic acid at P4' (Figure 4-2B). Therefore, the reverse turn or at least its stabilization by a hydrogen bond does not seem to be necessary for self-processing. As introduction of the HRV14 residues LeuGlyPro at P2'-P4' only slightly decreased the self-processing activity of HRV2 2A^{PRO} (Figure 4-2C), the P' region seemed not to be a major determinant of substrate specificity. However, it has been reported that peptides with phenylalanine, threonine, lysine or aspartic acid at P2' are cleaved 2-5 fold less efficiently than peptides with proline (Sommergruber *et al.* 1992). Thus, it seems possible that the mutation of proline to leucine is responsible for the slight decrease in self-processing efficiency.

As a consequence, we started to concentrate on the P region and were surprised to find that also mutating P3-P1 did not significantly alter cleavage efficiency (Figure 4-2D). Especially serine at P2 is known to be not well accepted by HRV2 2A^{pro} at least in *trans*. Sommergruber *et al.* showed that a peptide with serine at P2 was cleaved with a relative efficiency of only 0.15 in respect to the peptide with the wild-type cleavage sequence (Sommergruber *et al.* 1992). However, tyrosine at P1 was shown to be even better accepted than the wild-type alanine. Therefore, the presence of tyrosine at P1 is possibly compensating the harmful effect of serine at P2.

Neither the introduction of HRV14 residues at the P3-P1 region nor mutating the P2'-P4' region alone severely impaired self-processing. A combination of mutations at both sides of the cleavage site seems to be required to stop HRV2 2A^{pro} from performing the *cis* reaction (Figure 4-3). The most severe effect could be obtained by maintaining the mutations at P3-P1 and additionally mutating proline at P2' to leucine (Figure 4-3C). Furthermore, the finding that cleavage was still severely impaired when the wild-type residue threonine was reintroduced at P3 does not disagree with the idea that lysine is well accepted at P3 (Figure 4-3D). If lysine at P3 would contribute to the discrimination of the HRV14 cleavage site, one would expect an increase in self-processing activity upon reintroduction of the wild-type residue. However, as both cleavage sites are not processed at all, a contribution of lysine cannot be totally excluded. In contrast to our initial assumptions, these experiments showed that the P' region indeed seems to be important in the recognition of the substrate. Investigation of the HRV2 2A^{pro} structure revealed a putative S2' pocket made up of Arg15, Leu19, Phe20, Tyr39 and the main chain atoms of Asn16 (Figure 4-4A). Amongst these residues, Arg15 was found to be conserved within group A viruses whereas in group B viruses a conserved methionine was found at the equivalent position. However, mutating Arg15 to methionine did not significantly affect processing on the respective cleavage site (Figure 4-5A) indicating that Arg15 is not involved in the recognition of the P2' residue. Leu19 and Asn16 are conserved among group A and group B viruses. Thus, it seems that our prediction about the S2' pocket was incorrect.

However, the importance of proline at P2' in HRV2 2A^{pro} may arise from its fixed ϕ -angle. Through this fixed angle, it possibly stabilizes the type I reverse turn of the N-terminus, shaping the substrate into the correct formation to reach the active site. In contrast, the N-terminus of HRV14 2A^{pro} exhibits two additional amino acids. Thus, there would be no need for a tight turn in the substrate. Notably, the 3C proteinases (chymotrypsin-like proteinases like 2A^{pro}) of HRV2, HRV14 and PV1 also show preference for proline at P2' and an absolute

requirement for glycine at P1'. Investigation of the atomic structures (Matthews *et al.* 1994, Mosimann *et al.* 1997, Matthews *et al.* 1999) revealed that glycine and proline are probably responsible for a turn in the substrate that prevents clashing of the substrate with the β -strand bI1 (Semler and Wimmer 2002). As 2A^{pro} and 3C^{pro} are thought to have arisen by gene duplication (Petersen *et al.* 1999), these findings support the theory that proline at P2' could be important for a special turn in the substrate in HRV2 2A^{pro}, even though 2A^{pro} lacks the mentioned β -strand bI1. However, Sommergruber *et al.* found that a peptide corresponding to P8-P2' was nearly cleaved as efficiently as a peptide corresponding to P8-P8'. In contrast, a P8-P1' peptide was cleaved at a 30-fold reduced rate, indicating that the residue at P2' also strongly contributes to the binding affinity of the substrate to the enzyme (Sommergruber *et al.* 1992). However, in the absence of a 2A^{pro} structure with the substrate bound to the active site, this theory will remain just speculation.

5.2 NUP62 CONTAINS SEQUENCES THAT WERE FOUND TO BE CLEAVED IN *TRANS* BUT CANNOT BE ACCEPTED IN *CIS* BY HRV2 2A^{PRO}

Recently, it has been shown that proteins of the nuclear pore complex (NUPs) are cleaved upon poliovirus infection and that HRV2 2A^{pro} was able to induce cleavage of Nup98 in HeLa whole cell lysates (Park *et al.* 2008). Additionally, *in vitro* studies of Nup62 cleavage by HRV2 2A^{pro} identified multiple cleavage sites. Table 4-2 lists selected Nup62 cleavage sites in which alanine can be found at P1' and P2' and compares them with the wild-type cleavage site for 2A^{pro} self-processing (Park N. and Gustin K., pers. comm.).

The two cleavage sites giving rise to the fragments ND/cp5 and ND/cp6 contain alanine at P2'. Cleavage at these sites is not surprising as the cleavage sites fulfill the requirements of substrate specificity at the positions P4, P2 and P1' very well. These finding also correlates with the results presented in this thesis. The exclusive mutation of P2'-P4' (Figure 4-2C) or the single mutation of proline at P2' to alanine (Figure 4-6A) did not affect self-processing significantly. However, the fact that Nup62 is cleaved at the cleavage sites giving rise to ND/cp3 and cp8/cp1 indicates that the substrate requirements for *cis* and *trans*-cleavages can differ. Both cleavage sites lack glycine at P1' (mutated to alanine) and exhibit a poorly recognized residue at P2 (Sommergruber *et al.* 1992). In addition, the Nup62 cp8/cp1 cleavage

site contains alanine at P2'. Still, both of these cleavage sites were found to be cleaved in *trans*. In contrast, alanine at P2' in combination with the non-optimal residue serine at P2 severely impaired self-processing (Figure 4-6B) and HRV2 2A^{pro} was also not able to accept alanine at P1' in the *cis* reaction (Figure 4-6C).

Like 2A^{pro}, 3C^{pro} has an absolute requirement for glycine at P1'. Phe25 situated on β -strand bI1 of 3C^{pro} was proposed to be responsible for the discrimination against all other residues at P1' by occupying the space that would be needed by a side chain (Semler and Wimmer 2002). The same role was postulated for Leu19 of 2A^{pro} (Petersen *et al.* 1999). Indeed, superimposition of the structures of HRV2 2A^{pro} and 3C^{pro} strengthen this theory. The two structures superimpose with an rms-value of 1.25Å using the "Magic Fit" tool of the "DeepView – Swiss pdb viewer" (Guex and Peitsch 1997). The catalytic triad is found to superimpose very well. Additionally, the side chains of Phe25 and Leu19 are found to occupy the same space albeit arising from different β -strands. However, we show here that mutating Leu19 to alanine is not sufficient to restore self-processing on a substrate that contains alanine at P1'. Thus, Leu19 is at least not the only residue that is contributing to the discrimination of any side chains at P1'. To our knowledge, the corresponding mutation F25A in HRV2 3C^{pro} has not been tested so far. Therefore, data for comparison is unfortunately missing. It was also suggested that His18 itself and maybe Tyr85 could act as determinants for the specificity at P1'. Tyr85 was proposed to be rotated around its C α -C β bond during self processing, bringing it into a position where it could maybe influence substrate specificity at P1' (Petersen *et al.* 1999). Tyr85 is part of the so-called dityrosine flap that includes two tyrosines that are conserved amongst the 2A proteinases of rhinoviruses and enteroviruses. However, a 2A^{pro} structure with the substrate bound to the enzyme will be needed to reveal why only glycine can be accepted in the self-processing reaction while alanine can be accepted during *trans*-cleavages.

5.3 MET5: A HINGE AT WHICH THE N-TERMINUS IS ROTATED INTO THE ACTIVE SITE DURING SELF-PROCESSING?

As described in part 4.4, Skern *et al.* showed that a peptide with the sequence IVTRPIITTA*GPGPRYGGVG (underlined residues are the ones found in the equivalent positions of the HRV14 VP1-2A^{pro} junction) is not cleaved by HRV2 2A^{pro} (Skern *et al.* 1991). We showed

that this sequence (plus a variant of it) could also not be accepted in the self-processing reaction (Figure 4-7A and B). Residues seven and eight form β -strand bI2 of HRV2 2A^{pro}. Thus, mutation of these two residues was likely to interfere with the structure of the proteinase and hence with its activity. Nevertheless, the sequence is also not accepted in experiments with peptides in which these residues of the substrate do not need to form this β -strand. Thus, we focused our interest on the P2'-P5' region. Previous results had shown that mutations at P2'-P4' without additional mutations in the P3-P1 region had no dramatic effect on self-processing. Therefore, the presence of the bulky charged residue of arginine at position P5' instead of the wild-type methionine attracted our attention.

Sequence analysis revealed that methionine is the predominant amino acid at P5' in group B viruses, although methionine is not completely conserved (Figure 4-8B). Furthermore, Petersen *et al.* have already proposed that the region at Met5 could act as a hinge region at which the substrate is turned into the active site during self-processing (Petersen *et al.* 1999). We thought that rotation around this region would probably result in positioning the side chain of Met5 close to Lys109, supporting our theory that arginine at P5' could be responsible for the inability to self-process at the cleavage sites mentioned above. Additionally, Lys109 is conserved amongst group A viruses whereas in HRV14 this position is occupied by isoleucine. However, it should be mentioned that if only the ϕ and ψ angles of Met5 are adjusted in order to roughly fit the substrate into the active site, they will be found in forbidden regions in the ramachandran-plot (Figure 5-1). Furthermore, the side chain of Asp4 would clearly clash into the main chain of Asp105 and Cys106 (Figure 5-2). Nonetheless, the side chains of Met5 and Lys109 would clearly end up close together.

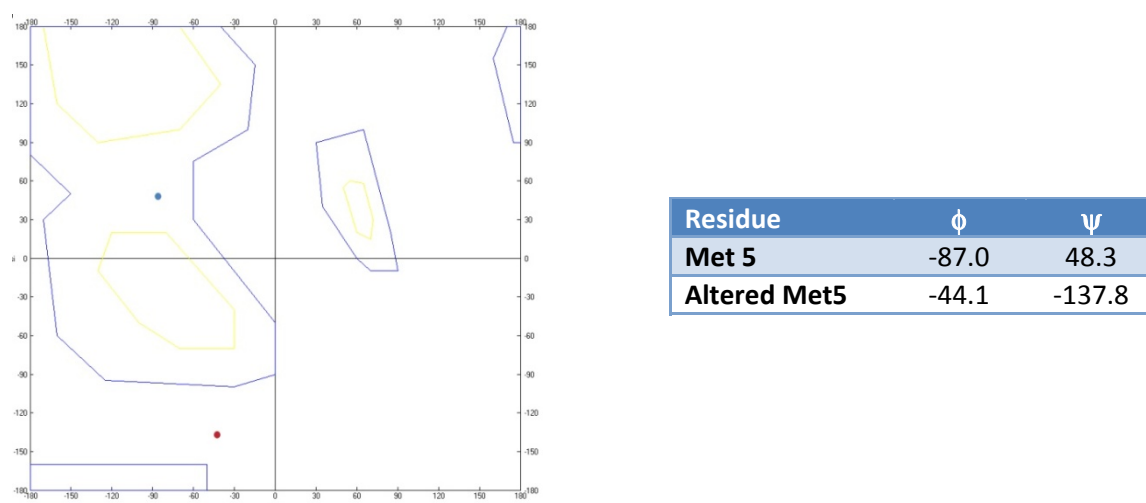


Figure 5-1 Ramachandran plot of Met5 in HRV2 2A^{pro}. In the crystal structure (PDB 2HRV) Met5 is found in an allowed region in the ramachandran plot (blue). Rotating the N-terminus into the active site around Met5 leads to a shift into a forbidden region (red).

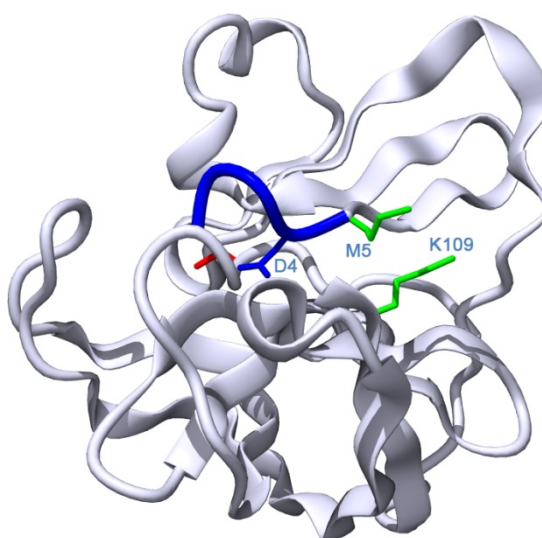


Figure 5-2 Structure of HRV2 2A^{pro} with the substrate rotated into the active site. Rotation was performed using the swiss pdb viewer (Guex and Peitsch 1997). Only the ϕ/ψ angles of Met5 have been adjusted. The active site cysteine is shown in red. The N-terminal five residues that are moved from their original position are depicted in blue (generated with the “protein movie generator” (Autin and Tuffery 2007)).

Unfortunately, the results of our mutational analysis disagreed with our proposed repulsion of arginine at P5' and Lys109. A cleavage site with the single mutation Met5 to arginine was processed at wild-type levels by HRV2 2A^{pro} (Figure 4-7C). Thus, not surprisingly the mutant K109I exhibited unaffected self-processing. Interestingly, the reverse mutant in

which the equivalent residue Ile112 of HRV14 2A^{pro} was mutated to lysine exhibited severely impaired self-processing, indicating a contribution to substrate recognition by this residue. However, as mentioned before, HRV14 2A^{pro} exhibits two additional amino acids in its N-terminal region in respect to the N-terminal region of HRV2 2A^{pro}. Thus, it is doubtful whether Met5 of HRV2 2A^{pro} and Arg5 of HRV14 2A^{pro} occupy equivalent positions in the structure as in the sequence alignment Met5 aligns with Gly7 of HRV14 2A^{pro}.

Recently, the solution structure of coxsackievirus B4 (CVB4) 2A^{pro} was solved (Baxter *et al.* 2006). This NMR-structure and the crystal structure of HRV2 2A^{pro} are the only 2A^{pro} structures available so far. Superimposition of the HRV2 2A^{pro} structure and the CVB4 2A^{pro} structure shows that Gly8 of CVB4 2A^{pro} is in the equivalent structural position to Met5 of HRV2 2A^{pro}. The fact that Gly7 of HRV14 aligns with Met5 of HRV2 2A^{pro} and Gly8 of CVB4 2A^{pro} (Figure 5-3) strongly implies that Gly7 and not Arg5 of HRV14 2A^{pro} is in the equivalent structural position to Met5 in HRV2 2A^{pro}.

				10						110				120																									
HRV2_2A	.	.	.	G	P	S	D	I	Y	V	H	V	G	N	L	I	Y	P	G	D	C	G	G	I	L	L	C	K	H	G	V	I	G	I	V	T	A	G
HRV14_2A	G	.	L	G	P	R	Y	G	G	I	Y	T	S	N	V	K	I	P	G	D	C	G	G	I	L	R	C	I	H	G	P	I	G	L	L	T	A	G
CVB4_2A	G	P	Y	G	H	Q	S	G	A	V	Y	V	G	N	Y	K	V	P	G	D	A	G	G	I	L	R	C	E	H	G	V	I	G	L	V	T	M	G

Figure 5-3 Sequence alignment of the 2A^{pro} sequences of HRV2, HRV14 and coxsackievirus B4.

In contrast to HRV2 2A^{pro}, a molecular model of CVB4 2A^{pro} self-processing is available. Baxter *et al.* modeled the substrate including the C-terminal eight residues of VP1 into the active site of the CVB4 2A^{pro} structure. This model shows that the substrate region of P3'-P8' forms a quite wide bulge with the side chains of Tyr3, His5, Gln6 and Ser7 exposed to the solvent. We investigated this model to evaluate whether a rotation around Gly8 is needed for the N-terminus to reach the active site in CVB4 2A^{pro}. Unfortunately, the ϕ/ψ angles of Gly8 vary quite strongly within the 17 NMR-structures of the CVB4 2A^{pro} that are deposited in the protein data base (PDB 1Z8R) (Table 5-2, Figure 5-4). Therefore, it is hard to judge whether a rotation around Gly8 in CVB4 2A^{pro} is needed for self-processing.

Molecule	Residue	ϕ	ψ
1Z8R_1	GLY8	63.7	23.2
1Z8R_2	GLY8	-157.3	37.8
1Z8R_3	GLY8	166.8	-51.6
1Z8R_4	GLY8	-156.6	140.8
1Z8R_5	GLY8	-161.3	-76.0
1Z8R_6	GLY8	97.2	84.0
1Z8R_7	GLY8	158.6	-28.5
1Z8R_8	GLY8	-170.8	60.4
1Z8R_9	GLY8	-160.1	179.3
1Z8R_10	GLY8	152.4	-36.1
1Z8R_11	GLY8	178.7	37.4
1Z8R_12	GLY8	140.1	-25.1
1Z8R_13	GLY8	-160.6	27.4
1Z8R_14	GLY8	143.1	-40.9
1Z8R_15	GLY8	-135.2	27.2
1Z8R_16	GLY8	169.4	43.5
1Z8R_17	GLY8	96.8	-29.6
1Z8R with modeled substrate	GLY8	-79.0	125.5

Table 5-2 ϕ/ψ angles of Gly8 in the 17 molecules of the CVB4 2A^{PRO} NMR-structure (1Z8R) as well as in the structure with the substrate modeled into the active site.

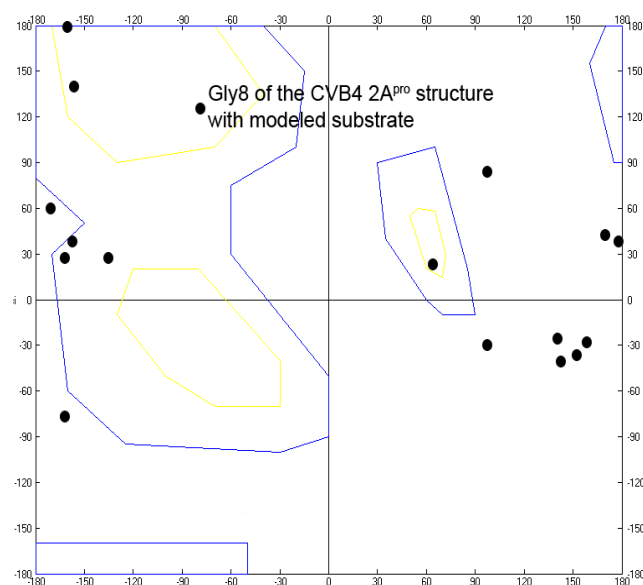


Figure 5-4 Ramachandran plot of Gly8 residues of the 17 CVB4 2A^{PRO} NMR structures deposited in the PDB file 1Z8R as well as of Gly8 of a structure with the N-terminus modeled into the active site (also see Table 5-2). The ϕ/ψ angles exhibit strong variation which makes it hard to judge whether rotation around Gly8 is needed for the N-terminus to reach the active site.

5.4 CONSTRUCTION OF HRV14/2 2A^{PRO} HYBRIDS

The construction of a hybrid 2A proteinase was intended to be a useful tool to investigate the differences of HRV2 and HRV14 2A proteinases. The N-terminal domain of HRV14 2A^{PRO} was fused with the C-terminal domain of HRV2 2A^{PRO} at the interdomain loop. Consequently, the catalytic triad of each enzyme was split. The general base His20 and Asp38 are provided by the N-terminal HRV14 domain whereas the nucleophilic cysteine (now Cys109) is provided by the C-terminal HRV2 domain. This arrangement is one of several possible reasons why the hybrid 2A^{PRO} was not able to perform self-processing. If the interactions between the two domains of the hybrid 2A^{PRO} are not optimal, it is likely that a correct orientation of the catalytic triad is not possible. The total sequence identity between HRV2 and HRV14 2A^{PRO} is only 40%. Figure 5-5A shows residues located at the interface between the two domains of HRV2 2A^{PRO}. The sequence alignment (Figure 5-5B) shows that these residues are not very well conserved. Thus, it seems likely that the N-terminal domain of HRV14 2A^{PRO} and the C-terminal domain of HRV2 2A^{PRO} cannot act together to form an active enzyme.

A second possible reason for the inactivity of the hybrid 2A^{PRO} is that the HRV14 cleavage site could not be accepted by the hybrid enzyme. As we have shown that HRV2 2A^{PRO} cannot accept the HRV14 cleavage site and as we know that the recognition of the P region of the substrate is exclusively mediated by residues of the C-terminal domain, this seemed to be a likely possibility. However, introduction of the HRV2 cleavage site into the hybrid enzyme did not improve self-processing (Figure 4-11B), indicating that the problem goes either beyond substrate recognition or that a hybrid substrate containing HRV14 and HRV2 residues is needed. In principle it is also possible that the hybrid 2A^{PRO} is not at all able to fold correctly. Finally, it is worth mentioning that a similar approach by Roetzer A. to construct an active hybrid 2A^{PRO} between HRV2 2A^{PRO} and CVB4 2A^{PRO} also failed (Roetzer 2004). Neither the construct with an N-terminal HRV2 domain and a C-terminal CVB4 domain nor the inverse construct were active in self-processing.

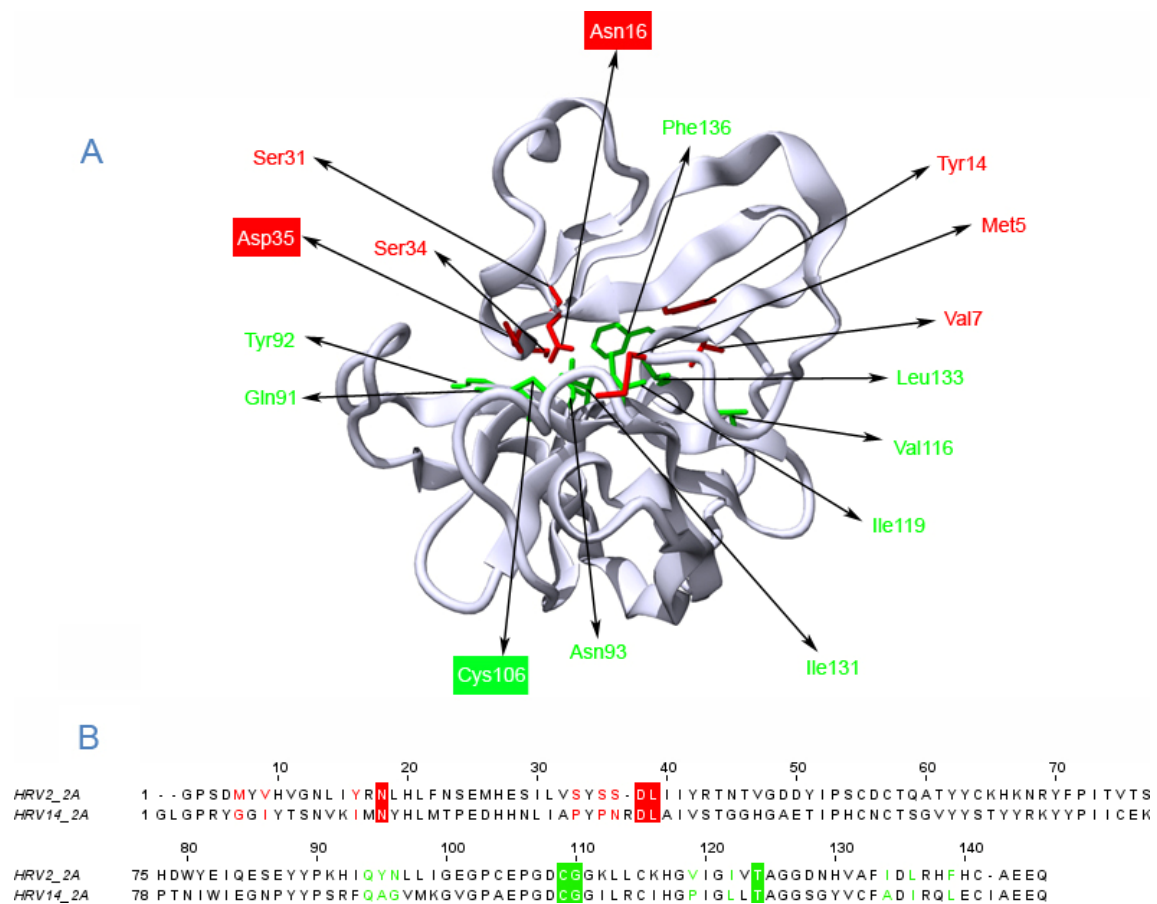


Figure 5-5 Residues situated at the interface of the N-terminal and C-terminal domain of HRV2 2A^{pro}. **(A)** Residues situated at the interface and directing towards the opposite domain. Residues provided by the N-terminal domain are colored red, those from the C-terminal domain are colored green. Residues that are conserved amongst HRV2 and HRV14 2A^{pro} are represented in reverse video. Residues Ser33, Leu36, Gly107 and Thr121 are also found at the interface but are hidden in this representation (generated with the “protein movie generator” (Autin and Tuffery 2007)). **(B)** Sequence alignment of HRV2 and HRV14 2A^{pro}. Conserved interface residues are given in reverse video (generated with JalView (Clamp *et al.* 2004)).

5.5 DOES THE VIRAL PROTEIN 2B INFLUENCE 2A^{PRO} SELF-PROCESSING?

It was stated by Hellen *et al.* that a VP1-2A^{pro} precursor acts as a representative model for investigating self-processing of 2A proteinases (Hellen *et al.* 1992). *In vitro* translation of mRNA coding for PV1 VP1-2A^{pro} for one hour followed by immunoprecipitation with antiserum directed against VP1 or 2A^{pro} showed that only a small amount of precursor remained uncleaved. Similar results were achieved when VP1 was replaced by the entire P1 region of structural proteins or 2A^{pro} was replaced by most of the P2 region of non-structural proteins.

However, recent results suggest that the protein 2B is involved in the self-processing reaction (Kirkegaard K., pers. comm.). PV1 mutants that had escaped the treatment with the 2A^{pro} specific inhibitor zVAM.fmk exhibited the mutation Y93C in 2A^{pro} as well as the mutations I6V, I6M, I2V and T18A in the protein 2B. This theory is further strengthened by the finding that an HRV14 VP1-2A^{pro}-2B construct with the mutation I94N in 2B was totally inactive in self-processing (Figure 4-13).

Furthermore, we show here that the processing of HRV2 and HRV14 VP1-2A^{pro}-2B constructs is delayed in respect to corresponding VP1-2A^{pro} constructs. Hellen *et al.* reported that no more than 5% of uncleaved precursor could be detected upon 60 minutes of translation, no matter whether they used a VP1-2A^{pro} construct or a construct made up of VP1 and nearly the entire P2 region of non-structural proteins. This is in contrast to our own results as Figure 4-12 shows that a minimum of 50% of uncleaved precursor could be detected at the time point of 60 minutes.

Deszcz *et al.* showed that HRV2 2A^{pro} was not sensitive to zVAM.fmk in *cis*, whereas HRV14 2A^{pro} was inhibited in the self-processing reaction (Deszcz *et al.* 2006). Therefore, we also wanted to test whether the presence of 2B influences the sensitivity of the *cis* reaction to zVAM.fmk. However, as we found that our inhibitor stocks seemed to be no longer active, these experiments had to be postponed.

5.6 METHIONINE AT POSITION 143 IN LB^{PRO} EXHIBITS COMPARABLE PERFORMANCE IN DISCRIMINATING PHENYLALANINE FROM P2 THAN LEUCINE AT POSITION 143

Recently, it has been found that the leader protease is severely impaired in self-processing on cleavage sites with phenylalanine at P2 or aspartic acid at P3 (Kuehnel *et al.* 2004). Furthermore, Leu143 was identified as a major determinant for the specificity at P2 (Mayer *et al.* 2008). Additionally, we were able to show that also methionine, which can be found at position 143 of some FMDV strains, is able to discriminate phenylalanine from the S2 pocket. However, the effect of phenylalanine at P2 is not that severe in the L143M variant than in the wild-type enzyme. The nature of the aberrant cleavage products remains unclear.

Only leucine or valine can be found at the P2 positions of all strains that have been sequenced so far. Additionally, position 143 is always occupied by a bulky hydrophobic side

chain in all isolates sequenced so far. This suggests that not cleaving substrates with phenylalanine at P2 has biological importance for the virus. Therefore, the construction of the S2 pocket may strongly contribute to the restricted number of substrates cleaved by Lb^{pro}. Indeed, the two isoforms of eukaryotic initiation factor 4G (eIF4GI and eIF4GII) remain the only cellular substrates identified so far.

Like the wild-type enzyme, the L143M mutant was strongly impaired in processing the cleavage site ADFG*RQTP. However, it was able to cleave the substrate with the single mutation L200F, albeit at a very low rate. Additionally, Mayer *et al.* have reported that mutating Leu143 to alanine could restore some cleavage activity on the ADFG*RQTP substrate, but not to wild-type levels (Mayer *et al.* 2008). These facts support the finding of Kuehnel *et al.* that aspartic acid at P3 also contributes to the discrimination of this cleavage site (Kuehnel *et al.* 2004). Thus, future work should also concentrate on the P3 residue and reveal, how the S3 pocket is able to discriminate aspartic acid.

6 APPENDIX

6.1 ABBREVIATIONS

2A^{pro}	Proteinase 2A
aa	Amino acid
Amp	Ampicillin
bp	Base pairs
cDNA	Complementary DNA
CIP	Calf intestine phosphatase
CITE	Cap-independent translation enhancer
Cp	Cleavage product
CTE	C-terminal extension
CVB	Coxsackie virus B
DNA	Deoxyribonucleic acid
dNTP	Deoxynucleotide triphosphate
DTT	Dithiothreitol
EDTA	Ethylenediaminetetraacetic acid
eIF3	Eukaryotic initiation factor 3
eIF4A	Eukaryotic initiation factor 4A
eIF4E	Eukaryotic initiation factor 4E
eIF4F	Eukaryotic initiation factor 4F
eIF4G	Eukaryotic initiation factor 4G
EM	Electron microscopy
EMCV	Encephalomyocarditis virus
FMDV	Foot and mouth disease virus
HAV	Hepatitis A virus
HeLa cells	Henrietta Lacks' cells
HRV	Human rhinovirus
ICAM-1	Intercellular adhesion molecule 1
ICTV	International committee on taxonomy of viruses
IRES	Internal ribosomal entry segment
kb	Kilo bases
kDa	Kilo Dalton
Lab^{pro}	Leader proteinase ab
LB	Luria Bertani
Lb^{pro}	Leader proteinase b
LDLR	Low density lipoprotein receptor
LFA-1	Leukocyte function-associated antigen-1
L^{pro}	Leader proteinase
LRP	Low density lipoprotein receptor related protein
Mac-1	Macrophage-1 antigen
mRNA	Messenger RNA
NF-κB	Nuclear factor κB
NMR	Nuclear magnetic resonance
NTP	Nucleotide triphosphate

NUP	Nuclear pore complex protein
ORF	Open reading frame
PABP	Poly-A binding protein
PAGE	Polyacrylamide gel electrophoresis
PCR	Polymerase chain reaction
PNK	Polynucleotide kinase
pol	Polymerase
Poly-A	Poly adenylation
PV	Poliovirus
RNA	Ribonucleic acid
RRL	Rabbit reticulocyte lysate
SDS	Sodiumdodecylsulfate
TAE	Tris-acetate-EDTA
TE	Tris-EDTA
UTR	Untranslated region
UV	Ultra-violet
VLDLR	Very low density lipoprotein receptor
VP1-4	Viral protein 1-4
VPg	Viral protein genome linked
wt	Wild-type
zVAD.fmk	Benzyloxycarbonyl-Val-Ala-Asp-fluoromethylketone
zVAM.fmk	Benzyloxycarbonyl-Val-Ala-Met-fluoromethylketone

6.2 LIST OF AMINO ACIDS

G	Gly	Glycine
A	Ala	Alanine
V	Val	Valine
L	Leu	Leucine
I	Ile	Isoleucine
M	Met	Methionine
P	Pro	Proline
S	Ser	Serine
T	Thr	Threonine
C	Cys	Cysteine
H	His	Histidine
F	Phe	Phenylalanine
Y	Tyr	Tyrosine
W	Trp	Tryptophane
N	Asn	Asparagine
Q	Gln	Glutamine
D	Asp	Aspartate
E	Glu	Glutamate
K	Lys	Lysine
R	Arg	Arginine

6.3 REFERENCES

- Acharya, R., E. Fry, D. Stuart, G. Fox, D. Rowlands, and F. Brown. 1989.** The three-dimensional structure of foot-and-mouth disease virus at 2.9 Å resolution. *Nature* 337: 709-16.
- Ambros, V., and D. Baltimore. 1980.** Purification and properties of a HeLa cell enzyme able to remove the 5'-terminal protein from poliovirus RNA. *J Biol Chem* 255: 6739-44.
- Arnold, E., M. Luo, G. Vriend, M. G. Rossmann, A. C. Palmenberg, G. D. Parks, M. J. Nicklin, and E. Wimmer. 1987.** Implications of the picornavirus capsid structure for polyprotein processing. *Proc Natl Acad Sci U S A* 84: 21-5.
- Arruda, E., A. Pitkaranta, T. J. Witek, Jr., C. A. Doyle, and F. G. Hayden. 1997.** Frequency and natural history of rhinovirus infections in adults during autumn. *J Clin Microbiol* 35: 2864-8.
- Autin, L., and P. Tuffery. 2007.** PMG: online generation of high-quality molecular pictures and storyboarded animations. *Nucleic Acids Res* 35: W483-8.
- Badorff, C., G. H. Lee, B. J. Lamphear, M. E. Martone, K. P. Campbell, R. E. Rhoads, and K. U. Knowlton. 1999.** Enteroviral protease 2A cleaves dystrophin: evidence of cytoskeletal disruption in an acquired cardiomyopathy. *Nat Med* 5: 320-6.
- Bahnemann, H. G. 1975.** Binary ethylenimine as an inactivant for foot-and-mouth disease virus and its application for vaccine production. *Arch Virol* 47: 47-56.
- Basavappa, R., R. Syed, O. Flore, J. P. Icenogle, D. J. Filman, and J. M. Hogle. 1994.** Role and mechanism of the maturation cleavage of VP0 in poliovirus assembly: structure of the empty capsid assembly intermediate at 2.9 Å resolution. *Protein Sci* 3: 1651-69.
- Baxt, B. 1987.** Effect of lysosomotropic compounds on early events in foot-and-mouth disease virus replication. *Virus Res* 7: 257-71.
- Baxt, B., and Y. Becker. 1990.** The effect of peptides containing the arginine-glycine-aspartic acid sequence on the adsorption of foot-and-mouth disease virus to tissue culture cells. *Virus Genes* 4: 73-83.
- Baxter, N. J., A. Roetzer, H. D. Liebig, S. E. Sedelnikova, A. M. Hounslow, T. Skern, and J. P. Waltho. 2006.** Structure and dynamics of coxsackievirus B4 2A proteinase, an enzyme involved in the etiology of heart disease. *J Virol* 80: 1451-62.
- Bayer, N., E. Prchla, M. Schwab, D. Blaas, and R. Fuchs. 1999.** Human rhinovirus HRV14 uncoats from early endosomes in the presence of bafilomycin. *FEBS Lett* 463: 175-8.
- Bazan, J. F., and R. J. Fletterick. 1988.** Viral cysteine proteases are homologous to the trypsin-like family of serine proteases: structural and functional implications. *Proc Natl Acad Sci U S A* 85: 7872-6.
- Beard, C. W., and P. W. Mason. 2000.** Genetic determinants of altered virulence of Taiwanese foot-and-mouth disease virus. *J Virol* 74: 987-91.
- Belsham, G. J., J. K. Brangwyn, M. D. Ryan, C. C. Abrams, and A. M. King. 1990.** Intracellular expression and processing of foot-and-mouth disease virus capsid precursors using vaccinia virus vectors: influence of the L protease. *Virology* 176: 524-30.
- Berinstein, A., M. Roivainen, T. Hovi, P. W. Mason, and B. Baxt. 1995.** Antibodies to the vitronectin receptor (integrin alpha V beta 3) inhibit binding and infection of foot-and-mouth disease virus to cultured cells. *J Virol* 69: 2664-6.
- Bienkowska-Szewczyk, K., and E. Ehrenfeld. 1988.** An internal 5'-noncoding region required for translation of poliovirus RNA in vitro. *J Virol* 62: 3068-72.
- Bienz, K., D. Egger, M. Troxler, and L. Pasamontes. 1990.** Structural organization of poliovirus RNA replication is mediated by viral proteins of the P2 genomic region. *J Virol* 64: 1156-63.

- Borman, A. M., R. Kirchweger, E. Ziegler, R. E. Rhoads, T. Skern, and K. M. Kean. 1997.** eIF4G and its proteolytic cleavage products: effect on initiation of protein synthesis from capped, uncapped, and IRES-containing mRNAs. *Rna* 3: 186-96.
- Burke, K. L., J. W. Almond, and D. J. Evans. 1991.** Antigen chimeras of poliovirus. *Prog Med Virol* 38: 56-68.
- Cao, X., I. E. Bergmann, R. Fullkrug, and E. Beck. 1995.** Functional analysis of the two alternative translation initiation sites of foot-and-mouth disease virus. *J Virol* 69: 560-3.
- Carrillo, E. C., C. Giachetti, and R. H. Campos. 1984.** Effect of lysosomotropic agents on the foot-and-mouth disease virus replication. *Virology* 135: 542-5.
- Carrillo, E. C., C. Giachetti, and R. Campos. 1985.** Early steps in FMDV replication: further analysis on the effects of chloroquine. *Virology* 147: 118-25.
- Cencic, R., C. Mayer, M. A. Juliano, L. Juliano, R. Konrat, G. Kontaxis, and T. Skern. 2007.** Investigating the substrate specificity and oligomerisation of the leader protease of foot and mouth disease virus using NMR. *J Mol Biol* 373: 1071-87.
- Clamp, M., J. Cuff, S. M. Searle, and G. J. Barton. 2004.** The Jalview Java alignment editor. *Bioinformatics* 20: 426-7.
- Colonna, R. J., J. H. Condra, S. Mizutani, P. L. Callahan, M. E. Davies, and M. A. Murcko. 1988.** Evidence for the direct involvement of the rhinovirus canyon in receptor binding. *Proc Natl Acad Sci U S A* 85: 5449-53.
- Crowder, S., and K. Kirkegaard. 2005.** Trans-dominant inhibition of RNA viral replication can slow growth of drug-resistant viruses. *Nat Genet* 37: 701-9.
- Curry, S., E. Fry, W. Blakemore, R. Abu-Ghazaleh, T. Jackson, A. King, S. Lea, J. Newman, and D. Stuart. 1997.** Dissecting the roles of VP0 cleavage and RNA packaging in picornavirus capsid stabilization: the structure of empty capsids of foot-and-mouth disease virus. *J Virol* 71: 9743-52.
- Dasso, M. C., and R. J. Jackson. 1989.** Efficient initiation of mammalian mRNA translation at a CUG codon. *Nucleic Acids Res* 17: 6485-97.
- de Los Santos, T., F. Diaz-San Segundo, and M. J. Grubman. 2007.** Degradation of nuclear factor kappa B during foot-and-mouth disease virus infection. *J Virol* 81: 12803-15.
- DeLano, D. L. 2002.** The PyMOL molecular graphics system computer program, version By DeLano, D. L., Palo Alto, CA, USA.
- Deszcz, L., R. Cencic, C. Sousa, E. Kuechler, and T. Skern. 2006.** An antiviral peptide inhibitor that is active against picornavirus 2A proteinases but not cellular caspases. *J Virol* 80: 9619-27.
- DeTulleo, L., and T. Kirchhausen. 1998.** The clathrin endocytic pathway in viral infection. *Embo J* 17: 4585-93.
- Devaney, M. A., V. N. Vakharia, R. E. Lloyd, E. Ehrenfeld, and M. J. Grubman. 1988.** Leader protein of foot-and-mouth disease virus is required for cleavage of the p220 component of the cap-binding protein complex. *J Virol* 62: 4407-9.
- Donaldson, A. I. 1987.** Foot-and-mouth disease: the principal features. *Irish Vet J* 41: 325-327.
- Donaldson, A. I., C. F. Gibson, R. Oliver, C. Hamblin, and R. P. Kitching. 1987.** Infection of cattle by airborne foot-and-mouth disease virus: minimal doses with O1 and SAT 2 strains. *Res Vet Sci* 43: 339-46.
- Donnelly, M. L., G. Luke, A. Mehrotra, X. Li, L. E. Hughes, D. Gani, and M. D. Ryan. 2001.** Analysis of the aphthovirus 2A/2B polyprotein 'cleavage' mechanism indicates not a proteolytic reaction, but a novel translational effect: a putative ribosomal 'skip'. *J Gen Virol* 82: 1013-25.

- Etchison, D., and S. Fout. 1985.** Human rhinovirus 14 infection of HeLa cells results in the proteolytic cleavage of the p220 cap-binding complex subunit and inactivates globin mRNA translation in vitro. *J Virol* 54: 634-8.
- Etchison, D., S. C. Milburn, I. Edery, N. Sonenberg, and J. W. Hershey. 1982.** Inhibition of HeLa cell protein synthesis following poliovirus infection correlates with the proteolysis of a 220,000-dalton polypeptide associated with eucaryotic initiation factor 3 and a cap binding protein complex. *J Biol Chem* 257: 14806-10.
- Fauquet, C. 2005.** Virus taxonomy: classification and nomenclature of viruses: eighth report of the International Committee on the Taxonomy of Viruses. Elsevier Academic Press, San Diego, Calif.; London.
- Fields, B. N., D. M. Knipe, and P. M. Howley. 2007.** Fields' virology. Wolters Kluwer/Lippincott Williams & Wilkins, Philadelphia, Pa.; London.
- Fox, G., N. R. Parry, P. V. Barnett, B. McGinn, D. J. Rowlands, and F. Brown. 1989.** The cell attachment site on foot-and-mouth disease virus includes the amino acid sequence RGD (arginine-glycine-aspartic acid). *J Gen Virol* 70 (Pt 3): 625-37.
- Gamarnik, A. V., and R. Andino. 1998.** Switch from translation to RNA replication in a positive-stranded RNA virus. *Genes Dev* 12: 2293-304.
- Gerber, K., E. Wimmer, and A. V. Paul. 2001a.** Biochemical and genetic studies of the initiation of human rhinovirus 2 RNA replication: identification of a cis-replicating element in the coding sequence of 2A(pro). *J Virol* 75: 10979-90.
- Gerber, K., E. Wimmer, and A. V. Paul. 2001b.** Biochemical and genetic studies of the initiation of human rhinovirus 2 RNA replication: purification and enzymatic analysis of the RNA-dependent RNA polymerase 3D(pol). *J Virol* 75: 10969-78.
- Glaser, W., R. Cencic, and T. Skern. 2001.** Foot-and-mouth disease virus leader proteinase: involvement of C-terminal residues in self-processing and cleavage of eIF4GI. *J Biol Chem* 276: 35473-81.
- Glaser, W., A. Triendl, and T. Skern. 2003.** The processing of eIF4GI by human rhinovirus type 2 2A(pro): relationship to self-cleavage and role of zinc. *J Virol* 77: 5021-5.
- Gradi, A., Y. V. Svitkin, H. Imataka, and N. Sonenberg. 1998a.** Proteolysis of human eukaryotic translation initiation factor eIF4GII, but not eIF4GI, coincides with the shutoff of host protein synthesis after poliovirus infection. *Proc Natl Acad Sci U S A* 95: 11089-94.
- Gradi, A., H. Imataka, Y. V. Svitkin, E. Rom, B. Raught, S. Morino, and N. Sonenberg. 1998b.** A novel functional human eukaryotic translation initiation factor 4G. *Mol Cell Biol* 18: 334-42.
- Gradi, A., Y. V. Svitkin, W. Sommergruber, H. Imataka, S. Morino, T. Skern, and N. Sonenberg. 2003.** Human rhinovirus 2A proteinase cleavage sites in eukaryotic initiation factors (eIF) 4GI and eIF4GII are different. *J Virol* 77: 5026-9.
- Gradi, A., N. Foeger, R. Strong, Y. V. Svitkin, N. Sonenberg, T. Skern, and G. J. Belsham. 2004.** Cleavage of eukaryotic translation initiation factor 4GII within foot-and-mouth disease virus-infected cells: identification of the L-protease cleavage site in vitro. *J Virol* 78: 3271-8.
- Greve, J. M., G. Davis, A. M. Meyer, C. P. Forte, S. C. Yost, C. W. Marlor, M. E. Kamarck, and A. McClelland. 1989.** The major human rhinovirus receptor is ICAM-1. *Cell* 56: 839-47.
- Guarne, A., J. Tormo, R. Kirchwegger, D. Pfistermueller, I. Fita, and T. Skern. 1998.** Structure of the foot-and-mouth disease virus leader protease: a papain-like fold adapted for self-processing and eIF4G recognition. *Embo J* 17: 7469-79.
- Guex, N., and M. C. Peitsch. 1997.** SWISS-MODEL and the Swiss-PdbViewer: an environment for comparative protein modeling. *Electrophoresis* 18: 2714-23.
- Gustin, K. E., and P. Sarnow. 2001.** Effects of poliovirus infection on nucleo-cytoplasmic trafficking and nuclear pore complex composition. *Embo J* 20: 240-9.

- Halperen, S., H. J. Eggers, and I. Tamm. 1964.** Evidence For Uncoupled Synthesis Of Viral Rna And Viral Capsids. *Virology* 24: 36-46.
- Hanecak, R., B. L. Semler, C. W. Anderson, and E. Wimmer. 1982.** Proteolytic processing of poliovirus polypeptides: antibodies to polypeptide P3-7c inhibit cleavage at glutamine-glycine pairs. *Proc Natl Acad Sci U S A* 79: 3973-7.
- Hellen, C. U., C. K. Lee, and E. Wimmer. 1992.** Determinants of substrate recognition by poliovirus 2A proteinase. *J Virol* 66: 3330-8.
- Herold, J., and R. Andino. 2001.** Poliovirus RNA replication requires genome circularization through a protein-protein bridge. *Mol Cell* 7: 581-91.
- Hewat, E. A., E. Neumann, J. F. Conway, R. Moser, B. Ronacher, T. C. Marlovits, and D. Blaas. 2000.** The cellular receptor to human rhinovirus 2 binds around the 5-fold axis and not in the canyon: a structural view. *Embo J* 19: 6317-25.
- Hofer, F., M. Gruenberger, H. Kowalski, H. Machat, M. Huettinger, E. Kuechler, and D. Blaas. 1994.** Members of the low density lipoprotein receptor family mediate cell entry of a minor-group common cold virus. *Proc Natl Acad Sci U S A* 91: 1839-42.
- Hogle, J. M., M. Chow, and D. J. Filman. 1985.** Three-dimensional structure of poliovirus at 2.9 Å resolution. *Science* 229: 1358-65.
- Hoover-Litty, H., and J. M. Greve. 1993.** Formation of rhinovirus-soluble ICAM-1 complexes and conformational changes in the virion. *J Virol* 67: 390-7.
- Hyde, J. L., J. H. Blackwell, and J. J. Callis. 1975.** Effect of pasteurization and evaporation on foot-and-mouth disease virus in whole milk from infected cows. *Can J Comp Med* 39: 305-9.
- ICTV. 2008.** www.ictvonline.org. International committee on taxonomy of viruses.
- Imataka, H., A. Gradi, and N. Sonenberg. 1998.** A newly identified N-terminal amino acid sequence of human eIF4G binds poly(A)-binding protein and functions in poly(A)-dependent translation. *Embo J* 17: 7480-9.
- Jackson, T., F. M. Ellard, R. A. Ghazaleh, S. M. Brookes, W. E. Blakemore, A. H. Corteyn, D. I. Stuart, J. W. Newman, and A. M. King. 1996.** Efficient infection of cells in culture by type O foot-and-mouth disease virus requires binding to cell surface heparan sulfate. *J Virol* 70: 5282-7.
- Jacobson, M. F., and D. Baltimore. 1968.** Morphogenesis of poliovirus. I. Association of the viral RNA with coat protein. *J Mol Biol* 33: 369-78.
- Joachims, M., P. C. Van Breugel, and R. E. Lloyd. 1999.** Cleavage of poly(A)-binding protein by enterovirus proteases concurrent with inhibition of translation in vitro. *J Virol* 73: 718-27.
- Kerekatte, V., B. D. Keiper, C. Badorff, A. Cai, K. U. Knowlton, and R. E. Rhoads. 1999.** Cleavage of Poly(A)-binding protein by coxsackievirus 2A protease in vitro and in vivo: another mechanism for host protein synthesis shutoff? *J Virol* 73: 709-17.
- Kirchweger, R., E. Ziegler, B. J. Lamphear, D. Waters, H. D. Liebig, W. Sommergruber, F. Sobrino, C. Hohenadl, D. Blaas, R. E. Rhoads, and et al. 1994.** Foot-and-mouth disease virus leader proteinase: purification of the Lb form and determination of its cleavage site on eIF-4 gamma. *J Virol* 68: 5677-84.
- Kitamura, N., B. L. Semler, P. G. Rothberg, G. R. Larsen, C. J. Adler, A. J. Dorner, E. A. Emini, R. Hanecak, J. J. Lee, S. van der Werf, C. W. Anderson, and E. Wimmer. 1981.** Primary structure, gene organization and polypeptide expression of poliovirus RNA. *Nature* 291: 547-53.
- Kitching, R. P. 2005.** Global epidemiology and prospects for control of foot-and-mouth disease. *Curr Top Microbiol Immunol* 288: 133-48.

- Kolatkar, P. R., J. Bella, N. H. Olson, C. M. Bator, T. S. Baker, and M. G. Rossmann. 1999.** Structural studies of two rhinovirus serotypes complexed with fragments of their cellular receptor. *Embo J* 18: 6249-59.
- Konig, H., and B. Rosenwirth. 1988.** Purification and partial characterization of poliovirus protease 2A by means of a functional assay. *J Virol* 62: 1243-50.
- Kuehnel, E., R. Cencic, N. Foeger, and T. Skern. 2004.** Foot-and-mouth disease virus leader proteinase: specificity at the P2 and P3 positions and comparison with other papain-like enzymes. *Biochemistry* 43: 11482-90.
- Laine, P., S. Blomqvist, C. Savolainen, K. Andries, and T. Hovi. 2006.** Alignment of capsid protein VP1 sequences of all human rhinovirus prototype strains: conserved motifs and functional domains. *J Gen Virol* 87: 129-38.
- Lamphear, B. J., R. Kirchweger, T. Skern, and R. E. Rhoads. 1995.** Mapping of functional domains in eukaryotic protein synthesis initiation factor 4G (eIF4G) with picornaviral proteases. Implications for cap-dependent and cap-independent translational initiation. *J Biol Chem* 270: 21975-83.
- Lamphear, B. J., R. Yan, F. Yang, D. Waters, H. D. Liebig, H. Klump, E. Kuechler, T. Skern, and R. E. Rhoads. 1993.** Mapping the cleavage site in protein synthesis initiation factor eIF-4 gamma of the 2A proteases from human Coxsackievirus and rhinovirus. *J Biol Chem* 268: 19200-3.
- Lau, S. K., C. C. Yip, H. W. Tsoi, R. A. Lee, L. Y. So, Y. L. Lau, K. H. Chan, P. C. Woo, and K. Y. Yuen. 2007.** Clinical features and complete genome characterization of a distinct human rhinovirus (HRV) genetic cluster, probably representing a previously undetected HRV species, HRV-C, associated with acute respiratory illness in children. *J Clin Microbiol* 45: 3655-64.
- Lee, Y. F., A. Nomoto, B. M. Detjen, and E. Wimmer. 1977.** A protein covalently linked to poliovirus genome RNA. *Proc Natl Acad Sci U S A* 74: 59-63.
- Leippert, M., E. Beck, F. Weiland, and E. Pfaff. 1997.** Point mutations within the betaG-betaH loop of foot-and-mouth disease virus O1K affect virus attachment to target cells. *J Virol* 71: 1046-51.
- Lonberg-Holm, K., and B. D. Korant. 1972.** Early interaction of rhinoviruses with host cells. *J Virol* 9: 29-40.
- Mader, S., H. Lee, A. Pause, and N. Sonenberg. 1995.** The translation initiation factor eIF-4E binds to a common motif shared by the translation factor eIF-4 gamma and the translational repressors 4E-binding proteins. *Mol Cell Biol* 15: 4990-7.
- Makela, M. J., T. Puhakka, O. Ruuskanen, M. Leinonen, P. Saikku, M. Kimpimaki, S. Blomqvist, T. Hyypia, and P. Arstila. 1998.** Viruses and bacteria in the etiology of the common cold. *J Clin Microbiol* 36: 539-42.
- Marlovits, T. C., C. Abrahamsberg, and D. Blaas. 1998a.** Soluble LDL minireceptors. Minimal structure requirements for recognition of minor group human rhinovirus. *J Biol Chem* 273: 33835-40.
- Marlovits, T. C., C. Abrahamsberg, and D. Blaas. 1998b.** Very-low-density lipoprotein receptor fragment shed from HeLa cells inhibits human rhinovirus infection. *J Virol* 72: 10246-50.
- Marlovits, T. C., T. Zechmeister, M. Gruenberger, B. Ronacher, H. Schwihla, and D. Blaas. 1998c.** Recombinant soluble low density lipoprotein receptor fragment inhibits minor group rhinovirus infection in vitro. *Faseb J* 12: 695-703.
- Matthews, D. A., W. W. Smith, R. A. Ferre, B. Condon, G. Budahazi, W. Sisson, J. E. Villafranca, C. A. Janson, H. E. McElroy, C. L. Gribskov, and et al. 1994.** Structure of human rhinovirus 3C protease reveals a trypsin-like polypeptide fold, RNA-binding site, and means for cleaving precursor polyprotein. *Cell* 77: 761-71.

- Matthews, D. A., P. S. Dragovich, S. E. Webber, S. A. Fuhrman, A. K. Patick, L. S. Zalman, T. F. Hendrickson, R. A. Love, T. J. Prins, J. T. Marakovits, R. Zhou, J. Tikhe, C. E. Ford, J. W. Meador, R. A. Ferre, E. L. Brown, S. L. Binford, M. A. Brothers, D. M. DeLisle, and S. T. Worland. 1999.** Structure-assisted design of mechanism-based irreversible inhibitors of human rhinovirus 3C protease with potent antiviral activity against multiple rhinovirus serotypes. *Proc Natl Acad Sci U S A* 96: 11000-7.
- Mayer, C., D. Neubauer, A. T. Nchinda, R. Cencic, K. Trompf, and T. Skern. 2008.** Residue L143 of the foot-and-mouth disease virus leader proteinase is a determinant of cleavage specificity. *J Virol* 82: 4656-9.
- Medina, M., E. Domingo, J. K. Brangwyn, and G. J. Belsham. 1993.** The two species of the foot-and-mouth disease virus leader protein, expressed individually, exhibit the same activities. *Virology* 194: 355-9.
- Mischak, H., C. Neubauer, B. Berger, E. Kuechler, and D. Blaas. 1988.** Detection of the human rhinovirus minor group receptor on renaturing Western blots. *J Gen Virol* 69 (Pt 10): 2653-6.
- Moore, D. M., and K. M. Cowan. 1978.** Effect of trypsin and chymotrypsin on the polypeptides of large and small plaque variants of foot-and-mouth disease virus: relationship to specific antigenicity and infectivity. *J Gen Virol* 41: 549-62.
- Mosimann, S. C., M. M. Cherney, S. Sia, S. Plotch, and M. N. James. 1997.** Refined X-ray crystallographic structure of the poliovirus 3C gene product. *J Mol Biol* 273: 1032-47.
- Muckelbauer, J. K., M. Kremer, I. Minor, G. Diana, F. J. Dutko, J. Groarke, D. C. Pevear, and M. G. Rossmann. 1995.** The structure of coxsackievirus B3 at 3.5 Å resolution. *Structure* 3: 653-67.
- Neff, S., and B. Baxt. 2001.** The ability of integrin $\alpha(v)\beta(3)$ to function as a receptor for foot-and-mouth disease virus is not dependent on the presence of complete subunit cytoplasmic domains. *J Virol* 75: 527-32.
- Neff, S., P. W. Mason, and B. Baxt. 2000.** High-efficiency utilization of the bovine integrin $\alpha(v)\beta(3)$ as a receptor for foot-and-mouth disease virus is dependent on the bovine $\beta(3)$ subunit. *J Virol* 74: 7298-306.
- Neff, S., D. Sa-Carvalho, E. Rieder, P. W. Mason, S. D. Blystone, E. J. Brown, and B. Baxt. 1998.** Foot-and-mouth disease virus virulent for cattle utilizes the integrin $\alpha(v)\beta(3)$ as its receptor. *J Virol* 72: 3587-94.
- Neubauer, C., L. Frasel, E. Kuechler, and D. Blaas. 1987.** Mechanism of entry of human rhinovirus 2 into HeLa cells. *Virology* 158: 255-8.
- Novak, J. E., and K. Kirkegaard. 1991.** Improved method for detecting poliovirus negative strands used to demonstrate specificity of positive-strand encapsidation and the ratio of positive to negative strands in infected cells. *J Virol* 65: 3384-7.
- Nugent, C. I., and K. Kirkegaard. 1995.** RNA binding properties of poliovirus subviral particles. *J Virol* 69: 13-22.
- Oliveira, M. A., R. Zhao, W. M. Lee, M. J. Kremer, I. Minor, R. R. Rueckert, G. D. Diana, D. C. Pevear, F. J. Dutko, M. A. McKinlay, and et al. 1993.** The structure of human rhinovirus 16. *Structure* 1: 51-68.
- Olson, N. H., P. R. Kolatkar, M. A. Oliveira, R. H. Cheng, J. M. Greve, A. McClelland, T. S. Baker, and M. G. Rossmann. 1993.** Structure of a human rhinovirus complexed with its receptor molecule. *Proc Natl Acad Sci U S A* 90: 507-11.
- Palmenberg, A. C. 1982.** In vitro synthesis and assembly of picornaviral capsid intermediate structures. *J Virol* 44: 900-6.
- Park, N., P. Katikaneni, T. Skern, and K. E. Gustin. 2008.** Differential targeting of nuclear pore complex proteins in poliovirus-infected cells. *J Virol* 82: 1647-55.

- Petersen, J. F., M. M. Cherney, H. D. Liebig, T. Skern, E. Kuechler, and M. N. James. 1999.** The structure of the 2A proteinase from a common cold virus: a proteinase responsible for the shut-off of host-cell protein synthesis. *Embo J* 18: 5463-75.
- Pfaff, E., H. J. Thiel, E. Beck, K. Strohmaier, and H. Schaller. 1988.** Analysis of neutralizing epitopes on foot-and-mouth disease virus. *J Virol* 62: 2033-40.
- Piccione, M. E., S. Sira, M. Zellner, and M. J. Grubman. 1995.** Expression in *Escherichia coli* and purification of biologically active L proteinase of foot-and-mouth disease virus. *Virus Res* 35: 263-75.
- Pierschbacher, M. D., and E. Ruoslahti. 1984a.** Variants of the cell recognition site of fibronectin that retain attachment-promoting activity. *Proc Natl Acad Sci U S A* 81: 5985-8.
- Pierschbacher, M. D., and E. Ruoslahti. 1984b.** Cell attachment activity of fibronectin can be duplicated by small synthetic fragments of the molecule. *Nature* 309: 30-3.
- Pilipenko, E. V., S. V. Maslova, A. N. Sinyakov, and V. I. Agol. 1992.** Towards identification of cis-acting elements involved in the replication of enterovirus and rhinovirus RNAs: a proposal for the existence of tRNA-like terminal structures. *Nucleic Acids Res* 20: 1739-45.
- Prchla, E., E. Kuechler, D. Blaas, and R. Fuchs. 1994.** Uncoating of human rhinovirus serotype 2 from late endosomes. *J Virol* 68: 3713-23.
- Renwick, N., B. Schweiger, V. Kapoor, Z. Liu, J. Villari, R. Bullmann, R. Miething, T. Briese, and W. I. Lipkin. 2007.** A recently identified rhinovirus genotype is associated with severe respiratory-tract infection in children in Germany. *J Infect Dis* 196: 1754-60.
- Rivera, V. M., J. D. Welsh, and J. V. Maizel, Jr. 1988.** Comparative sequence analysis of the 5' noncoding region of the enteroviruses and rhinoviruses. *Virology* 165: 42-50.
- Robertson, B. H., D. M. Moore, M. J. Grubman, and D. G. Kleid. 1983.** Identification of an exposed region of the immunogenic capsid polypeptide VP1 on foot-and-mouth disease virus. *J Virol* 46: 311-6.
- Roetzer, A. 2004.** Untersuchung der Wechselwirkung von enteroviralen 2A Proteinasen mit dem eukaryontischem Initiationsfaktor eIF4GI, Department of medical biochemistry. Medical University of Vienna, Vienna.
- Rossmann, M. G., E. Arnold, J. W. Erickson, E. A. Frankenger, J. P. Griffith, H. J. Hecht, J. E. Johnson, G. Kamer, M. Luo, A. G. Mosser, and et al. 1985.** Structure of a human common cold virus and functional relationship to other picornaviruses. *Nature* 317: 145-53.
- Rotbart, H. A. 1995.** Human enterovirus infections. ASM Press, Washington, D.C.
- Ryan, M. D., A. M. King, and G. P. Thomas. 1991.** Cleavage of foot-and-mouth disease virus polyprotein is mediated by residues located within a 19 amino acid sequence. *J Gen Virol* 72 (Pt 11): 2727-32.
- Sangar, D. V., S. E. Newton, D. J. Rowlands, and B. E. Clarke. 1987.** All foot and mouth disease virus serotypes initiate protein synthesis at two separate AUGs. *Nucleic Acids Res* 15: 3305-15.
- Savolainen, C., S. Blomqvist, M. N. Mulders, and T. Hovi. 2002.** Genetic clustering of all 102 human rhinovirus prototype strains: serotype 87 is close to human enterovirus 70. *J Gen Virol* 83: 333-40.
- Schertler, S. 2008.** Investigating the cleavage specificities of picornaviral 2A proteinases, Department of medical biochemistry. University of Vienna, Vienna.
- Schober, D., P. Kronenberger, E. Prchla, D. Blaas, and R. Fuchs. 1998.** Major and minor receptor group human rhinoviruses penetrate from endosomes by different mechanisms. *J Virol* 72: 1354-64.

- Seipelt, J., H. D. Liebig, W. Sommergruber, C. Gerner, and E. Kuechler. 2000.** 2A proteinase of human rhinovirus cleaves cytokeratin 8 in infected HeLa cells. *J Biol Chem* 275: 20084-9.
- Semler, B. L., and E. Wimmer. 2002.** Molecular biology of picornaviruses. ASM Press, Washington, D.C.
- Skern, T., W. Sommergruber, D. Blaas, P. Gruendler, F. Fraundorfer, C. Pieler, I. Fogy, and E. Kuechler. 1985.** Human rhinovirus 2: complete nucleotide sequence and proteolytic processing signals in the capsid protein region. *Nucleic Acids Res* 13: 2111-26.
- Skern, T., W. Sommergruber, H. Auer, P. Volkmann, M. Zorn, H. D. Liebig, F. Fessl, D. Blaas, and E. Kuechler. 1991.** Substrate requirements of a human rhinoviral 2A proteinase. *Virology* 181: 46-54.
- Sommergruber, W., G. Casari, F. Fessl, J. Seipelt, and T. Skern. 1994.** The 2A proteinase of human rhinovirus is a zinc containing enzyme. *Virology* 204: 815-8.
- Sommergruber, W., J. Seipelt, F. Fessl, T. Skern, H. D. Liebig, and G. Casari. 1997.** Mutational analyses support a model for the HRV2 2A proteinase. *Virology* 234: 203-14.
- Sommergruber, W., H. Ahorn, A. Zophel, I. Maurer-Fogy, F. Fessl, G. Schnorrenberg, H. D. Liebig, D. Blaas, E. Kuechler, and T. Skern. 1992.** Cleavage specificity on synthetic peptide substrates of human rhinovirus 2 proteinase 2A. *J Biol Chem* 267: 22639-44.
- Sonenberg, N., M. A. Morgan, W. C. Merrick, and A. J. Shatkin. 1978.** A polypeptide in eukaryotic initiation factors that crosslinks specifically to the 5'-terminal cap in mRNA. *Proc Natl Acad Sci U S A* 75: 4843-7.
- Sousa, C., E. M. Schmid, and T. Skern. 2006.** Defining residues involved in human rhinovirus 2A proteinase substrate recognition. *FEBS Lett* 580: 5713-7.
- Spector, D. H., and D. Baltimore. 1974.** Requirement of 3'-terminal poly(adenylic acid) for the infectivity of poliovirus RNA. *Proc Natl Acad Sci U S A* 71: 2983-7.
- Stanway, G., P. J. Hughes, R. C. Mountford, P. D. Minor, and J. W. Almond. 1984.** The complete nucleotide sequence of a common cold virus: human rhinovirus 14. *Nucleic Acids Res* 12: 7859-75.
- Staunton, D. E., S. D. Marlin, C. Stratowa, M. L. Dustin, and T. A. Springer. 1988.** Primary structure of ICAM-1 demonstrates interaction between members of the immunoglobulin and integrin supergene families. *Cell* 52: 925-33.
- Staunton, D. E., V. J. Merluzzi, R. Rothlein, R. Barton, S. D. Marlin, and T. A. Springer. 1989.** A cell adhesion molecule, ICAM-1, is the major surface receptor for rhinoviruses. *Cell* 56: 849-53.
- Strebel, K., and E. Beck. 1986.** A second protease of foot-and-mouth disease virus. *J Virol* 58: 893-9.
- Toyoda, H., M. J. Nicklin, M. G. Murray, C. W. Anderson, J. J. Dunn, F. W. Studier, and E. Wimmer. 1986.** A second virus-encoded proteinase involved in proteolytic processing of poliovirus polyprotein. *Cell* 45: 761-70.
- Trono, D., R. Andino, and D. Baltimore. 1988.** An RNA sequence of hundreds of nucleotides at the 5' end of poliovirus RNA is involved in allowing viral protein synthesis. *J Virol* 62: 2291-9.
- Voss, T., R. Meyer, and W. Sommergruber. 1995.** Spectroscopic characterization of rhinoviral protease 2A: Zn is essential for the structural integrity. *Protein Sci* 4: 2526-31.
- Wang, Q. M., R. B. Johnson, W. Sommergruber, and T. A. Shepherd. 1998.** Development of in vitro peptide substrates for human rhinovirus-14 2A protease. *Arch Biochem Biophys* 356: 12-8.
- Yamamoto, T., C. G. Davis, M. S. Brown, W. J. Schneider, M. L. Casey, J. L. Goldstein, and D. W. Russell. 1984.** The human LDL receptor: a cysteine-rich protein with multiple Alu sequences in its mRNA. *Cell* 39: 27-38.

Zhao, X., B. J. Lamphear, D. Xiong, K. Knowlton, and R. E. Rhoads. 2003. Protection of cap-dependent protein synthesis in vivo and in vitro with an eIF4G-1 variant highly resistant to cleavage by Coxsackievirus 2A protease. *J Biol Chem* 278: 4449-57.

CURRICULUM VITAE

David Neubauer Blechturm-gasse 1/16, 1050 Vienna +436505314959 david.neubauer@univie.ac.at

PERSONAL INFORMATION

DATE OF BIRTH	16.11.1981
PLACE OF BIRTH	Linz
CITIZENSHIP	Austrian
GENDER	Male

EDUCATION

1987-1991	Elementary school in Altenberg bei Linz
1991-1995	Secondary school in Altenberg bei Linz
1995-1999	High school (BORG Honauerstraße) in Linz
2000-2008	Student of chemistry at the University of Vienna

PUBLICATIONS / ATTENDANCE AT CONFERENCES

Mayer, C., D. Neubauer, A. T. Nchinda, R. Cencic, K. Trompf, and T. Skern. 2008.
Residue L143 of the foot-and-mouth disease virus leader proteinase is a determinant of cleavage specificity. *J Virol* 82: 4656-9.

AUGUST 2007	Attendance at the EMBO workshop "RNA viruses: replication, evolution and drug design", Vienna.
AUGUST 2008	Attendance and poster presentation at the VIZIER/SPINE2 workshop "Structural virology", Vienna.
SEPTEMBER 2008	Attendance and poster presentation at the annual meeting of the ÖGBM (Austrian society for biochemistry and molecular biology), Graz.

MISCELLANEOUS

LANGUAGES	German, English
COMPUTER SKILLS	Microsoft Office, Adobe Photoshop, Swiss PDB viewer, PyMOL, Clone Manager, basics in LATEX
HOBBIES	Volleyball, ultimate frisbee, hiking, playing the guitar, singing, reading, biking,...

LEBENS LAUF

David Neubauer Blechturm gasse 1/16, 1050 Vienna +436505314959 david.neubauer@univie.ac.at

PERSÖNLICHE INFORMATIONEN

GEBURTSDATUM	16.11.1981
GEBURTSORT	Linz
STAATSBÜRGERSCHAFT	Österreich
GESCHLECHT	Männlich

AUSBILDUNG

1987-1991	Volksschule in Altenberg bei Linz
1991-1995	Hauptschule in Altenberg bei Linz
1995-1999	BORG Honauerstraße, Linz
2000-2008	Chemie Studium an der Universität Wien

VERÖFFENTLICHUNGEN / TEILNAHME AN KONFERENZEN

Mayer, C., D. Neubauer, A. T. Nchinda, R. Cencic, K. Trompf, and T. Skern. 2008.
Residue L143 of the foot-and-mouth disease virus leader proteinase is a determinant of cleavage specificity. J Virol 82: 4656-9.

AUGUST 2007	Teilnahme am EMBO Workshop "RNA viruses: replication, evolution and drug design", Wien.
AUGUST 2008	Teilnahme und Poster Präsentation beim VIZIER/SPINE2 workshop "Structural virology", Wien.
SEPTEMBER 2008	Teilnahme und Poster Präsentation an der Jahrestagung der österreichischen Gesellschaft für Biochemie und molekulare Biologie (ÖGBM), Graz.

SONSTIGE FÄHIGKEITEN

SPRACHEN	Deutsch, Englisch
COMPUTER KENNTNISSE	Microsoft Office, Adobe Photoshop, Swiss PDB viewer, PyMOL, Clone Manager, Grundkenntnisse in LATEX
HOBBIES	Volleyball, Ultimate Frisbee, Wandern, Gitarre spielen, Singen, Lesen, Radfahren,...